IMPACTS OF CONNECTED AND AUTONOMOUS VEHICLES ON DEEP
REINFORCEMENT LEARNING CONTROLLED INTERSECTION SYSTEMS

by

Li Song

A dissertation submitted to the faculty of
The University of North Carolina at Charlotte
in partial fulfillment of the requirements
for the degree of Doctor of Philosophy in
Infrastructure and Environmental Systems

Charlotte

2022

Approved by:

_____

Dr. Wei Fan

_____

Dr. Martin Kane

_____

Dr. David Weggel

_____

Dr. Jay Wu

_____

Dr. John Diemer

ABSTRACT

LI SONG. Impacts of connected and autonomous vehicles on deep reinforcement learning controlled intersection systems. (Under the direction of DR. WEI FAN)

Connected and autonomous vehicle (CAV) technologies could significantly change the car-following behaviors and affect the performance of the intersection systems. As it is expected to have a long transition time during which human driven vehicles (HDVs) and CAVs will coexist, it is important to investigate the impacts of CAVs on the intersection systems under different market penetration rates (MPRs). Also, the currently used Highway Capacity Manual does not consider the impacts of CAVs when calculating the intersection capacity. Though highly needed, a new guideline for estimating the intersection capacity under different MPRs of CAVs is becoming a critical issue for transportation planners and engineers. Furthermore, combining the intersection traffic signal control (TSC) systems with deep reinforcement learning (DRL) provides a new potential solution to improve the efficiency, safety, and sustainability of the intersection system. However, the training procedure of the DRL TSC system requires large samples and takes a long time to converge. Furthermore, it is common to have several intersections along corridors or in networks. A single DRL agent is unable to control several intersections as this may result in exponential explosion in the action space. Hence, a modification of the DRL TSC framework to improve the training efficiency and a multi-agent control framework to control several intersections are needed.

To better prepare and guide both intersection planning and operations under different MPRs of CAVs and traffic demands, this dissertation provides an intensive evaluation of the

impacts of CAVs in several signal intersection systems, as well as an in-depth analysis on intersection capacity adjustments that consider varying MPRs of CAVs. Also, a transfer-based DRL TSC framework is proposed and tested at different MPRs of CAVs and traffic demand levels. A multi-agent DRL TSC with shared traffic states between downstream and upstream intersections is investigated in a corridor. It is concluded that 100% MPR of CAVs can increase the saturation flow rate of the through-only lane by 126.8%. Meanwhile, transfer-based models could significantly improve training efficiency and model performance. The multi-agent DRL TSC also enables coordination between intersections. The insights of this research should be helpful and valuable to transportation researchers and traffic engineers in calculating intersection capacity, designing intelligent intersections, improving intersection efficiency, and implementing DRL-controlled traffic signals under the mixed flow with CAVs.

ACKNOWLEDGEMENTS

TABLE OF CONTENTS

LIST OF TABLES

LIST OF FIGURES

LIST OF ABBREVIATIONS

ACC   Adaptive Cruise Control

AV   Autonomous Vehicle

CACC   Cooperative Adaptive Cruise Control

CAV   Connected and Autonomous Vehicle

CV   Connected Vehicle

DQN   Deep Q Network

DRL   Deep Reinforcement Learning

FHWA   Federal Highway Administration

HDV   Human Driven Vehicle

IDM   Intelligent Driver Model

MARL   Multi-agent Reinforcement Learning

MPR   Market Penetration Rate

NCDOT   North Carolina Department of Transportation

RL   Reinforcement Learning

TSC   Traffic Signal Control

V2I   Vehicle to Infrastructure

V2V   Vehicle to Vehicle

CHAPTER 1: INTRODUCTION

1.1.   Problem Statement and Motivation

In the past decades, emerging technologies that could assist or automatically control the driving process of traditionally human-driven vehicles have drawn great interest from researchers and engineers. With the development of Vehicle to Vehicle (V2V) and Vehicle to Infrastructure (V2I) communication technologies, connected and autonomous vehicles (CAVs) could make driving-informed decisions based on multi-source data, such as the speed/location of the surrounding vehicles and the signal timing schemes of surrounding intersections. The requirement of the time gap for successive vehicles could also be sharply decreased, and this could significantly change the car-following behaviors and affect the performance of the transportation systems. However, it is expected to have a long transition period during which human driven vehicles (HDVs) and intelligent vehicles will coexist (Sharon & Stone, 2017). Hence, research on the impacts of CAV technologies and the mixed flow of HDVs and CAVs is needed.

CAVs will have a profound influence on the performance of the currently used transportation system, especially for the intersection that has complex traffic conditions. Several proposed intersection control systems require a modification of the existing intersections, particularly for high market penetration rates (MPRs) of Autonomous Vehicles (AVs) or Connected Vehicles (CVs) (Algomaiah & Li, 2019; Dresner & Stone, 2008). Reconstruction of those intersections or installing the V2I equipment would take a long time. For example, the autonomous interaction management (AIM) system replaces signals with a reservation-based central control system. For this purpose, the AIM requires more than a 90% MPR of the CAVs (Dresner & Stone, 2008). However, there is still a long way to go for intelligent vehicles to be

fully applicable in currently used traffic environments. Meanwhile, currently used Highway Capacity Manual (HCM) methods do not consider the impacts of CAVs on the transportation system. Evaluating the capacity of intersections under the impacts of CAVs is becoming a critical issue to be resolved for transportation planners and engineers. Consequently, new guidelines for estimating the capacity of intersections, including the consideration of CAV involvement in mixed traffic conditions, need to be established. Moreover, research needs to analyze the impacts of the CAV MPRs on the intersection capacity and modify the intersection capacity adjustments factors for engineer applications.

For intersection TSC, pre-timed or actuated signal schemes have been widely utilized in real-world intersections. With the rapid development of learning-based artificial intelligence technologies, combining the management of transportation systems with deep reinforcement learning (DRL) technologies provides a new potential solution to improve the efficiency, safety, and sustainability of intelligent transportation systems. Several studies designed an intelligent signal control system that assumed 100% MPR of CAVs so that the signal controller could obtain the full information on the vehicles and set the signal phase according to the environment information (Guo et al., 2019). Also, it is noted that most research studies indicated a generally positive effect of intelligent vehicles, while some others found that the intelligent vehicles could improve the system performance only after certain MPRs (Algomaiah & Li, 2019; Jiang et al., 2017; Lee et al., 2013). Since there is still a long way to achieve high MPRs of CAVs, it is practical and important to investigate the impacts of mixed flow and determine the MPRs of CAVs that are sufficient to train a relatively good DRL-controlled TSC system.

Moreover, the DRL training procedure of the DRL-controlled TSC system requires a lot of samples and takes a long time to converge (Xu et al., 2019). With the variations in the traffic

flow at the intersection across time and space, it is extremely hard to train a model that could accommodate several traffic scenarios for real-world applications. Currently, transfer learning enables the reuse of previously trained action policy developed from a similar task to initialize the learning of a target task, and it is expected to improve the training efficiency, sample efficiency, and training performance (Kiran et al., 2021; Xu et al., 2019). Hence, a modification of the currently used DRL framework and reusing pre-trained models under similar traffic scenarios provided by transfer learning may provide a feasible solution to improve the training procedure of the DRL.

Furthermore, it is common to have several intersections on the roadways or networks. However, a single DRL agent is unable to control several intersections as this may result in exponential explosion in the action space. Hence, a multi-agent control framework for several intersections is needed. Additionally, the upstream and downstream intersections could impact each other, and the signal coordination could further improve the traffic performance in corridor or network intersection systems. With the infrastructure to infrastructure (I2I) communication technology, the intersections can also share traffic states with one another. In this way, it is important to investigate the performance of multi-agent DRL-controlled intersection signals and cooperate signals by sharing the state information with each other.

The results of this study could provide a theoretical basis for researchers to investigate the impact of CAVs on currently used intersections and DRL-controlled signalized intersections. The calibration methods and results of intersection capacity adjustment factors for different CAV penetration rates could provide a guideline for transportation engineers/planners to modify intersection capacity considering the impacts of CAVs. Also, the proposed frameworks could provide a foundation for better intelligent vehicle operations and intersection signal controls.

Moreover, the results could give a solid reference to researchers and engineers for better designing, planning, and operating future intelligent intersection systems under a variety of mixed traffic environments.

1.2.   Study Objectives

The main goals of this research project include an investigation of the impacts of CAV penetration rates and deep reinforcement learning controlled signal schemes on the intersection systems. The proposed work in this research is intended to complete the following objectives:

1. To conduct a comprehensive review of the state-of-the-art and state-of-the-practice on CAV technologies, DRL-controlled signal schemes, and their impacts on the intersection efficiency;

2. To identify potential scenarios of the traffic environments for the intersection case studies;

3. To use a simulation method to measure the intersection capacity and performance at different MPRs of CAVs;

4. To modify the DRL framework by transfer learning and analyze the performance of the transfer-based DRL-controlled signal system at different traffic volumes and MPRs of CAVs; and

5. To investigate the performance of the multi-agent DRL-controlled intersection system with shared traffic states between downstream and upstream intersections in a corridor.

1.3.   Expected Contributions

This research aims to evaluate the influence of different MPRs of CAVs on a typical pre-timed intersection and a DRL-controlled signalized intersection. The outcomes from this research are expected as follows:

1. Review of CAV technologies, DRL-controlled traffic signal system, and intersection mobility analysis considering different MPRs of CAVs;

2. Identification of potential intersections and simulation scenarios under different traffic demands and MPRs of CAVs;

3. Microscopic simulation settings for CAVs and specific parameters for car-following models and DRL-controlled traffic signal models;

4. Guidelines on the intersection capacity adjustments under different MPRs of CAVs for engineer applications;

5. Frameworks of transfer-based DRL-controlled signal intersection and multiagent DRL-controlled signal intersections with shared states;

6. Guidelines on the impacts of CAV penetration rates on the performance of transfer-based DRL-controlled signal intersection.

1.4.   Dissertation Overview

The dissertation is structured as shown in Figure 1.1. In this chapter, the motivation of the research has been explained, followed by the study objectives and expected outcomes.

Chapter 2 summarizes a comprehensive review of the current state-of-the-art and state-of-the-practice on CAVs technologies and the impacts of different MPRs of CAVs on the intersection system. The traffic flow control methods for CAVs, intersection capacity analysis

methods, and intersection modeling scenarios are summarized. Moreover, traffic signal control methods based on deep reinforcement learning technologies are also introduced. A variety of suitable evaluation criteria for measuring intersection system performance and assessing possible impacts of the mixed traffic are examined and presented. These works could give a clear picture of the CAV technology and intelligent traffic signal control methods in the existing intersection capacity and performance studies considering the impacts of different MPRs of CAVs.

Chapter 3 presents the basic information for the identification of intersection and simulation scenarios. The basic settings for the intersection layouts, traffic signal schemes, and traffic demands are all introduced. Empirical methods are implemented to provide an initial traffic signal scheme and theoretical intersection capacity as a reference value. Scenarios with different traffic demands and MPRs of CAVs are also designed for further simulation.

Chapter 4 introduces the methodologies and parameter settings of the microscopic traffic simulation models used in this research. The car-following behaviors and settings of HDVs and CAVs are described in detail. Meanwhile, the potential scenarios for the isolated intersection are introduced.

Chapter 5 discusses the simulation results of the impact of CAVs on the intersection capacity under different scenarios. The intersection capacity is first analyzed by calculating adjustment factors for saturation headway and saturation traffic flow rate for each lane under different MPRs of CAVs. Then, the fitted curves and functions for the maximum throughput of the whole intersection under different MPRs of CAVs are calibrated and investigated. Also, this research investigates the effects of different control models of AVs and CAVs on the intersections with different signal control methods under different market penetration rates and traffic demands.

Chapter 6 proposes a transfer-based DRL traffic signal control (TSC) system framework. Then, different model settings will be modified and tested. The simulation results will explore the training efficiency and model performances of the transfer learning on the DRL TSC system. The impacts of CAVs on the traffic performance of the proposed DRL-based TSC system will be examined under different traffic demands and MPRs of CAVs.

Chapter 7 presents the basic settings for the proposed multi-agent DRL TSC system in a corridor with seven intersections. Considering the coordination between upstream and downstream intersections, the traffic performances of the basic multi-agent reinforcement learning (MARL) model and the MARL model with shared states will be investigated.

Chapter 8 concludes the dissertation by summarizing the proposed models and research results. Suggestions for future research directions are also provided.

```
┌─────────────────────────────┐
│   Chapter 1. Introduction   │
└─────────────────────────────┘
              │
              ▼
┌─────────────────────────────┐      ┌──────────────────────────────┐
│ Chapter 2: Literature Review│◄ ─ ─ │ Literature Review on Basic   │
└─────────────────────────────┘      │ Signal Control Strategy at   │
              │                       │ Intersections                │
              ▼                       └──────────────────────────────┘
┌─────────────────────────────┐
│ Chapter 3: Intersections    │◄ ─ ─ ┌──────────────────────────────┐
│ Scenarios Identification    │      │ Development of Traffic       │
└─────────────────────────────┘      │ Simulation Models            │
              │                       └──────────────────────────────┘
              ▼
┌─────────────────────────────┐      ┌──────────────────────────────┐
│ Chapter 4: Microscpic       │◄ ─ ─ │ Adjustment Factors for       │
│ Simulation Methodologies    │      │ Saturation Headway and       │
└─────────────────────────────┘      │ Saturation Traffic Flow Rate │
              │                       │ under different MPRs of CAVs  │
              ▼                       └──────────────────────────────┘
┌─────────────────────────────┐
│ Chapter 5: Impact of CAVs on│◄ ─ ─ ┌──────────────────────────────┐
│ Intersection Capacity       │      │ Literature Review on Deep    │
└─────────────────────────────┘      │ Reinforcement Learning       │
              │                       │ Controlled Traffic Signal    │
              ▼                       │ Systems                      │
┌─────────────────────────────┐      └──────────────────────────────┘
│ Chapter 6: Impacts of CAVs  │◄ ─ ─ ┌──────────────────────────────┐
│ on Deep Reinforcement       │      │ Development of Transfer-based│
│ Learning Controlled Systems │      │ Deep Reinforcement Learning  │
└─────────────────────────────┘      │ Controlled Signal Systems    │
              │                       └──────────────────────────────┘
              ▼
┌─────────────────────────────┐
│ Chapter 7: Multi-Agent Deep │
│ Reinforcement Learning      │
│ Controlled Traffic Signal   │
│ Systems                     │
└─────────────────────────────┘
              │
              ▼
┌─────────────────────────────┐
│ Chapter 8: Summary And      │
│ Conclusions                 │
└─────────────────────────────┘
```

Figure 1.1 Dissertation Structure

CHAPTER 2: LITERATURE REVIEW

2.1. Introduction

This chapter provides a comprehensive review of the current state-of-the-art and state-of-the-practice on CAV technologies and their impacts on intersection systems. This should give a clear picture of CAV technologies and intersection control strategies. The rest of this chapter is organized as follows. Section 2.2 presents concepts and taxonomy of CV, AV, and CAV technologies, followed by the descriptions of current technologies in use and benefits of CAVs. Section 2.3 shows existing deployments and market penetration rate prediction of CAVs. Section 2.4 introduces traffic flow control strategies for AVs and CAVs. Section 2.5 presents empirical and simulation-based intersection capacity analysis methods. A variety of suitable evaluation criteria for measuring intersection system performance and assessing possible impacts of the mixed flow of HDVs with CAVs are evaluated and presented. Section 2.6 presents recent studies that implemented deep reinforcement learning technologies in traffic signal controls. Section 2.7 describes several intersection modeling scenarios developed and specific parameters used when modeling CAVs. Finally, section 2.8 concludes this chapter with a summary.

2.2. Connected and Autonomous Vehicles Concepts and Potential Benefits

The term 'intelligent vehicles' refers to vehicles that are equipped with communication and/or autonomous driving technologies. This section gives the concepts, taxonomy, and potential benefits of the CV, AV, and CAV.

2.2.1. Connected Vehicles

2.2.1.1. Concepts of the Connected Vehicles

CVs are vehicles that are implemented with wireless communication technologies to facilitate vehicle-to-vehicle (V2V), vehicle-to-infrastructure (V2I), and vehicle-to-pedestrian (V2P) communication. Specifically, CV denotes the manual or autonomous vehicle which is capable of communicating with other vehicles/infrastructures/people to collect or transmit information on the driving environment to guide driver's maneuvers (Hendrickson et al., 2014). The V2V communication can transfer the state of the subject CV (e.g. speed, acceleration, and location) to surrounding CVs to implement applications such as hazard alerts, lane changing assistance, and rear-end/head-on collision avoidance. V2I communication can enable vehicles to obtain information from the infrastructure including signal stage, speed, volume, travel time, queue length, and stops. V2P communication allows vehicles to communicate with pedestrians' smartphones and provides warnings to avoid vehicle-to-pedestrian collisions especially for pedestrians in blind spots.

2.2.1.2. Potential Benefits of the Connected Vehicles

According to the National Highway Traffic Safety Administration (NHTSA), CV technologies have the potential to decrease about 80% of non-injury vehicle crashes (USDOT, 2020). By applying connected vehicle technologies, drivers can be notified in advance of the traffic information (such as vehicle's speed, location, gap to the front vehicle, and an accident occurred ahead), and possible collision with pedestrians or other vehicles. Such information aims to assist drivers to reduce travel time and avoid potential crashes that cannot be observed/predicted by the driver. Meanwhile, information for speed coordination and route re-planning enables CVs to improve mobility, safety, efficiency, and reduce air pollution.

As improving safety issues are the main objective of CVs, Table 2.1 summarizes the potential safety benefits and the maturity of CV technologies. Through V2V communication,

drivers could be alerted to potential causes of crash such as merging vehicles, vehicles in the driver's blind spot, and sudden brake of the front vehicle. Through V2I communication, drivers could be alerted of red lights, working/school/no-passing zones, and speed limit violations.

Table 2.1 Safety Benefits and Maturity of Connected Vehicle Technologies

Type	Technology	Safety Benefits	Safety Improvement	Maturity
V2I	Red light warning	Warning for red light	High	High
V2I	Stop gap assist	Warning for minimum stop gap	Medium	High
V2I	Reduce speed warning	Warning for speeding	Medium	High
V2I	Traffic Signal Coordination	More benefit for intersection capacity	Low	Medium
V2V	Lane Change Warning	Lane change information from CVs	High	High
V2V	Forward Collision Warning	Avoid Rear-End crashing	High	High
V2V	Electronic Emergency Brake Light	Avoid Rear-End crashing	High	High
V2V	Left Turn Assist	Opposite direction	High	Medium
V2V/V2I	Do Not Pass Warning	Opposite direction	High	High
V2V/V2I	Intersection Movement Assist	Junction crossing	High	Medium
V2V/V2I	Blind Spot Warning	Avoid traffic collision due to the blind spot	High	Medium
V2V/V2I	Emergency Vehicle Priority	Give priority to the emergency vehicle	High	High
V2X	Pedestrian Crossing Warning	Notification of pedestrian crossing the street	High	Low

2.2.2. Autonomous Vehicles

2.2.2.1. Taxonomy of Autonomous Vehicles

The basic concept of the AV refers to using intelligent technology to replace some or all of the human operations on driving electronic or mechanical vehicles (Shladover, 2018). Regarding the concept of automation, different taxonomies of the autonomous vehicle were

proposed. In 2013, the NHTSA proposed a 4-level category for the automation degree/level of the vehicle. Then, a 5-level automation degree category was introduced by the Society of Automotive Engineers International (SAE) in 2014 (SAE, 2016). In 2016, NHTSA adopted SAE's taxonomy for the automation levels of the autonomous vehicle, and now the 2016 SAE's taxonomy for the automation level of the autonomous vehicle has become commonly used as an industry standard (NHTSA, 2016).

Regarding the 2016 SAE's autonomous vehicle taxonomy, the increase of the automation level would correspondingly decrease the engagement of human labor required to monitor the driving environment and control the vehicle. From Level 0 to Level 5, the allocation of vehicle control function between the vehicle and the driver increases along the gradient: full driver control (Level 0), the vehicle assists/augments primary driver control (Level 1), the vehicle having at least one automated driver assistance system (Level 2), both the vehicle and driver control safety-critical functions (Level 3), fully-autonomous in certain driving scenarios (Level 4), and fully-autonomous in all driving scenarios (Level 5). Table 2.2 provides an outline of the five automation levels (including Level 0 which indicates no automation) (Kockelman and Boyles, 2018; NHTSA, 2016). According to the Federal Automated Vehicles Policy of the U.S. Department of Transportation, a vehicle is denoted as AV if it has levels 3-5 automated systems (NHTSA, 2016). Also, according to (Shladover, 2018), "autonomous" is not strictly limited to a specific level of autonomy and any level of autonomy could be defined as an autonomous vehicle, and this definition for the AV is adopted in this research.

Table 2.2 Outline of Five Automation Levels (NHTSA, 2016)

Level	Vehicle Controls	Environment Monitoring
L0	No automation. Drivers are **solely responsible** and control all vehicle functions (braking, steering, throttle, and motive power).	**Drivers take sole responsibility** for monitoring the roadway environment and traffic; some systems may provide **information or warnings** to the driver (such as traffic sign/signal information and collision warnings).
L1	Driver assistance. Drivers are **solely responsible**, but drivers are **assisted with primary vehicle controls** (either steering or acceleration /deceleration). Also, only one of the primary control systems is in work at any one time.	**Drivers take the solely responsible** for monitoring the environment. Also, the system provides **information and warnings** as with L0.
L2	Partial automation. Drivers **share the authority of primary controls** with the system and may be physically disengaged from operating the vehicles. The system may undertake steering and acceleration/deceleration function. Drivers can cede active primary control in certain situations and are expected to **take control on short notice**.	**Drivers are responsible** for monitoring the environment and are expected to be available for control at all times. **The system could obtain driving information** from the environment. Information and Warnings may still be provided to the driver.
L3	Conditional automation. Drivers can **cede the system control** of safety-critical functions and are expected to **take control under certain conditions** with sufficient transition time.	**The system could obtain driving information** from the environment. When ceding control and transiting back to driver control, drivers can rely heavily on the system to monitor environments.
L4	High automation. **The system undertakes all safety-critical driving functions** and monitors the driving environment in certain locations or scenarios. Drivers only need to provide destination or navigation input but are **not expected to take control** at any time during the trip.	The system will perform all the monitoring in certain driving scenarios.
L5	Full automation. **The system undertakes all safety-critical driving functions** and monitors the environment in all scenarios. Vehicles are **not** restricted by the locations and conditions they can travel to. Drivers only need to provide destination or navigation input but are **not expected to take control** at any time during the trip.	System could take the whole responsibility for the monitoring in all driving scenarios.

2.2.2.2. Potential Benefits of Autonomous Vehicles

Driving includes several functions, including perception, control, planning, localization, and management. Even with an automation level less than L3, the driving assistance system notices drivers with some traffic information that is critical for safety or some information that could not be obtained by the drivers themselves. The information from the sensor could help the drivers to adjust their driving strategies and avoid possible collisions or congestions.

Table 2.3 summarizes a total of 20 intelligent automation technologies on different automation levels and the corresponding safety benefits, safety improvements, and maturity of these technologies (Kockelman and Boyles, 2018). Presently, the technologies at Levels 1 and 2 are commercially available, while some of Levels 3 technologies are still being tested for commercial applications and are under development.

Table 2.3 Benefits and Maturity of Autonomous Vehicle Technologies

Automation Level	Technology	Safety Benefits	Safety Improvement	Maturity
Level 0	Adaptive headlights	Improve light condition and visibility of environment	Intermediate	High
	Forward collision warning	Prevent rear-end collision	High	High
	Blind spot monitoring	Reduce crash risk caused by blind spots (such as merging and weaving areas)	High	High
	Traffic sign recognition	Inform and alert the driver	Intermediate	Medium
	Lane departure warning	Prevent lane departure crashes	High	Medium
	Left-turn assist	Prevent potential conflict	High	Medium
	Pedestrian collision warning	Prevent pedestrian collision	High	Medium
	Rear cross traffic alert	Prevent backing collision	High	Medium
Level 1	Electronic stability control	Prevent rollover	High	High
	Adaptive cruise control	Prevent rear-end collision	High	High
	Cooperative adaptive cruise control	Prevent rear-end collision	Low	Medium
	Parental control	Prevent speeding	Intermediate	Medium
	Automatic emergency	Prevent rear-end collision	High	Medium

	braking			
	Lane keeping	Prevent lane departure crashes	High	Medium
Level 2	Traffic jam ass	Driving assist	Low	Medium
	High speed automation	Driving assist	High	Medium
	Automated assistance in roadwork and congestion	Driving assist	High	Medium
Level 3	On-highway platooning	Driving assist, prevent rear-end crashes	Intermediate	Medium
	Automated operation for military applications	Prevent human fatalities	Unknown	Low
Level 4/5	Self-driving vehicle	Replace human drivers	High	Low
	Emergency stopping assistant	Response when lose control human drivers	High	Low

2.2.3. Connected and Autonomous Vehicles

2.2.3.1. Concepts of the Connected and Autonomous Vehicle

If any AV has V2V, V2I, or V2X functions to collect and transmit information, it is defined as a connected and autonomous vehicle (Shladover, 2018). CV communication technologies permit widely, timely, standardized, and secure communication with unities equipped with communications equipment. The additional information collected could help CAVs to utilize the Cooperative Adaptive Cruise Control (CACC) system. For CAVs with the CACC system, they could follow their predecessors with a higher accuracy, shorter response time, and shorter headway compared to AVs with Adaptive Cruise Control (ACC) systems (Shladover et al., 2012). Therefore, CAV could be treated as the combination of the CV technologies and AV technologies, and CV technologies could supply, enhance, or have synergistic effects on AV technologies to some extent (Shladover, 2018), though connectivity is not a mandatory characteristic of AVs (Hendrickson et al., 2014).

2.2.3.2. Potential Benefits of Connected and Autonomous Vehicles

As the CAVs are the vehicles that are incorporated with both automation systems and communication systems, the potential benefits of CAVs combine the benefits of AVs and CVs. In summary, CAVs could bring several potential benefits including improvement of safety, efficiency, roadway/intersection capacity, mobility, and reduction in travel time and emissions.

As mentioned by Li and Kockelman (2016), CAVs may significantly reduce the number of crashes and decrease current crash costs in the U.S. by at least $126 billion per year. CAVs can also increase mobility by providing opportunities to people who cannot afford a vehicle, people who prefer not to drive, people with disabilities, and elderly people who cannot drive safely (Duncan et al., 2015). The communication and automation technologies also enable CAVs to drive more smoothly than human drivers, with smaller following gaps and harmonized speeds, and these will also reduce vehicle emissions by reducing the stop-and-go frequency. Also, with the help of the smart parking system, CAVs could get the information on nearby parking lots and park themselves automatically after arriving at the destination. This technology could save a significant amount of time for the passengers. Additionally, CAVs could save/rationalize land use and improve the infrastructure design by narrowing the width of the lanes and removing median barriers and even traffic lights in the future.

2.3.   Deployment of and Market Forecast for AVs

With the rapid development of vehicle automation and communication technologies, Level 1 and Level 2 automation systems have already been commercially implemented in intelligent vehicles for many years. Meanwhile, Level 3 conditional automation systems are still under development and are being tested in different experimental fields. Moreover, Level 4 AVs

(conditional automation vehicles) can reduce driver stress and increase productivity, and Level 5 AVs (fully automated vehicles) are expected to significantly improve the system performance.

2.3.1. Deployment of the Autonomous Vehicles

The vision of vehicle automation was initiated as early as 1918 (Pendleton et al., 2017). In 1939, General Motors exhibited the concept of AV, and the autonomous technology was mainly concentrated on controlling speed, break, lane change control, and other basic cruise control functions (Shladover et al., 2012). Even though there have been a lot of uncertainties as to the release date of the fully autonomous vehicle for the public, the Digital and 4th Industrial Revolutions gave a tremendous boost to rapid technological development in this field. All these intelligent technologies further promote several on-roads and experiment field tests for AVs with different autonomous technologies (Christie et al., 2016).

As early as the 1950s, General Motors and Radio Corporation of America Sarnoff Laboratory jointly initialized the early phase of research and development (R&D) of AV technologies (Shladover, 2018). From 1964 to 2003, several other AV programs were deployed and tested in different countries/areas, including the United States of America, European Union, Canada, United Kingdom, China, Japan, Australia, United Arab Emirates, Singapore, Korea, etc. (Bloomberg, 2017). Under the cooperation of government institutes, universities, and companies, several CAV related research projects were established, including the pilot of automated commercial taxi/bus, vehicle platooning, technologies of driving environment recognition, smart parking, and V2X communication (Shladover, 2018). In 2004, the US government accelerated the research and development of AV technology by the Defense Advanced Research Projects Agency's (DARPA) Grand Challenges Program. This program challenged AVs to traverse a desert area in 2005 and 2007. Researchers also managed to test the performance of AVs on open

urban roadways through the DARPA's Urban Challenge Program (Pendleton et al., 2017; Shladover, 2018). Since then, research and development have continued to rapidly evolve in both academia and industrial fields. Other projects are also under field trials concerning mixed traffic flow of AVs and HDVs, including Safe Road Trains for the Environment (SARTRE) and Europe's KONVOI system.

The automation technologies developed by institutes and universities have also been rapidly transferring into the commercial fields. Several commercial companies planned or started to investigate the technologies of AVs. Volvo announced the development of the autonomous vehicle technology in 2006 and tested its AV program, "Drive Me Pilot", in 2017. Volvo also planned to bring its unsupervised AV to the market around 2021. Tech giant Google also started to develop AVs in 2009. By 2017, Google's AV fleet, "WAYMO", completed three million miles of test driving in the U.S. In 2014, TESLA announced that its AV technology would be capable of self-driving about 90% of the travel time. At present, TESLA vehicles are equipped with a self-driving assistance system. By 2020, many other vehicle companies, including Audi, BMW, Mercedes-Benz, Ford, GM, Toyota, Volkswagen, and Nissan, developed their own commercial AVs (Faisal et al., 2019). Meanwhile, Level 2 AVs and some CV technologies are now available to the public. Many commercial intelligent vehicles have already been equipped with adaptive cruise control (ACC), collision avoidance and alert, parking assist systems, and lane departure warning systems (Fagnant and Kockelman, 2015).

As summarized in Bloomberg (2017), 36 cities around the world announced to host field tests for AVs, or planned to start piloting experiments in the near future. Meanwhile, 18 other cities are making long-range surveys of the planning, regulatory, law, and governance issues associated with the application of AVs. These piloting cities were undertaking a variety of AV

application tests. The testbed locations are generally isolated places or low population density areas of the city, such as isolated test sites, racing tracks, parks, campuses, renewal districts, highways, and former international mega-event sites. Hence, as mentioned in Bloomberg (2017), even though several trials were being undertaken, there still needs to be more tests to guide fully self-driving AVs in complex environments of the urban areas.

2.3.2. Market Forecast for Autonomous Vehicles

With the help of intelligent technologies from virtual identity and machine learning algorithms, some of Level 3 conditional automation technologies (such as platooning and traffic congestion assistance) have been implemented in field experiments and are under test for market implementation in the near future. According the report of (PTOLEMUS, 2017), it was indicated that Level 2 vehicles will comprise the largest portion of new sales during the next decade (2020 – 2030). Sales for Conditional automation Level 3 and High automation Level 4 vehicles were all expected to increase steadily in the next decade. And Level 4 vehicles with highly automated systems were expected to be available for the market around 2025.

However, since Level 3 AVs are still under testing for fully commercial application and the technology of full automation Level 5 is still under development phase, many researchers expect that the mixed flow of human driven vehicles (HDVs) and AVs will co-exist for a long period. Several previous studies also gave a prediction of the market penetration rate for autonomous vehicles in the next decades. Navigant Research (2016) estimated that 75% of all light-duty vehicles around the world (almost 100 million sales annually) will be equipped with automation assistance systems by 2035. In accordance with this timeline, Litman (2020) provided a prediction that AVs' beneficial impacts on safety and congestion are likely to appear between 2050 and 2080. Litman (2020) also expected that human driving may be restricted after

2060 as the randomness of human driving behaviors might result in disruptive effects on the automation systems. Moreover, as autonomous vehicles are relatively costly and rare in the early stage, benefits, such as reducing driver stress/operations and independent mobility, are more likely to be available for affluent users in the early stage. Hence, the AV sharing might be more applicable in the early stage when AVs are available for commercial adoption. Likewise, only when the price of AVs becomes affordable for common users, benefits of the affordable taxi, micro-transit services, and independent mobility could be available for moderate-income users.

Litman (2020) gave predictions of the sales, travel, and fleet projections of the AVs from 2030 to 2080. By 2050, with optimistic predictions, AVs are supposed to comprise 50% of all vehicle sales, 40% of all vehicle travel, and 30% of all vehicles. Meanwhile, the market penetration rates (MPRs) of the AVs are expected to be around 50% in 2060. TransAID, (2019) predicted the fleet penetration rates of different vehicle types (i.e., HDV, CV, AV, and CAV) from 2025 to 2060. In this report, the Level 4 technology is supposed to be feasible in 2035 and HDVs still will have 15% MPRs in 2060.

2.4. Traffic Flow Controls of CAVs

CAVs are automatically or partially controlled by the designed systems. These automation systems with fixed rule/logic make the movement behaviors of the CAVs different from manually controlled vehicles. The heterogeneous driving behaviors among different drivers would result in significant randomness in longitudinal movements (travel speed and acceleration/deceleration) of the vehicles. Also, the CAV controlled system would give a more rapid response to emergency circumstances (such as sudden braking of the front vehicle and dashing out of a pedestrian) than human drivers. The differences between CAVs and HDVs require specific models to describe the traveling behaviors of such intelligent vehicles. In the

simulation, the traveling behaviors of the CAVs could be divided into two parts, i.e., a car-following control model for longitudinal movements and a lane-changing control model for lateral movements.

2.4.1. Longitudinal Movement Control of CAVs

The main difference between HDVs and CAVs is the controller for the longitudinal movements (which mainly controls the travel speed), acceleration/deceleration, and car following gaps between vehicles. Also, the longitudinal movements of AVs significantly improve the efficiency of the roadway/intersection systems. Hence, this section mainly focuses on reviewing studies on the longitudinal movements of the CAVs.

The Lidar sensor technology allows AVs to obtain the surrounding environment information, especially on the distance and speed of front and current vehicles. In this case, AVs could adjust their speeds according to the down-stream traffic situations. Furthermore, with the communication technology (V2V, V2I, or V2X), the CAVs could communicate with one another to share their locations, speeds, and accelerations. Meanwhile, CAVs would change their travel behaviors according to the information received, such as a crash ahead and the status of intersection signals. The communication technology helps CAVs to connect and potentially form a platoon, and this cooperative traveling behavior could significantly improve the efficiency of the transportation system. All these traveling behaviors of CAVs are beyond the capability of the human drivers and make the car-following behaviors of intelligent vehicles (AVs and CAVs) different from the traditional car-following behaviors of normal HDVs.

The Intelligent Driver Model (IDM) and MICroscopic Model for Simulation of Intelligent Cruise Control (MIXIC) models are the two most often used benchmark car-following control models for AVs, and they have been implemented in many studies, which are shown in

Table 2.4. Several studies also modified these models to describe the longitudinal movements of intelligent vehicles. Meanwhile, the ACC System has been widely implemented in AVs. Thus, an ACC control model has been proposed and adopted in the simulation of AVs in several studies. Moreover, the CACC System has been widely utilized for CAVs. Hence, a specific CACC control model is proposed to describe the longitudinal movements of CAVs. The following section gives a more specific introduction of these four longitudinal movement control models for AVs and CAVS.

Table 2.4 Longitudinal Movement Control Model for AVs and CAVs

Methodology	Vehicles	Reference paper
Intelligent Driver Model (IDM)	AV, HDV, CV	Kesting et al., 2007, 2008; Milanés and Shladover, 2014; Talebpour and Mahmassani, 2016; Treiber et al., 2000
IDM with constant-acceleration heuristic	AV, HDV	Kesting et al., 2010
Cooperative IDM	AV, CV, HDV	Zhou et al., 2017
MICroscopic Model for Simulation of Intelligent Cruise Control (MIXIC)	CV, CAV	Deng, 2016; Talebpour and Mahmassani, 2016; van Arem et al., 1997; Van Arem et al., 2006
Adaptive Cruise Control (ACC)	AV	Milanés and Shladover, 2014; Porfyri et al., 2018; Treiber et al., 2000
Cooperative Adaptive Cruise Control (CACC)	CAV	Shladover et al., 2012

2.4.1.1. Cruise Control Modes

2.4.1.1.1 Intelligent Driver Model

IDM was first proposed by Treiber, Hennecke, and Helbing (2000), and it was commonly used in the simulations to control the acceleration and deceleration of HDVs and AVs based on the condition of the front vehicle in a single-lane situation (Treiber and Kesting, 2013). The IDM has a simple model structure and accident-free logic that can be used to describe the longitudinal

movement characteristics of the AVs with the ACC system. Also, the IDM does not include an explicit reaction time of the driver and it has a continuously differentiable acceleration/deceleration function (Treiber and Kesting, 2013). By modifying specific parameters according to specific cases, the IDM can be used for an AV with the ACC system or in a HDV situation.

2.4.1.1.2 Improved Intelligent Driver Model

In most situations, the IDM can provide plausible acceleration and deceleration rates. However, when the distance gap to the front vehicle is significantly lower than the desired distance gap, the IDM would result in an unrealistically high deceleration rate for the current vehicle to stop (Do et al., 2019). For HDVs, drivers would not suddenly brake/decelerate when the front vehicle is not suddenly decelerating to stop even if the distance gap is very small.

To mitigate this issue, Kesting et al. (2010) further combined the IDM with the Constant Acceleration Heuristics (CAH) to determine different acceleration/deceleration rates in different scenarios. The basic assumption of the CAH was that the front vehicle will not accelerate/decelerate suddenly in the following few seconds (Kesting et al., 2010). If the IDM produces an unrealistically high deceleration and the CAH deceleration is in a comfortable deceleration range, the AV with the ACC system would decelerate at a rate of the CAH deceleration minus the comfortable deceleration. In this way, the IDM controlled vehicle could avoid the unrealistic deceleration situation. Results showed that the road capacity is essentially improved, even with only a 50% MPR of IDM-CAH-controlled vehicles.

Additionally, several other modified IDMs were applied to simulate CAVs in different situations. To improve safety in non-stationary traffic situations, Derbel et al. (2012) modified the desired minimum gap between vehicles in the IDM. Zhou et al. (2017) developed a cooperative intelligent demand model (CIDM) using the IDM as the benchmark model and

examined the system performance of CAVs. The results showed that the increasing percentage of CAVs will reduce the total travel time and smooth traffic oscillations caused by the freeway merging or lane drop sections.

2.4.1.2. Cruise Control Systems

2.4.1.2.1 Microscopic Model for Simulation of Intelligent Cruise Control

The communication function helps the CAV with the CACC system to obtain the information on the surrounding vehicles and infrastructures. A car-following model specific to the CAV with the CACC system is needed. A stochastic simulation model, the MICroscopic Model for Simulation of Intelligent Cruise Control (MIXIC), was developed by Van Arem et al. (1997), and it has been widely used for cooperative CAV simulations. The MIXIC model is capable of characterizing the V2V communication process and can share speed, acceleration, and deceleration between the front and current CAVs. Moreover, in contrast to the IDM that only models a single lane, the MIXIC is capable to model two-, three-, and four-lane situations. This makes the adjusted traffic flow model controlled by the MIXIC more reliable and closer to the reality of CAVs with the CACC system.

The basic acceleration controller in the MIXIC model can be divided into two main parts: one is the acceleration controller part, which calculates the reference acceleration values, and another part is a vehicle model which transforms the reference acceleration values into actually realized acceleration values (Bart Van Arem et al., 2006). Therefore, the reference acceleration rate was determined by a controller and then transformed into a vehicle model for real actions. Van Arem et al. (2006) utilized the MIXIC to study the impact of CAVs with the CACC system in the highway-merging scenario from four to three lanes (lane drop scenario). The results showed that a low CACC system penetration rate ($< 40\%$) would decrease the average speed,

increase speed variances, and result in more shock waves before and after the merging area. Only when the CACC system penetration rate was over 60% would the CACC-equipped CAVs improve the stability and efficiency of the traffic flow in the merging area. Talebpour and Mahmassani (2016) employed the IDM and MIXIC to investigate the effects of CVs and CAVs on traffic flow stability and throughput. The results indicated that the increase of the market penetration rate of CAVs can improve the traffic flow stability and the throughput of roadways.

2.4.1.2.2 Adaptive Cruise Control System

With the development of the intelligent driving assistance system (IDAS), the intelligent vehicle could control or assist drivers with several driving tasks. An early stage of the IDAS is a cruise control (CC) system. The primary function of the CC-equipped vehicle is to maintain the desired speed set by a driver. After that, the CC system evolves towards ACC and CACC systems. These systems mainly control the acceleration/deceleration of AVs for longitudinal movements. The ACC system controls brake and throttle systems to change the travel speed and maintains a safe following gap based on a predefined speed and gap distance between preceding and current vehicles.

Numerous cruise control systems have been proposed for intelligent vehicles in previous studies. The IDM, ACC, and CACC are the three most commonly used cruise control models that control the longitudinal movements of intelligent vehicles (Milanés and Shladover, 2014; Porfyri et al., 2018; Treiber et al., 2000). The ACC system was proposed and dynamically controlled by four modes: cruising control, gap control, gap-closing control, and collision avoidance mode (Milanés and Shladover, 2014; Mintsis, 2018; Xiao et al., 2017).

Ioannou and Stefanovic (2005) found that the smoothly controlled speed of AVs with the ACC system would be beneficial to the environment. However, several studies also pointed out that the use of the ACC system was unlikely to change lane capacity significantly or even

decrease the performance of the transportation systems because of the unstable interaction between HDVs and AVs (Virdi et al., 2019; Yang et al., 2017). The disturbances among the traffic of AVs with the ACC system and HDVs were mainly caused by the high-acceleration maneuver, lane cutting-in, lane exiting, and sudden braking. Also, when a vehicle with the ACC system is following a HDV, it still needs a transfer time for the driver to take control of the vehicle for emergency circumstances. Hence, the safety distance gap between HDV and ACC vehicle is equal to or even larger than the gap between two HDVs.

2.4.1.2.3 Cooperative Adaptive Cruise Control System

The CACC system is a functional extension of the ACC system, and it enables cooperative platoon driving by sharing the acceleration, deceleration, and vehicle positions by V2V, V2I, or V2X communications. The additional information collected could help CAVs with a CACC system follow the front vehicle with a higher accuracy, shorter response time, and shorter distance gap compared to ACC vehicles (Shladover et al., 2012). The communication allows the CACC-system-equipped CAVs to have a significantly shorter time headway (i.e., 0.5 seconds) compared to the ACC (i.e., 1.4 seconds). The acceleration/deceleration of the subject CACC vehicle is controlled based on the gap distance and speed difference with respect to the preceding vehicle. In the simulation, the parameters that determine the longitudinal movements of CAVs with the CACC system are shared among the CACC-platooned vehicles. Also, CACC-platooned CAVs do not need to guarantee the minimum safety distance theoretically, but there still has to be a minimum safety distance and a collision-free function for CACC-platooned CAVs to protect cybersecurity and communication delay scenarios in the simulation.

Several studies investigated the impacts of the ACC/CACC system by using the microscopic traffic simulators. Arnaout and Arnaout (2014) found that the ACC-equipped vehicles would only have a slight impact on capacity. Delis et al. (2015) indicated that the CACC

system performs better than the ACC system with respect to both traffic stability and capacity. Amoozadeh et al. (2015) tested the impact of message falsification disturbances and radio jamming attacks on the acceleration and following distance of CACC vehicles. Results indicated that security attacks could reduce traffic safety and result in traffic flow instability and rear-end collisions.

Several studies also pointed out that a significant improvement in the system performance requires a certain market penetration rate (MPR) of the CACC-equipped vehicles. Arnaout and Arnaout (2014) utilized simulations to investigate the effects of the CACC on the traffic flow on a multilane highway. Results showed that low MPRs of CACC vehicles would have a slight impact on the traffic flow. Shladover et al. (2012) indicated that a 40% market penetration rate (MPR) of CACC-equipped vehicles is a critical threshold to achieve a 10% improvement of the capacity. Also, 100% MPR of CACC-equipped vehicles could double the capacity compared to the scenario with 100% MPR of HDVs.

Several studies also conducted field tests for the performance of the CACC system. Shladover et al. (2012) tested the performance of the ACC and CACC vehicles by collecting and analyzing the field experiments data. Results showed that increasing the market penetration rate (MPR) of ACC vehicles would slightly increase the roadway capacity. However, increasing CACC vehicles could significantly increase the roadway capacity. Milanes et al. (2014) conducted a field trial of four vehicles equipped with the CACC system to exchange information. The result indicated that the CACC system needs a lower response time to the speed change of the leading vehicle. Hence, the CACC system could improve traffic/string stability with cooperative speed adjustment and less following gaps. Another field trial of the CACC vehicles in the Connect and Drive project also suggested that vehicles with the CACC system could form

a platoon of vehicles with a 0.7 second headway. This could significantly improve the string stability of the traffic flow (Ploeg et al., 2011).

2.4.2. Latitudinal Movement Control of CAVs

A safe, smooth, and efficient lane changing behavior is essential to fulfil latitudinal movements of an AV. Several studies have also proposed a specific lane changing control model for AVs/CAVs. Nilsson et al. (2015) proposed a pragmatic model to determine a safe following gap and time interval to perform the lane changing maneuver. Field test results of the proposed model on a VOLVO V60 vehicle indicated a good performance of real-time ability, safety, and efficiency. Shi et al. (2019) proposed a hierarchical reinforcement learning approach for modeling the automated lane changing control process. The proposed approach could output the lane changing decision and maneuver with the consideration of safety. Results indicated that the AV could smoothly and safely change to the target lane. Wang et al. (2019) adopted a deep deterministic policy gradient reinforcement learning to control continuous lane changing behavior in dynamic driving situations. Simulation results showed the reinforcement learning agent vehicle could smoothly and stably change to the target lane under diverse driving environments.

2.5. Intersection Capacity Analysis Methods

2.5.1. Empirical Methods

Compared to the freeway system, traffic conditions in the intersection system are more complex as there have been many more conflict points and different types of transportation users (e.g., vehicles, cyclists, and pedestrians). To analyze the impact of CAVs at intersections, the capacity (or maximum throughput) of the intersection has been frequently utilized as a

performance indicator in many previous studies. In summary, there are two main ways to improve the throughput of the intersection: (1) Increasing the number of vehicles that crossed the intersection during a time unit; (2) Decreasing the average travel time for the vehicle to cross the intersection.

2.5.1.1. HCM's research work

Highway Capacity Manual (HCM, 2010) provided several empirically calibrated equations to calculate the capacity of conventional intersections considering different roadway, geometric, traffic, and control conditions. The capacity of the intersection could be modified by several adjustment factors. Also, the volume capacity ratio was implemented as a performance indicator for the intersection.

2.5.1.2. Brilon and Wu's research work

Brilon and Wu (2001) developed a conflict-based technique to calculate the capacity of the unsignalized intersection. The proposed method simplified the theoretical structure of the conventional gap acceptance method. Based on the calibrated parameters, the proposed method could measure traffic performance such as capacity, average delay, and queue length.

2.5.1.3. Dahl and Lee's research work

Dahl and Lee (2012) modified the gap acceptance method to estimate roundabout capacity by calibrating gap acceptance parameters for trucks and passenger vehicles separately. Results indicated that increasing the percentage of the trucks would decrease the capacity of the intersection, and the modified model could calculate the capacity more accurately than the unmodified model.

2.5.1.4. Abhishek et al.'s research work

Abhishek et al. (2019) improved the gap acceptance model to calculate unsignalized intersection capacity by incorporating driver impatience behaviors with merging behaviors. Also, the modified approach allowed different gap acceptance behaviors for different drivers or vehicles. Moreover, the modified model implemented a novel queueing model to calculate the mean service time, and hence, facilitating the calculation of minor road capacity for an unsignalized intersection.

In summary, the capacity/throughput has been measured and served as a key performance indicator for the intersections. Table 2.5 exhibits several empirical methods that were proposed to measure the capacity of intersections.

Table 2.5 Summaries of Empirical Methods on Intersection Capacity Analysis

No.	Reference	Intersection Type	Method	Capability of the Method
1	HCM, 2010	Signal/unsignalized Intersection, Roundabout	Empirical calibrated equations	• Considering different roadway, geometric, traffic, and control conditions
2	Brilon and Wu, 2001	Unsignalized Intersection	Conflict-based technique	• Simplifying the theoretical structure compared to gap acceptance method
3	Dahl and Lee, 2012	Roundabout	Modified gap acceptance method	• Calculating the capacity more accuracy than unmodified model
4	Abhishek et al., 2019	Unsignalized Intersection	Modified gap acceptance model	• Incorporating driver impatience behavior with merging behavior; • Allowing different gap acceptance behaviors; • Facilitating the calculation of minor road capacity for an unsignalized intersection

2.5.2. Simulation Based Methods

2.5.2.1. Impacts of CAVs under 100% Market Penetrate Rates

2.6.2.1.1 Li et al.'s research work

Li et al. (2014) jointly optimized signal timing and trajectories of the CAVs at an isolated intersection. Compared with a traditional actuated signal control scheme, the simulation results showed that the proposed control method could increase intersection throughput by 2.7–20.2% and reduce the average delay by 16.2–36.9% based on different traffic demands.

2.6.2.1.2 Abdelhameed et al.'s research work

Abdelhameed et al. (2015) utilized a hybrid fuzzy-genetic controller to minimize the travel time of CAVs while avoiding possible collisions at the intersection. Results indicated a 91% increase in throughput and about 62–72% decrease in delay compared to the pre-timed traffic light controller and the un-optimized fuzzy logic controller.

2.6.2.1.3 Chen and Kang's research work

Chen and Kang (2016) proposed a win-fit reservation management scheme for CAVs to cross an intersection without possible collisions. Results showed a reduction in trip delay by 31–95% compared with first-come-first-service and signal control schemes.

2.6.2.1.4 Liu et al.'s research work

Liu et al. (2018) developed a trajectory planning approach for autonomous intersection management (TP-AIM). The proposed system assigned priority and collision-free trajectories to CAVs. Results indicated a 20% increase in the throughput of the intersection. Moreover, a 10% reduction in delay could be observed compared to a traffic light controller.

2.6.2.1.5 He et al.'s research work

He et al. (2018) introduced a conflict-avoidance-based approach to coordinate CAVs at an unsignalized intersection with all-direction turn lanes. The simulation results indicated that the proposed approach outperformed traditional signal control by increasing 50% of the throughput and decreasing 60% of the travel time.

2.6.2.1.6 Wei et al.'s research work

Wei et al. (2018) proposed a game theory method to maximize throughput and minimize the accidents and congestion of the CAVs at the intersection. A platoon formation model and a strategic game theory model were proposed to control CAV movements at the intersection. Results showed that the proposed control method could increase the throughput by 140% and 43% in light and heavy traffic demand conditions, respectively.

2.6.2.1.7 Sun et al.'s research work

Sun et al. (2018) developed a MCross scheme to maximize intersection capacity with CAVs. Several simulation examples indicated that the proposed scheme could almost double the intersection capacity (i.e., by 99.51%) compared to a signal control scheme.

In summary, several studies designed an intersection control system that assumed 100% market penetration rate (MPR) of CAVs so that vehicles could obtain full information and be controlled by the system controller (Guo et al., 2019). Table 2.6 exhibits a summary of the studies on simulation-based intersection capacity analysis with 100% MPR of CAVs.

Table 2.6 Capacity Analysis Studies of CAVs under 100% Market Penetrate Rate

No.	Reference	Aim and method	Criteria	Main result
1	Li et al., 2014	Optimize signal timing and trajectories	Throughput, Delay	Increase intersection throughput by 2.7–20.2% compared with actuated signal control
2	Abdelhameed et al., 2015	Minimize the travel time of CAVs while avoiding possible collisions	Throughput, Delay	Increase throughput by 91% compared to the pre-timed traffic light controller and the un-optimized fuzzy logic controller
3	Chen and Kang, 2016	Conflict-avoidance-based approach to coordinate CAVs	Delay	Reduce trip delay by 31%-95% compared with FCFS and signal control schemes

4	Liu et al., 2018	Assign priority and collision-free trajectories to CAVs	Throughput, Delay	Increase throughput by 20% compared to signal control scheme.
5	He et al., 2018	Conflict-avoidance-based approach to coordinate CAVs	Throughput, Travel time	Increase throughput by 50% compared to signal control scheme
6	Wei et al., 2018	Game theoretic framework to maximize throughput and minimize the accidents and congestion of the CAVs	Throughput	Increase the throughput by 140% and 43% in light and heavy traffic demand conditions, respectively
7	Sun et al., 2018	MCross scheme to maximize intersection capacity	Throughput	Almost double the intersection capacity by 99.51% compared to signal control scheme

2.5.2.2. Impacts of CAVs under Mixed Traffic Environment

Several proposed intersection control systems required a modification of the existing intersection systems, and several of them required high market penetration rates (MPRs) of AVs or CVs (Algomaiah and Li, 2019; Dresner and Stone, 2008). However, reconstruction of those intersections or installing the V2I equipment would take a long time. Hence, it is reasonable to expect for a longer time for AVs to achieve high MPRs or be fully applicable in those intersection systems.

Additionally, several studies pointed out that a significant improvement in the system performance requires a certain MPR of the CAVs. Arnaout and Arnaout (2014) utilized simulations to investigate the effects of the CACC-equipped CAVs on the traffic flow on a multilane highway. Results showed that low MPRs of CACC-equipped CAVs would have a slight impact on the traffic flow.

2.6.2.2.1 Shladover et al.'s research work

Shladover et al. (2012) indicated that a 40% market penetration rate (MPR) of CACC-equipped vehicles is a critical threshold to achieve a 10% improvement of the roadway capacity.

Also, 100% MPR of CACC-equipped vehicles could double the capacity compared to the scenario of 100% MPR of HDVs.

2.6.2.2.2 Lee and Park's research work

Lee and Park (2012) proposed a cooperative vehicle intersection control system to remove signals while guaranteeing the safety of CVs. Simulation on a four-way single-lane approach intersection with the proposed system indicated that the throughput and total travel time were improved by 8% and 33% compared to an actuated signal control system.

2.6.2.2.3 Jiang et al.'s research work

Jiang et al., (2017) utilized an optimization method to control the speed of CAVs at an isolated intersection. Results indicated that benefits grow with the MPRs of CAVs until they level off at about a 40% MPR. Also, with a 60% MPR of CAVs, the throughput of the intersection would be improved by 7.06% and 10.80% under saturated flow rate (v/c = 1) and oversaturated flow rate (v/c = 1.2) conditions, respectively.

2.6.2.2.4 Sharon and Stone's research work

Sharon and Stone (2017) proposed a hybrid autonomous intersection management (H-AIM) system to accommodate mixed traffic conditions. H-AIM could identify approaching HDVs by sensor technologies. Compared to the basic AIM system, the H-AIM can improve the throughput and delay with only a 10% market penetration rate of CAVs. With a 50% MPR of CAVs, the H-AIM can increase the throughput of a four-way intersection and a three-way intersection by 10% and 6%, respectively.

2.6.2.2.5 Algomaiah and Li's research work

Algomaiah and Li (2019) proposed a first-come-first-serve reservation-based system at the intersection with different MPRs of CAVs. Simulation results indicated that the proposed control system outperforms traffic signals after a 75% MPR of CAVs. Additionally, the proposed

system would increase the throughput by 50% with a 100% MPR of CAVs compared to a signal control system.

In summary, simulation-based models were frequently utilized to evaluate the impacts of AV/CAV technologies on the intersection capacity/throughput. Table 2.7 summarizes previous capacity analysis studies on intelligent vehicles at intersections considering different MPRs. Additionally, Table 2.8 summarizes previous studies which utilized other performance criteria to evaluate impacts of intelligent vehicles at intersections considering different MPRs. The evaluation criteria for the performance of CAVs at the intersection mainly included efficiency (delay, travel time, speed, throughput, density, queuing length), safety (collision avoidance, resolving conflict), and ecology (energy/fuel consumption, emission).

Microscopic simulation software has been widely used in previous studies, such as VISSIM, SUMO, AIMSUN, which can be generally integrated with MATLAB and JAVA. It is noted that most studies indicated a positive effect of intelligent vehicles, while some others found that the intelligent vehicles could improve the system performance only after certain MPRs (Algomaiah and Li, 2019; Jiang et al., 2017; Lee et al., 2013). Moreover, several studies found that the interaction between intelligent vehicles with HDVs would result in a negative impact on system performance (Du et al., 2017). This is in line with the phenomenon that low MPRs of intelligent vehicles would decrease system performance (Virdi et al., 2019; Yang et al., 2017).

Table 2.7 Capacity Analysis Studies of CAVs under Mixed Traffic Environment

No.	Reference	Veh.	Object and method	Software	Criteria	Main result
1	Shladover et al. 2012	HDV, CV, AV, CAV	Simulation ACC and CACC based on field	AIMSUN	Capacity	• 40% market penetration rate (MPR) of CACC-equipped vehicles is a critical threshold to

			experiment data (for time gap settings) to estimate the effect on roadway capacity			achieve a 10% improvement of the capacity. • 100% MPR of CACC-equipped vehicles could double the capacity
2	Lee and Park, 2012	CV	Cooperative Vehicle Intersection Control	VISSIM	Through-put, Delay, Emission	• The throughput and total travel time were improved by 8% and 33% compared to actuated signal control system
3	Jiang et al., 2017	CAV	Optimizing speed of CAVs	VISSIM, Matlab	Fuel, CO2, Through-put	• Benefits grow with the MPRs of CAVs until they level off at about 40% MPR.
4	Sharon and Stone, 2017	CAV	Hybrid autonomous intersection management	SUMO	Queue length, Through-put	• H-AIM can decrease delays for AVs even at a 1% MPR. • With 50% MPR of CAVs, increase the throughput for four-way intersection and three-way intersection by 10% and 6%, respectively.
5	Algomaiah and Li, 2019	CAV	A first-come-first-serve reservation at intersection	VISSIM	Through-put, delay	• The proposed control system outperforms traffic signals after a 75% MPR of CAVs.

Table 2.8 Performance Measures of CAVs under Mixed Traffic Environment

No.	Reference	Veh.	Object and method	Software	Criteria	Main result
1	Lee et al., 2013	CV	Cumulative travel-time responsive (CTR) real-time intersection control	VISSIM, Matlab	Delay, speed	• The CTR algorithm improves the system performance after a 30% MPR of CVs. • CTR algorithm outperformed the actuated controls after a 70% MPR of CVs.
2	Guler et al., 2014	CV	Optimizing the departure sequences	Matlab	Delay	• CVs with MPRS from 0% up to 60% can significantly reduce the average delay. • The average delay could be significantly reduced even with low MPRs (20–40%).
3	Yang et al.,	CV,	Optimization	Java	Stops,	• This algorithm performs

	2016	AV	of departure sequence and trajectory by maximize the speed entering the intersection		Delay	• better than the actuated signal control after a 50% MPR of CVs. • Even a 50% information level for CVs could significantly decrease the delay and stops.
4	Yang et al., 2017	CAV	Eco-CACC system that computes the fuel-optimum vehicle trajectory	Integration	Fuel	• Eco-CACC system produces vehicle fuel savings up to 40% at a 100% MPR of CAVs. • Lower MPRs of CAVs increase fuel consumption on multi-lane roads, and the system decreases the fuel consumption only after a 30% MPR of CAVs.
5	Du et al., 2017	CV	Coordinate CVs at adjacent signalized intersections.	–	Fuel	• Increase the MPRs of CVs would decrease fuel consumption. • Fuel consumption will increase if the CV is following an HDV.
6	Pourmehrab et al., 2018	AV	Headway minimization	Matlab	Travel Time	• The average travel time decreases with higher MPRs of AVs.
7	Zhao et al., 2018	AV	Minimize the fuel consumption for platoons	Matlab	Fuel, Travel time	• Both fuel consumption and travel time decrease with the increasing MPRs of AVs. • The benefits of cooperation between AVs and HDVs are most evident for lower MPRs, and a platoon size of 5 can reduce 22% fuel consumption under a 60% MPR of AVs.
8	Liang et al., 2019	CV, AV, SGV	Jointly optimizing the signal phase and timing plan along with speed guidance	Java	Delay, stops	• The average delay and number of stops decrease with higher MPRs of CV, AVs, and SGVs (HDV with speed guidance-enabled vehicles). • The marginal benefits decrease rapidly when MPRs of the CVs exceed 40%.
9	Virdi et al., 2019	CAV	Safety assessment of mixed flow	VISSIM	Conflict	• CAVs at low penetration rates increase conflicts at signalized intersections while decrease conflicts at priority-controlled intersections.

2.6.   Reinforcement Learning for Intersection Signal Control

Optimizing traffic signal control with a reinforcement learning method has received great attention in previous studies (Haydari & Yilmaz, 2020; X. Liang et al., 2019; Vidali, 2018). The TSC agent is trained to learn an optimal policy for developing the signal phase and timing plan based on the information gathered from the traffic environment. With regards to the number of RL agents, these studies could be classified into centralized TSC with a single agent RL (for an isolated intersection or the entire intersection network) or decentralized TSC with multi-agent RL (for a network of intersections). The state of vehicles (numbers, locations, speeds, or other traffic performance criteria) is usually presented by image-like representation format (i.e., discrete traffic state encoding) or feature-based state vectors (Haydari & Yilmaz, 2020). The actions are commonly defined as binary action sets (whether or not to prolong the green time) or multi-phase sets (usually four or eight green phases). Due to the large scale of the state and action representation, many recent TSC studies employed deep learning (neural networks) to approximate Q-values, which are returns for taking an action *A* at a state *S* (Zhang et al., 2021). Based on the target estimated by the deep learning, the deep reinforcement learning (DRL) could be classified into value-based (estimating Q value), policy-based (estimating action policy probability), and state-value-based method (estimating both Q value and action policy probability, such as actor-critic (A2C) framework).

Table 2.9 summarizes several deep reinforcement learning studies for traffic signal control systems. One of the earliest neural-network-based RL models for TSC was proposed in (Arel et al., 2010). However, it was different from the typical deep Q network (DQN) algorithm as it did not include experience replay method and the target network. After that, Genders and Razavi (2016) implemented a convolutional neural network (CNN) to approximate the Q values

for a single intersection with four green phases. The simulation in SUMO showed a better result compared to that using a single-layer neural network Q-learning approach. Wei et al. (2018) introduced a DQN-based TSC, called IntelliLight, and utilized CNN to extract traffic features from the real-world camera data collected in China. The IntelliLight was also selected as a benchmark in another research work (Xu et al., 2019). This research introduced a transfer learning framework with source task selection and batch learning. Results based on the real-world data from China indicated a quicker model convergence and better traffic performance compared to non-transfer models. Shi and Chen (2018) also utilized transfer learning to speed up the training procedure of multi-agent DRL TSC with long short-term memory (LSTM) layers (a type of recurrent neural network, RNN) for Q-value approximation. The results on 2-by-2 grids of intersections indicated a lower average delay compared to Q-learning and pre-timed signal under both low and high traffic demands. Moreover, Zhang et al. (2021) trained a DQN for TSC with a partial detection of vehicles. Results indicated that the DQN-controlled TSC could efficiently reduce the average waiting time even with a low detection rate.

Table 2.9 Summary of Deep Reinforcement Learning Studies on Traffic Signal Control

Paper	Scenario	Approach	Simulator	Result comparison
(S. Shi & Chen, 2018)	2 by 2 grid of intersections	Transfer DQN-RNN, multi-agent,	USTCMTS	Fixed-timed signal, Q-learning
(Xu et al., 2019)	Single intersection, real data	Targeted Transfer DQN, CNN and LSTM, single-agent	SUMO	IntelliLight
(Zhang et al., 2021)	Single intersection	DQN, single-agent	SUMO	Fixed-time signal
(X. Liang et al., 2019)	Single intersection	Double dueling DQN-CNN, single-agent	SUMO	Fixed-time signal, actuated signal, DQN
(Genders & Razavi,	Single intersection	DQN-CNN, single-agent	SUMO	Q-learning with a shallow neural

Paper	Scenario	Approach	Simulator	Result comparison
2016)				network
(Hua Wei et al., 2018)	Single intersection, real data	DQN-CNN (IntelliLight), single-agent	SUMO	Fixed-time signal, Self-organizing TSC, DQN
(Wan & Hwang, 2018)	Single intersection	Modified DQN, single-agent	VISSIM	Fixed-time signal, standard DQN
(Genders & Razavi, 2019)	Single intersection	Asynchronous n-step Q-learning, single-agent	SUMO	actuated signal, random control
(Chu et al., 2020)	5 by 5 grid of Monaco city map	A2C-RNN, Multi-agent	SUMO	Q-learning, DQN, A2C

2.7.   **Intersection Modeling Scenarios and Parameters**

Jiang et al. (2017) utilized an optimization method to control the speed of CAVs at an isolated single-lane intersection. With a 60% MPR of the CAVs, simulation results indicated that the intersection throughput would be improved by 7.06% and 10.80% under saturated flow (v/c = 1) and oversaturated flow (v/c = 1.2) conditions, respectively.

Sharon and Stone (2017) proposed a hybrid autonomous intersection management (H-AIM) system. The performance of the system was tested by the simulations at a four-way intersection and a three-way intersection. Compared to the basic AIM system, the H-AIM can improve throughput and delay with only a 10% MPR of CAVs. With 50% MPR of CAVs, the H-AIM can increase the throughput for four-way intersection and three-way intersection by 10% and 6%, respectively.

Yang et al. (2017) proposed an eco-CACC system to compute optimal fuel consumption trajectories for CACC-equipped CAVs. When vehicles were traveling at signalized single-lane and multi-lane intersections, the increase of MPRs of CACC vehicles would decrease fuel consumption and air pollution correspondingly. The proposed system could save about 40% of

the fuel consumption with a 100% market penetration rate of eco-CACC vehicles. Moreover, when vehicles were traveling at a multi-lane intersection, the proposed system would increase fuel consumption if the MPRs of eco-CACC vehicles are over 30%.

Sun et al. (2018) developed an intelligent intersection system with continuous flow design and tandem control to maximize the intersection capacity with CAVs. Numerical examples for unbalanced flow, heavy left-turn traffic, heavy conflicting movements, and all demands flow cases were tested. Simulation results indicated that the proposed scheme could almost double the intersection capacity compared to a signal control scheme.

He et al. (2018) introduced a conflict-avoidance-based approach to coordinate CAVs at an unsignalized intersection with all-direction turn lanes. The traffic demands per lane were increased from 100 to 1000 veh/hr. The simulation results indicated that the proposed approach outperformed traditional traffic lights by increasing 50% of the throughput and decreasing 60% of the travel time.

Algomaiah and Li, (2019) proposed a first-come-first-served reservation-based system at the intersection considering different MPRs of CAVs. The geometrical designs of the intersection included different combinations of dedicated and shared lanes. Traffic demands from 400 to 1000 vehicles/hour/lane and three communication ranges (600, 800, 1000 ft) were tested in simulations. Throughput and delay results indicated that the proposed control system outperformed a traffic signal scheme after a 75% MPR of CAVs.

In summary, Table 2.10 exhibits several intersection modeling scenarios using simulation methods to analyze the impacts of CAVs. Note that the following parameters were used in the simulation models for CAVs with the CACC system (Milanés & Shladover, 2014; Mintsis, 2018; Xiao et al., 2017).

- Minimum gap when the vehicle is stopped (m)

- Maximum acceleration (m/s^2)

- Maximum deceleration (m/s^2)

- The maximum deceleration in case of emergency (m/s^2)

- Desired headway (s), Speed control factor, and Reaction time (s)

- The driver imperfection [0, 1]

- The control gain determining the rate of speed deviation (for Speed control mode)

- The control gain determining the rate of positioning deviation (for Gap closing control mode, Gap control mode, and Collision avoidance mode, respectively)

- The control gain determining the rate of the positioning deviation derivative (for Gap closing control mode, Gap control mode, and Collision avoidance mode, respectively)

Table 2.10 Summary of Intersection Modeling Scenarios with CAVs

No.	Reference	Intersection Type	Scenarios	Findings
1	Jiang et al., 2017	Single lane signalized intersection	Mixed flow; Traffic demands: non-saturated (v/c = 0.5), saturated (v/c = 1), oversaturated (v/c = 1.2)	• Increase the throughput by 7.06% and 10.80% with 60% MPR of CAVs under saturated (v/c = 1) and oversaturated (v/c = 1.2) conditions, respectively
2	Sharon and Stone, 2017	A four-way intersection and a three-way intersection	Mixed flow; Traffic demands from low to high (150 - 750 vehicles/hour/lane)	• With 50% MPR of CAVs, the H-AIM can increase the throughput for four-way intersection and three-way intersection by 10% and 6%, respectively.
3	Yang et al., 2017	Single lane and multilane signalized intersections	Mixed flow	• Increase the fuel consumption if the MPR of eco-CACC vehicles are over 30%
4	Sun et al., 2018	An intersection with continuous flow design and tandem control	Unbalanced flow, heavy left-turn traffic, heavy conflicting movements, all demands flow cases	• Increase intersection capacity by 99.51% compared to signal control
5	He et al., 2018	Unsignalized intersection with all-direction turn lanes	Increase traffic demands from 100 – 1000 (vehicles/hour/lane)	• Increase 50% of the throughput compared to signal control scheme

| 6 | Algomaiah and Li, 2019 | Next-generation interchange with different combinations of dedicated and shared lanes | Mixed flow; Communication range (600, 800, 1000 ft); Traffic demands from 400 to 1000 vehicles/hour/lane | • Increase about 50% of the throughput with 100% MPR of CAVs compared to signal control scheme;
• 800 ft communication range shows a relatively lower delay |

2.8. Summary

This chapter provides a comprehensive review of the current state-of-the-art and state-of-the-practice on studies related to the connected vehicles, automated vehicles, and connected and autonomous vehicles. Deployment and market penetration rate prediction, traffic flow control strategy for CAVs, intersection capacity analysis methods (empirical-based and simulation-based methods), deep reinforcement learning controlled signal system, and intersection modeling scenarios and parameters of CAVs are all introduced and reviewed. This chapter is intended to provide a fundamental and solid reference to develop control strategies for CAVs at the intersection, and conduct effective simulations and impact analyses in future tasks.

CHAPTER 3: IDENTIFICATION OF INTERSECTIONS AND SCENARIOS

3.1.   Introduction

This chapter will identify potential intersection scenarios and collect necessary data related to selected intersections. Based on the literature review part, a hypothetical isolated four-way intersection will be developed, used and tested as a basic scenario. The intersection layout, pre-timed signal schemes, and potential traffic demands are determined. An empirical method for intersection capacity calculation is introduced and implemented. Specific scenarios considering different traffic demands and MPRs of CAVs are given. The following sections are organized as follows. Section 3.2 presents the information on a hypothetical isolated four-way intersection. Section 3.3 introduces empirical methods for intersection capacity calculation. Section 3.4 calculates an initial pre-timed signal scheme and capacity for the intersection. Finally, section 3.5 concludes this chapter with a summary.

3.2.   Typical Isolated Intersection Scenario

In this chapter, a hypothetical isolated four-way intersection (cross-intersection) is proposed and used to set up a basic scenario for the simulation. This intersection will also be tested with different market penetration rates (MPRs) of CAVs. The results of these scenarios will be further tested in real-world intersections. This isolated intersection is introduced in this section.

3.2.1. Intersection Layout

As shown in Figure 3.1, the isolated intersection has four two-way approaches. The angle of the intersection is vertical. Also, the entrance and exit of each approach have four lanes. Each

entrance (or inlet) has one lane for left-turn-only traffic, one lane for through-only traffic, and one lane for though and right-turn traffic.
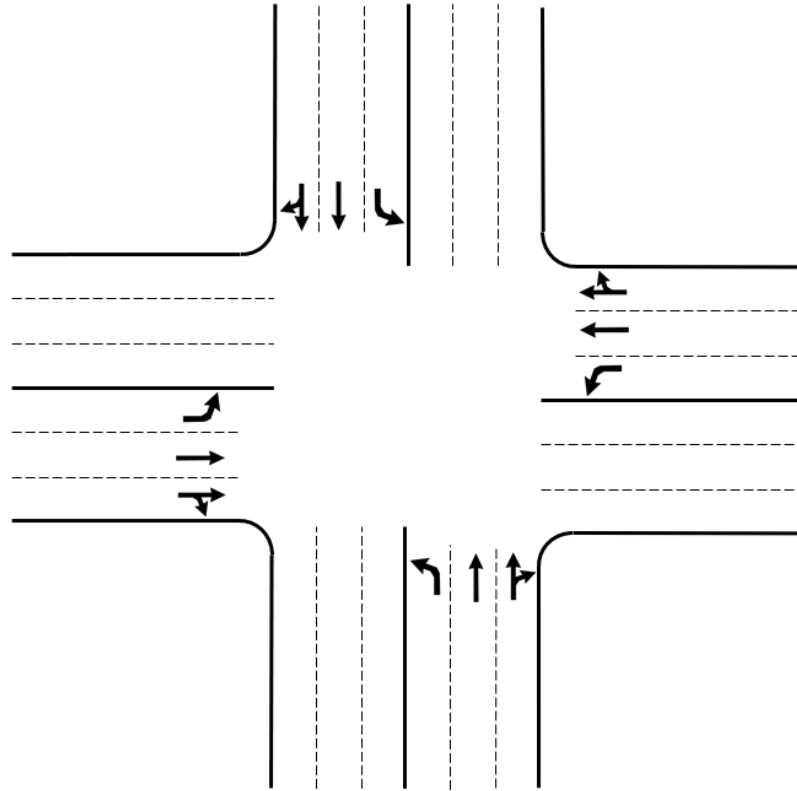
Figure 3.1 Layout of the Hypothetical Isolated Four-Way Intersection

3.2.2. Pre-timed Signal Schemes

Pre-timed signal control is a type of control where the signal cycle length, phase durations, and phase sequences are predetermined and fixed. A pre-timed signal scheme is utilized in the hypothetical isolated intersection. The capacity of the intersection could be calculated based on the Highway Capacity Manual (HCM, 2010). The maximum throughput could also be determined by the simulation method. As shown in Figure 3.2, eight potential signal phases are usually selected to accommodate different traffic volume scenarios.
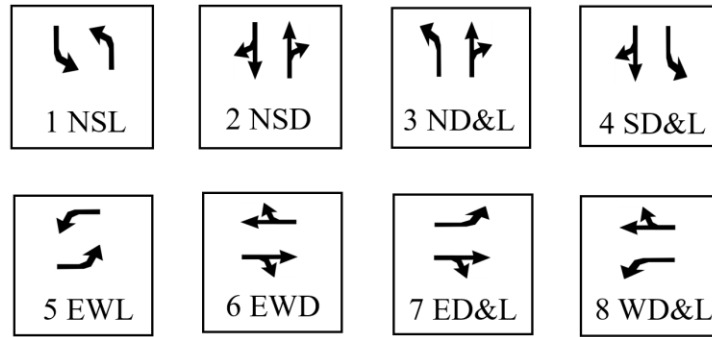
Figure 3.2 Potential Signal Phase of the Intersection

3.2.3. Potential Traffic Demands

For hypothetical isolated four-way intersection scenarios, different traffic demands for each direction will be considered. Under a specific pre-timed signal scheme, the capacity of the intersection is calculated based on the empirical method introduced by the Highway Capacity Manual (HCM, 2010). Then the maximum throughput is calculated with 100% HDVs based on the simulation method. Moreover, to investigate the impact of CAVs on the traffic flow, different MPRs of CAVs will be considered during the simulation (increase from 0% to 100% by 25% per step). Then the maximum throughput under different MPRs of CAVs will be recalculated by the simulation method. Following are the steps to determine potential traffic demands for the hypothetical isolated intersection.

- Calculate the capacity with a pre-timed signal scheme by the empirical method.

- Calculate the maximum throughput of the intersection by the simulation method.

- Determine the traffic demands based on the maximum throughput.

- Determine the volume of the CAVs based on the market penetration rate of the CAVs.

3.3. Empirical Method for Intersection Capacity Analysis

3.3.1. Quick-Estimation Method

The empirical method for intersection capacity calculation is based on the first five-step of the Quick-Estimation Method (QEM) that was introduced in the 2010 Highway Capacity Manual (HCM). The HCM defines capacity as the maximum number of vehicles that can pass through the intersection under certain traffic, roadway, and signalization conditions during a 15-min period. The QEM determines the critical movements based on the signal phases and calculates the critical phase volumes. Then the intersection capacity is calculated based on the maximum traffic volume that the intersection could accommodate in an hour. In general, Figure 3.3 provides the first five-step of the QEM.

- Step 1: Identify intersection traffic movements, number of lanes, and calculate hourly traffic volumes per lane. Usually, the hourly traffic volumes are modified to represent the peak 15-minute period.

- Step 2: Design a signal phasing plan and determine the traffic movements in each phase. Each phase usually accommodates two nonconflicting movements. The treatment (protected, permitted, etc.) of each left-turn movement is determined mainly based on the left-turn volume and the opposing through traffic volume.

- Step 3: Determine the critical volume per lane group that must be accommodated for each phase. The lane group is divided by the traffic movements in each phase. For example, the exclusive left-turn lane with a protected left-turn phase is usually designated as a specific lane group. The critical movement volume determines the amount of green time that should be assigned to the phase in one signal cycle.

- Step 4: Sum the critical phase volumes per phase to determine the overall critical volume that the intersection needs to accommodate.

- Step 5: Calculate the overall intersection capacity by determining the maximum critical volume that the intersection can accommodate per cycle. The maximum critical volume is determined by the saturated traffic flow. For signal lane cross-intersection, the HCM QEM recommended 1,710 vph for most purposes.
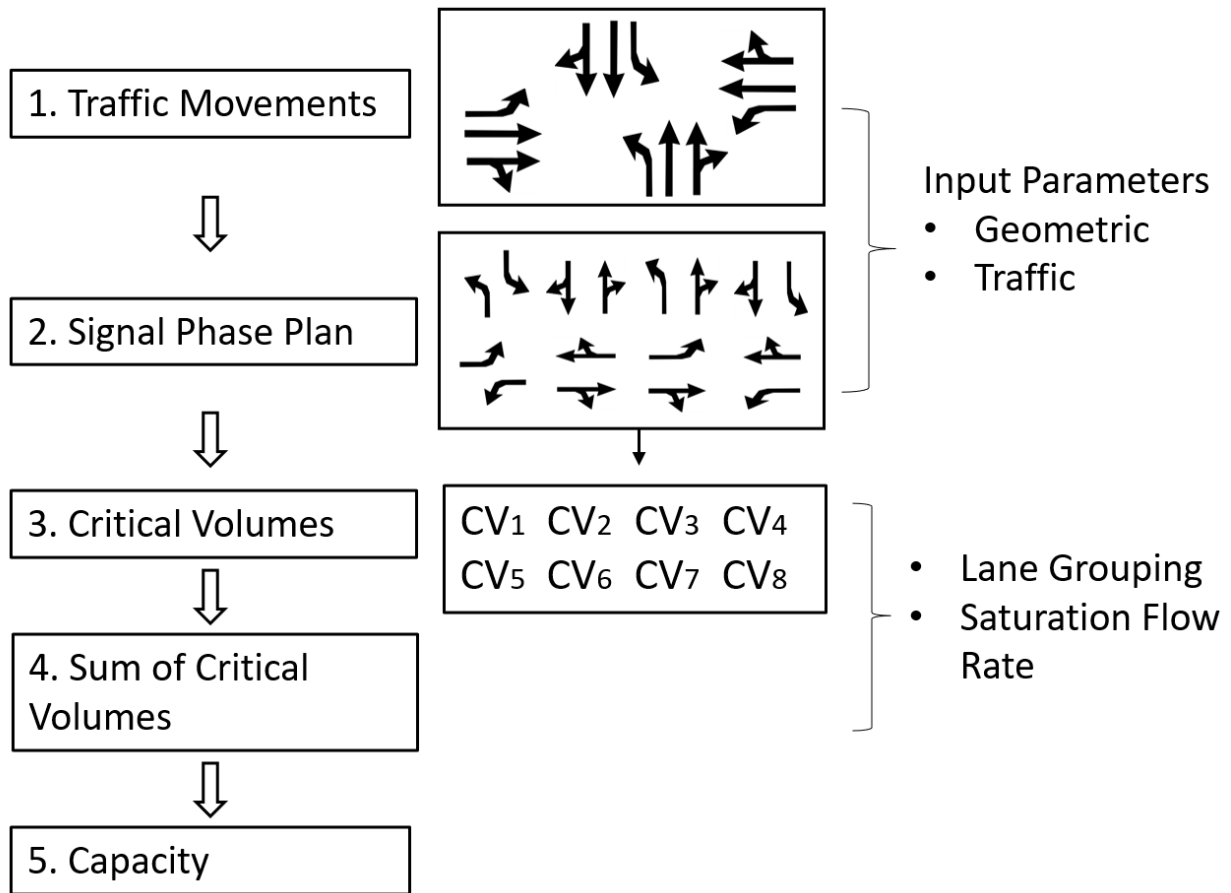
Figure 3.3 Illustration of the Quick Estimation Method Framework for Capacity Estimation

3.3.2. Intersection Capacity Calculation

To determine the capacity of the intersection, the saturation flow of the lane group in each phase should be firstly calculated. The saturation flow s_o of a lane is the maximum traffic that the lane could accommodate per hour,

$$s_o = \frac{3600}{h} \tag{3.1}$$

where, h denotes the average headway of the traffic, s.

HCM 2010 usually recommended a base saturation flow rate, i.e., 1,900 passenger cars per hour per lane (pc/hr/ln). The saturation flow rate of the lane group capacity is usually adjusted for a variety of conditions,

$$s = s_o N f_w f_{HV} f_g f_p f_{bb} f_a f_{LU} f_{LT} f_{RT} f_{Lpb} f_{Rpb} \tag{3.2}$$

where s is the saturation flow rate (or Capacity) of the lane group, veh/hr. s_o indicates the base saturation flow rate per lane, pc/h/ln. N denotes the number of lanes in the lane group.

For each lane group at a signal intersection, the lane group capacity is computed as the product of adjusted saturation flow rate and effective green time per cycle ratio. Then the signal intersection capacity is expressed as an hourly rate, with units of vehicles per hour. The capacity of the signal intersection is the sum of the lane group capacity,

$$c = \sum_i s_i \frac{g_i}{c} \tag{3.3}$$

where c indicates the capacity of the signal intersection. s_i expressed the saturation flow rate for all lanes in lane group i. g_i/c is the effective green time per cycle ratio for lane group i.

The intersection signal phase must be timed to accommodate the most intense traffic movements. An initial pre-timed signal plan could be calculated as follows.

- Step1 Develop a basic phase plan.

- Step 2: Convert all traffic volumes to through vehicle equivalents.

- Step 3 Determine critical lane volumes.

- Step 4 Determine Yellow and All-Red Intervals.

- Step 5 Determine lost time.

- Step 7 Allocate effective green time to each phase.

First, the maximum sum of critical lane volumes V_C is given as,

$$V_C = \frac{1}{h}\left[3{,}600 - Nt_L\left(\frac{3{,}600}{C}\right)\right] \tag{3.4}$$

where N indicates the number of phases. t_L is the total time loss in one phase. C is the cycle length.

For the total lost time per phase,

$$t_L = l_1 + l_2 \tag{3.5}$$

where l_1 denotes the start-up lost time, i.e., additional time for each initial headway. l_2 indicates the clearance lost time, i.e., the time between the front wheel of the last pass vehicle that crosses the stop line and the start of green for the next phase. The recommended value for t_L is 4 s.

Meanwhile, the effective green time g_i, i.e., the amount of time that vehicles can move in one phase, is given as,

$$g_i = G_i + Y_i - t_{Li} \tag{3.6}$$

where G_i denotes the actual green time for movements i. Y_i is the sum of yellow and all red time for movements i, $Y_i = y_i + ar$, y_i is yellow time, ar is all-red time. t_{Li} indicates the total lost time for movements i.

The allocation of the effective green time G_i to each phase is based on the critical volume to the maximum sum of critical volume ratios,

$$G_i = (C - Nt_L)\frac{CV_i}{V_C} \tag{3.7}$$

where C is the cycle length. N is the total number of the phase. t_L is the total time loss per phase. CV_i is the critical volume for phase i. V_C is the sum of critical volume in one signal cycle.

3.4. Intersections Identification

A hypothetical isolated four-way intersection is selected as a basic scenario. An initial pre-timed signal scheme is calculated for this typical intersection. Meanwhile, this typical

intersection is tested with different traffic demands and market penetration rates (MPRs) of CAVs. Later, two types of real-world intersections in North Carolina, including one isolated intersection and two adjacent intersections, will also be tested to analyze the impacts of CAVs on the intersection system performance.

3.4.1. Scenarios for Typical Isolated Intersection

3.4.1.1. Pre-timed Signal Schemes and Capacity for the Intersection

According to the methods introduced in the Empirical Method section, an initial signal scheme and the corresponding intersection capacity could be determined. The following basic settings for the hypothetical isolated intersection are made as follows:

1. The intersection has four approaches, and each approach (or inlet) has one lane for left-turn-only traffic, one lane for through-only traffic, and one lane for though and right-turn traffic.

2. The pre-timed signal scheme is implemented. The cycle length is 100 s.

3. The traffic demands for left-turn and right-turn movements are both set as 15% of the direct traffic demands. The traffic demands are the same in each approach.

Step1. Develop a phase plan:

For this intersection, a protected left-turn phase will be used for all left-turn movements. The four phases signal scheme is set as: North-South direct movements, North-South left-turn movements, East-West direct movements, and East-West left-turn movements.

Step 2. Convert volumes to through vehicle equivalents (TVU):

The saturation flow ratio is unknown for this hypothetical intersection. According to assumption 3, the hourly through traffic demand is assumed as X. Then the left- and right-turn traffic demands are both 0.15X. The equivalent movement factor for left- and right-turn traffic is

1.05 and 1.32. Table 3.1 shows the detailed through vehicle equivalents in the East Boundary approach.

Table 3.1 Assumed Through Vehicle Equivalents in the East Boundary

Approach	Movement	Volume (Veh/h)	Equivalent	Volume (TVU/h)	Lane group volume (TVU/h)	# of lanes	Volume/lane (TVU/h/ln)
EB	L	0.15X	1.05	0.1575X	0.1575X	1	0.1575X
	T	X	1	X	1.198X	2	1.198X/2= 0.599 X
	R	0.15X	1.32	0.198X			

Step 3. Determine critical lane volumes:

According to the step 1, a typical four phase scheme is given. The critical volumes for each phase are presented in Table 3.2. The maximum sum of critical lane volumes V_C is obtained as:

$$Vc = (0.1575 + 0.599) \cdot 2X = 1.513X$$

Table 3.2 Critical Lane Volume in Each Phase

Phase stage	Ring 1		Ring 2		Critical volumes
Phase A1	EB-T&R	0.599X	WB-T&R	0.599X	0.599X
Phase A2	EB-L	0.1575X	WB-L	0.1575X	0.1575X
Phase B1	SB-T&R	0.599X	NB-T&R	0.599X	0.599X
Phase B2	SB-L	0.1575X	NB-L	0.1575X	0.1575X

Step 4. Determine Yellow and All-Red Intervals and lost time:

The default timing of yellow (change) and all red (clearance) interval for each phase:

$$y_{EW} = 3s$$

$$ar_{EW} = 1s$$

Because $l_1 = e = 2$, the lost time per phase is given as:

$$t_L = l_1 + (y + ar - e) = y + ar = Y = 4 \ s$$

Step 5. Obtain the traffic demands:

With the loss time and given phase schemes, the maximum sum of critical lane volumes V_C could be calculated as:

$$V_C = \frac{1}{h}\left[3{,}600 - Nt_L\left(\frac{3{,}600}{C}\right)\right] = \frac{1}{1.9}\left[3{,}600 - 4 \times 4\left(\frac{3{,}600}{100}\right)\right] = 1592 \text{ veh/hr}$$

Hence, the traffic demand for direct movements X is:

$$X = 1592/1.513 = 1052$$

The detailed traffic demand for each direction is shown in Table 3.3. The sum of traffic demand in each approach is given as:

$$Sum\ of\ traffic\ demand\ =\ (158 + 1052 + 158) \times 4 = 5472 \text{ veh/hr}$$

Table 3.3 Calculated Through Vehicle Equivalents in the East Boundary

Approach	Movement	Volume (Veh/h)	Equivalent	Volume (TVU/h)	Lane group volume (TVU/h)	# of lanes	Volume/lane (TVU/h/ln)
EB	L	158	1.05	166	166	1	166
	T	1052	1	1052	1260	2	630
	R	158	1.32	208			

Step 6. Allocate effective green time to each phase:

Based on the through vehicle equivalents for each lane group, the total effective green time g_i and specific green time for each phase are given as:

$$g_i = G_i + Y_i - t_{Li} = 100 - 4 * 4 = 84\ s$$

$$G_{pA1} = G_{pB1} = (C - Nt_L)\frac{CV_i}{V_C} = 84 * \frac{630}{1592} = 33\ s$$

$$G_{pA2} = G_{pB2} = (C - Nt_L)\frac{CV_i}{V_C} = 84 * \frac{166}{1592} = 9s$$

3.4.1.2. Intersection Capacity Based on Empirical Method

The intersection capacity could be calculated by summing the capacity of all lane groups. To obtain the lane group capacity, the basic lane capacity is calculated. For the HDVs, the headway is set as 1.9 s. the basic saturation flow rate per lane:

$$s_0 = \frac{3600}{1.9} = 1895 \quad veh/hr/lane$$

This basic saturation flow rate is adjusted for different conditions. The adjustment factors for left-turn movements with exclusive lane is $f_{LT} = 0.95$. Meanwhile, the right-turn movement with shared lane is given as $f_{RT} = 1.0 - (0.15)P_{RT} = 1 - 0.15 \times 0.15 = 0.9775$.

The exclusive left-turn lane capacity:

$$c_{left} = s_i \frac{g_i}{C} = 1895 \times 0.95 \times 9/100 = 1625 \text{ pcu/hr}$$

The direct traffic only lane capacity:

$$c_{direct} = s_i \frac{g_i}{C} = 1895 \times 33/100 = 625 \text{ pcu/hr}$$

The direct and right traffic (i.e., shared right) lane capacity:

$$c_{sharedRight} = s_i \frac{g_i}{C} = 1895 \times 0.9775 \times 33/100 = 611 \text{ pcu/hr}$$

The total capacity of the intersection is given by adding of all lane groups in 4 approaches:

$$\text{Capacity} = 4 \times (162 + 625 + 611) = 4 \times 1398 = 5592 \text{ pcu/hr}$$

The capacity calculated by the empirical method is nearly to the sum of saturated traffic demands (5,472 pcu/hr) calculated in the previous section. This value would be compared with the capacity (i.e., maximum through) obtained by the simulation methods.

3.5.   Summary

In this chapter, a hypothetical isolated four-way intersection is proposed to set up a basic scenario for the simulation. The layout, pre-timed signal schemes, and potential traffic demands

of the intersection are all introduced. An initial pre-timed signal scheme and capacity are calculated based on the empirical capacity analysis method. Specific simulation scenarios to investigate the impacts of CAVs under different traffic demands and MPRs are also identified. This is the basic preparation for simulating intersection capacity with CAVs and investigating the potential impacts of CAV technologies on the intersection system in future tasks.

CHAPTER 4: MICROSCOPIC SIMULATION METHODOLOGIES

4.1.   Introduction

As discussed in the potential intersections conducted in Chapter 3, this chapter specifies microscopic simulation models for different types of vehicles and the transfer-based deep reinforcement learning framework for the traffic signal control. A hypothetical isolated four-way intersection is selected as a basic scenario. The following sections are organized as follows. Section 4.2 describes the microscopic simulation models for HDVs and CAVs. The basic parameters for specific traffic simulation models of HDVs and CAVs are also discussed. Section 4.3 presents the potential simulation scenarios for the isolated intersection. Finally, section 4.4 concludes this chapter with a summary.

4.2.   Microscopic Simulation Model for Vehicles

The microscopic simulation method is implemented in this research to investigate the impacts of CAVs on the intersection capacity. The main difference in microscopic simulation models of the HDVs and CAVs is the control mode of longitudinal movements (which mainly controls the travel speed), acceleration/deceleration, and car following gaps between vehicles. In this research, The IDM is implemented for modeling HDVs. The ACC system is utilized to model CAVs when the CAV is following a HDV. The CACC system is implemented to model CAVs when the CAV is following a CAV. The longitudinal movements controls of the CAVs are expected to significantly improve the efficiency of the roadway/intersection systems.

4.2.1.   Traffic Simulation Model for Human Driving Vehicles

4.2.1.1. Intelligent Driving Model

The IDM is implemented for modeling HDVs according to Treiber et al. (2000). The IDM calculates the acceleration rates of the subject vehicle by balancing the ratio of the current velocity versus the desired speed minus the ratio of the desired gap versus the current gap with respect to the preceding vehicle (Treiber, Hennecke, and Helbing 2000).

$$a_{i,k} = a_{max}[1 - (\frac{v_{i,k}}{v_d})^\delta - (\frac{s^*(v,\Delta v)}{s_{i,k}})^2] \tag{4.1}$$

$$s^*(v_{i,k}, \Delta v) = s_0 + max\left[0, \left(v_{i,k}t_d + \frac{v, \Delta v}{2\sqrt{a_{max}d_c}}\right)\right] \tag{4.2}$$

where $a_{i,k}$ denotes the acceleration of the subject vehicle i in time step k. a_{max} represents the maximum acceleration allowed; $v_{i,k}$ is the current speed of the subject vehicle. v_d is the desired speed. δ represents the acceleration exponent. $s^*(v, \Delta v)$ denotes the desired minimum gap. Δv represents the speed difference between the subject vehicle and the preceding vehicle. $s_{i,k}$ is the current distance to the preceding vehicle. s_0 represents the linear jam distance. s_1 denotes the non-linear jam distance. t_d denotes the desired time gap. d_c is the comfortable deceleration.

4.2.2. Traffic Simulation Models for Connected and Autonomous Vehicles

The ACC system and CACC system are utilized for CAV simulation according to previous works (Liu et al., 2018; Xiao et al., 2017). When the CAV is following a HDV, then the car-following system is changed into the ACC mode. When the CAV is following a CAV, then the car-following system is switched into the CACC mode for a closer car-following behavior.

4.2.2.1. Adaptive Cruise Control

The ACC system, which is a variant of the IDM, is proposed and dynamically controlled by four modes, i.e., cruising control, gap control, gap-closing control, and collision avoidance mode (Milanés and Shladover 2014; Xiao, Wang, and Van Arem 2017; Mintsis 2018).

4.2.2.1.1 Cruising Control Mode

This controller aims to keep the ACC vehicle traveling at a desired speed.

$$a_{i,k+1} = k_1(v_d - v_{i,k}) \tag{4.3}$$

where $a_{i,k+1}$ represents the acceleration recommended for the i-th subject vehicle at the time step $k + 1$; v_d denotes the desired speed; $v_{i,k}$ indicates the speed of the subject vehicle i at the current time step k, and k_1 denotes the control gain parameter determining the acceleration by the speed deviation. Typical values for k_1 range between 0.3 to 0.4 s^{-1} in (Xiao et al., 2017), and this study selects 0.4 s^{-1} for k_1.

4.2.2.1.2 Gap Control Mode

The gap control mode of the ACC system is triggered when the gap and speed deviation with respect to the preceding vehicle are less than 0.2 m and 0.1 m/s, respectively (Xiao et al., 2017). The acceleration of the subject vehicle i at the next time step $k + 1$ is calculated based on the gap and speed deviations.

$$a_{i,k+1} = k_2 s_{i,k} + k_3(v_{i-1,k} - v_{i,k}) \tag{4.4}$$

where $s_{i,k}$ denotes the gap deviation of the subject vehicle i at the current time step k. $v_{i-1,k}$ represents the current speed of the preceding vehicle (index in i - 1); k_2 and k_3 denotes the control gains on the gap and speed deviations, respectively. Typical values for the optimal gains are $k_2 = 0.23\ s^{-2}$ and $k_3 = 0.07\ s^{-1}$ (Xiao et al., 2017).

The gap deviation of the subject vehicle is defined according to (Milanés & Shladover, 2014).

$$s_{i,k} = x_{i-1,k} - x_{i,k} - d_0 - t_d v_{i,k} \tag{4.5}$$

where $x_{i-1,k}$ and $x_{i,k}$ represent the current positions of the preceding vehicle and the subject vehicle, respectively. $v_{i,k}$ is the current speed of the subject vehicle. t_d indicates the desired time gap for the ACC vehicle.

4.2.2.1.3 Gap-closing Control Mode

The gap-closing control mode was proposed in (Milanés & Shladover, 2016) and is activated when the gap to the preceding vehicle is smaller than $100\ m$. When the gap is between $100\ m$ and $120\ m$, the subject vehicle retains the previous control mode to provide hysteresis in the control process and perform a smooth transfer between two modes (Liu et al., 2018; Xiao et al., 2017). The formula of the gap-closing control mode is calculated by recalibrating the parameters of control gains in Equation (4.4), and this study utilizes $k_2 = 0.04\ s^{-2}$ and $k_3 = 0.8$ s^{-1} according to (Xiao et al., 2017).

4.2.2.1.4 Collision Avoidance Mode

The collision avoidance mode aims to avoid imminent rear-end collisions, and it is activated when the gap to the preceding vehicle is smaller than $100\ m$, and the gap and speed deviations are less than 0 and 0.1 m/s, respectively (Mintsis, 2018). If the gap is between 100 m and 120 m, the subject vehicle retains the previous control mode to provide hysteresis in the control process and performs a smooth transfer between the two modes (Liu et al., 2018; Xiao et al., 2017). The collision avoidance control mode was also derived by calibrating the parameters of gap control gains in Equation (4.4), and this study sets $k_2 = 0.8\ s^{-2}$ and $k3 = 0.23\ s^{-1}$ according to (Mintsis, 2018).

4.2.2.2. Cooperative Adaptive Cruise Control

The CACC system, which could collect information from V2V and/or V2I communications, is a functional extension of the ACC system. It is noted that, when a CAV is

following a CAV, the car-following system is changed into CACC mode. The additional information collected could help CAVs with the CACC system follow their predecessors with higher accuracy, shorter response time, and shorter headway compared to ACC vehicles (Shladover et al., 2012).

4.2.2.2.1 Cruising Control Mode

The speed controller for the CACC system is the same as that for the ACC system. The cruising control mode is triggered when the time-gap with respect to the preceding vehicle is larger than 2 s, and the gain k_1 in Equation (4.3) is set as $0.4\ s^{-1}$ according to (Liu et al., 2018; Xiao et al., 2017).

4.2.2.2.2 Gap Control Mode

The gap control mode for the CACC system is activated when the gap and speed deviations are smaller than 0.2 m and 0.1 m/s, respectively (Xiao et al., 2017). Compared to the gap control mode of the ACC vehicle, the speed of the subject CACC vehicle at the next time step $k + 1$ is calculated by:

$$v_{i,k+1} = v_{i,k} + k_4 e_{i,k} + k_5 \dot{e}_{i,k} \tag{4.6}$$

$$\dot{e}_{i,k} = v_{i-1,k} - v_{i,k} - t_d a_{i,k} \tag{4.7}$$

where $\dot{e}_{i,k}$ is the first-order derivative of the gap deviation $e_{i,k}$. The values of the control gains k_4 and k_5 in Equation (4.6) are calibrated as $0.45\ s^{-2}$ and $0.25\ s^{-1}$, respectively (Xiao et al., 2017).

4.2.2.2.3 Gap-closing Control Mode

The gap-closing control mode in CACC is activated when the time-gap is less than 1.5 s. If the time-gap is between 1.5 s and 2 s, the subject vehicle would retain the previous control mode as a transition process (Liu et al., 2018; Xiao et al., 2017). The Gap-closing control

function is also calculated by calibrating the optimal gains in Equation (4.6), and they are set as $k_4 = 0.01 \; s^{-2}$ and $k_5 = 0.05 \; s^{-1}$ according to (Xiao et al., 2017).

4.2.2.2.4 Collision Avoidance Mode

The collision avoidance mode helps the CACC vehicle to change the velocity more smoothly and carefully when the time-gap to the preceding vehicle is less than 1.5 s and the gap deviation is negative (Mintsis, 2018). The collision avoidance controller is also derived by calibrating the parameters of the gap control gains in Equation (4.6), and this study sets $k_4 = 0.45$ s^{-2} and $k5 = 0.05 \; s^{-1}$ according to (Mintsis, 2018).

4.2.3. Basic Parameters for Specific Traffic Simulation Models

The default lane change model "LC2013" in SUMO is employed for all vehicles. Table 4.1 indicates the basic parameters of the car-following behaviors of the HDVs and CAVs. According to the HCM (2016), the base saturation flow rate for HDV is 1900 passenger cars per hour per lane. In this case, the desired headway for HDVs is set as 1.9 s. The recommend headways for CAVs are adopted according to (Milanés & Shladover, 2014; Mintsis, 2018). When a CAV is following a CAV, the desired headway is 0.6 s. When a CAV is following a HDV, the car-following behavior will shifted into ACC mode and the desired headway is 1.1 s. To model heterogeneous driving behaviors of the human drivers, the maximum speed for the HDV follows a normal distribution N(1, 0.2) with respect to the speed limits. Also, the reaction time for HDV is 0.7 s, while the reaction time for the CAV is always 0.1 s. Moreover, Table 4.2 shows other specific parameters for ACC/CACC-controlled CAVs which are set according to previous research and projects (Liu et al., 2018; Mintsis, 2018; Porfyri et al., 2018)

Table 4.1 Basic Parameters in Car-following Models

Vehicle Type	Control Mode	Acceleration (m/s^2)	Deceleration (m/s^2)	Desired time gap (s)	Speed Deviation	Reaction time (s)
HDV	IDM	3	6.5	1.9	0.2	0.7
CAV-HDV	ACC	3.5	7.5	1.1	0	0.1
CAV-CAV	CACC	3.5	7.5	0.6	0	0.1

Table 4.2 Specific Factors for Traffic Simulation Models

Factors	Default	Description	Models
minGap	2.5	Minimum Gap when standing (m)	all models
maxDecel	9	The maximum deceleration ability of vehicles of this type in case of emergency (in m/s^2)	all models
delta	4	acceleration exponent	IDM
stepping	0.25	the internal step length (in s) when computing follow speed	IDM
speedControlGain	-0.4	The control gain determining the rate of speed deviation (Speed control mode)	ACC
gapClosingControlGainSpeed	0.8	The control gain determining the rate of speed deviation (Gap closing control mode)	ACC
gapClosingControlGainSpace	0.04	The control gain determining the rate of positioning deviation (Gap closing control mode)	ACC
gapControlGainSpeed	0.07	The control gain determining the rate of speed deviation (Gap control mode)	ACC
gapControlGainSpace	0.23	The control gain determining the rate of positioning deviation (Gap control mode)	ACC
collisionAvoidanceGainSpace	0.8	The control gain determining the rate of positioning deviation (Collision avoidance mode)	ACC
collisionAvoidanceGainSpeed	0.23	The control gain determining the rate of speed deviation (Collision avoidance mode)	ACC
speedControlGainCACC	-0.4	The control gain determining the rate of speed deviation (Speed control mode)	CACC
gapClosingControlGainGap	0.005	The control gain determining the rate of positioning deviation (Gap closing control mode)	CACC
gapClosingControlGainGapDot	0.05	The control gain determining the rate of the positioning deviation derivative (Gap closing control mode)	CACC
gapControlGainGap	0.45	The control gain determining the rate of positioning deviation (Gap control mode)	CACC
gapControlGainGapDot	0.0125	The control gain determining the rate of the positioning deviation derivative (Gap control mode)	CACC
collisionAvoidanceGainGap	0.45	The control gain determining the rate of positioning deviation (Collision avoidance mode)	CACC
collisionAvoidanceGainGapDot	0.05	The control gain determining the rate of the positioning deviation derivative (Collision avoidance mode)	CACC

Source: SUMO User Documentation. https://sumo.dlr.de/docs

In this research, the total waiting time, CO_2 emission, and fuel consumption are utilized to investigate the traffic performance of the intersection system. All these three criteria are retrieved from the SUMO software. The waiting time of a vehicle/lane is calculated by accumulating the time when the vehicle speed decreases to a value below 0.1m/s. Also, the waiting time would be reset to 0 after the vehicle moves. The emission and fuel consumption models of the gasoline-powered passenger car (Euro norm 4) are developed and calculated by the HBEFA3 (version 3.1). The details of the calculation procedure and emission/fuel consumption factors could be referred to the HBEFA3 (Hausberger S., Rexeis M., Zallinger M., 2009).

4.3. Potential Intersection Simulation Scenarios

This section identifies potential intersections and collects necessary data related to the intersection simulation. A hypothetical isolated four-way intersection is selected as a basic scenario. An initial pre-timed signal scheme is calculated for this typical intersection.

4.3.1. Scenarios for Typical Isolated Intersection

All simulation scenarios are processed in the Simulation of Urban MObility (SUMO) by the TraCI-Python interface. Each training episode of the simulation is 3600-s with a 0.1-s time step. A ten-minutes (600 s) warm-up period is added at the beginning of each simulation. This warm-up period aims to eliminate the impacts of insufficiency of traffic generation at the first ten minutes of the simulation. The pre-timed signal scheme has a 100 s cycle length and the phases are set as North-South direct movements (33 s), North-South left-turn movements (9 s), East-West direct movements (33 s), East-West left-turn movements (9 s). The yellow and all-red time is 4 s per phase.

In the microscopic simulation scenarios, saturated traffic throughput (or maximum throughput) is utilized to estimate the capacity of the intersection. The traffic generation follows the uniform distribution to maintain the peak-hour traffic demands all the time. The maximum throughput is obtained by increasing the traffic demands of the intersection and obtain a stable throughput value. Then, traffic demands with different MPRs of CAVs are also tested to obtain the maximum throughput. The detailed simulation scenarios are given as follows.

1). For scenarios with only HDVs, increasing the traffic demands from 500 to 8000 veh/hr, each simulation would get the throughputs with different traffic demands and the traffic performance in the scenario with maximum throughput.

2). For scenarios with the CAVs, the MPRs of CAVs would increase from 0 to 100 % with 10% per step. Then, each simulation would obtain the throughputs with different traffic demands and the traffic performance in the scenario with maximum throughput.

4.4.   Summary

In this chapter, microscopic simulation models for different types of vehicles are introduced. After that, basic parameters for specific traffic simulation models are also specified for different types of vehicles. Specific scenarios for this typical intersection are designed considering different traffic demands and MPRs of CAVs. These are basic preparations for simulating intersection capacity with CAVs in the next tasks. The impacts of different traffic demands and MPRs of CAVs will be further investigated on an isolated intersection and DRL traffic signal control system.

CHAPTER 5: IMPACT OF CAVS ON INTERSECTION CAPACITY

5.1. Introduction

This chapter presents the impacts of CAVs on the designed intersection scenarios under different MPRs of CAVs. The following sections are mainly organized into two parts. In the first part, a hypothetical isolated four-way intersection is utilized as a basic scenario for the lane-level and intersection-level capacity analyses. The intersection capacity is first analyzed by calculating the adjustment factors of the saturation headway and saturation traffic flow rate for each lane under different MPRs of CAVs. Then, the fitted curves and functions for the maximum throughput of the whole intersection under different MPRs of CAVs are calibrated and investigated. In the second part, this research aims to investigate the effects of different control models of AVs and CAVs (i.e., IDM controlled AVs, ACC controlled AVs, and CACC controlled CAVs) on the intersections with different signal control methods (i.e., pre-timed signal, gap-based actuated signal, and delay-based actuated signalized intersections). Meanwhile, the impacts of AV/CAV market penetration rates on the intersection with different traffic demands are also investigated. Finally, this chapter concludes with a summary.

5.2. Intersection Capacity Analysis Methods

5.2.1. Intersection Capacity Analysis with the Lane Level

As defined in HCM (2016), saturation headway is the average headway between the fifth and fifteen vehicles in a standing queue when the intersection signal light changes from red to green. The first four headways are not included due to the impacts of start-up loss time. The headway is calculated by the time gap when two successive vehicles (front bumper) are passing over the stop line. In this research, the base saturation headway rate s_0 is obtained by dividing

3600 s by the saturation headway of the human driven vehicles h_{HDV}. Considering the impacts of CAVs, the saturation flow rate s^* could be adjusted by the headway adjustment factor f_h, according to equation (5.1) or the saturation flow rate (SFR) adjustment factor f_s, according to equation (5.3).

$$f_{h\,(CAV\,rate=\,\alpha)} = \frac{headway_{CAV\,rate=\,\alpha}}{headway\,_{HDV}} \tag{5.1}$$

$$s^* = \frac{3600}{f_h \times h_{HDV}} \tag{5.2}$$

$$f_{s\,(CAV\,rate=\,\alpha)} = \frac{1}{f_{h\,(CAV\,rate=\,\alpha)}} \tag{5.3}$$

$$s^* = f_s \times s_0 = f_s \frac{3600}{h_{HDV}} \tag{5.4}$$

5.2.2. Intersection Capacity Analysis with the Intersection Level

In the simulation, the maximum throughput of the isolated intersection is obtained with the increase in traffic demands. The capacity (simulated maximum throughput) of the isolated intersection is obtained under different MPRs of CAVs conditions. After that, the traffic performances are investigated under maximum throughput scenarios. The fitted curves and adjustment factors for the intersection capacity under different MPRs of CAVs are analyzed.

5.3. Intersection Capacity Analysis Results

5.3.1. Lane Level Results

With the increase of the traffic demand for each lane, the lane level throughput reaches a maximum value, which represents the saturated traffic demand. In this study, lanes in each approach of the hypothetical four-way intersection include one exclusive through traffic lane, one exclusive left-turn traffic lane, and one shared-right-and-through traffic lane. In each

simulation, the first 600s of the 3600s simulation is set as the warm-up time. The traffic is generated with a uniform distribution. The average values of all headways for the fifth to the fifteenth vehicle crossing the stop line when the light changed from red to yellow are obtained. Table 5.1 presents the saturation headway for each lane of the isolated intersection under saturated traffic demand scenarios. With the increase of MPRs of CAVs, the saturation headways for each lane also present different degrees of reduction. In the simulation, the desired time gap value for HDV, ACC-mode-controlled CAV, and CACC-mode-controlled CAV is 1.9 s, 1.1 s, and 0.6 s, respectively. It is noted that the time gap is only part of the headway, which also includes the travel time used for the length of the front vehicle. The saturation headway for the exclusive through traffic lane is 2.117 for only-HDV conditions. Also, the saturation headways for the exclusive left-turn and shared-right lane are slightly larger than the exclusive through lane due to the impacts of turning vehicles. With 100% CAVs, the saturation headways for the exclusive through traffic lane, exclusive left-turn traffic lane, and shared-right-and-through traffic lane decrease by 55.8%, 48.9%, and 42.4%, respectively.

Table 5.1 Saturation Headway for Each Lane under Different MPRs of CAVs

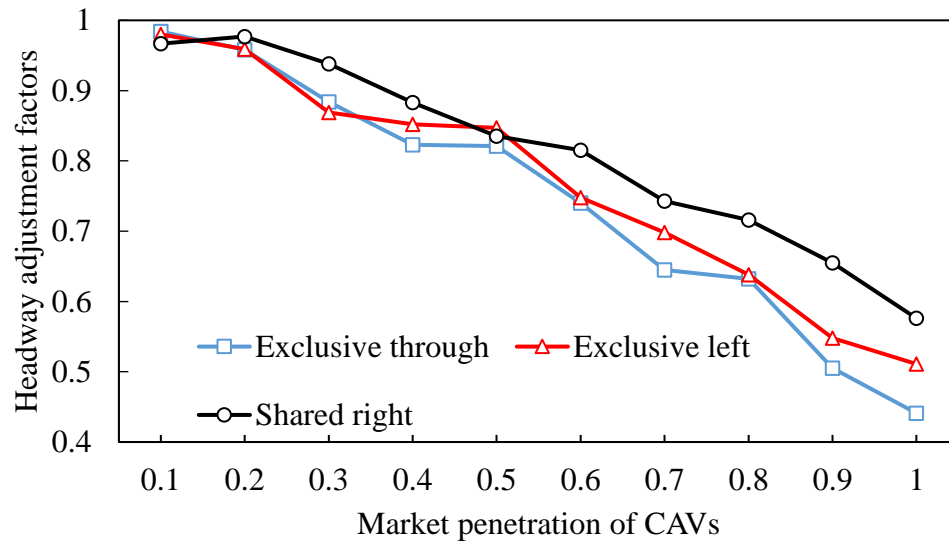|	Headway (s)		
CAV rate	Exclusive through	Exclusive Left	Shared right
0	2.117	2.298	2.317
0.1	2.083	2.252	2.24
0.2	2.029	2.203	2.263
0.3	1.871	1.996	2.174
0.4	1.742	1.957	2.045
0.5	1.738	1.945	1.934
0.6	1.566	1.718	1.888
0.7	1.367	1.604	1.722
0.8	1.311	1.369	1.604
0.9	1.068	1.26	1.518
1	0.934	1.174	1.335

According to the saturation headway results shown in Table 5.1, the adjustment factors for the saturation headway and saturation flow rate under different MPRs of CAVs are summarized in Table 5.2. The adjustment factors are used to modify the condition with only HDVs. Under 100% MPRs of CAVs, the saturation headways of through-only, left-turn-only, and shared-right-and-through traffic lanes are about 0.441, 0.511, and 0.576, respectively, with regard to the condition with only HDVs. Meanwhile, with 100% MPRs of CAVs, the saturation flow rates for the through-only, left-turn-only, and shared-right-and-through traffic lanes could increase about 126.8%, 95.7%, and 73.6%, respectively, compared to the only HDVs condition.

Figure 5.1 and Figure 5.2 also indicate the tendency of the saturation headway and saturation flow rate adjustment factors under different MPRs of CAVs. Contrary tendency results are observed in saturation flow rate adjustment factors as they are the reciprocal (or inverse) of the saturation headway adjustment factors. It is noted that the saturation headway adjustment factors for the exclusive through lane are smaller than the exclusive left-turn lane after 40% MPRs of CAVs. Also, saturation headway adjustment factors of the exclusive through lane and exclusive left-turn lane are always smaller than the shared-right-and-through traffic lane. The exclusive through traffic lane shows the largest deduction as it is not affected by the turning vehicles. The shared-right-and-through traffic lane has the minimum deduction in the headway as it both includes turning and straight vehicles. The heterogeneous traffic movements (mixed turning and straight movements) could have negative impacts on the deduction of headways.
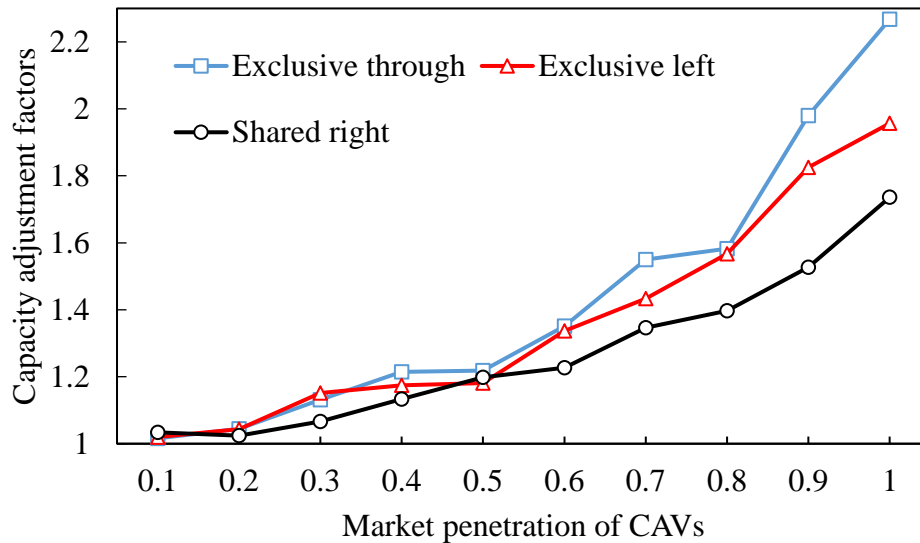
Table 5.2 Adjustment Factors for Saturation Headway and Saturation Flow Rate for Each Lane under Different MPRs of CAVs

	Saturation headway adjustment factors			Saturation flow rate adjustment factors		
CAV	Exclusive	Exclusive	Shared	Exclusive	Exclusive	Shared

rate	through	left	right	through	left	right
0						
0.1	0.984	0.98	0.967	1.016	1.02	1.034
0.2	0.958	0.959	0.977	1.044	1.043	1.024
0.3	0.884	0.869	0.938	1.131	1.151	1.066
0.4	0.823	0.852	0.883	1.215	1.174	1.133
0.5	0.821	0.847	0.835	1.218	1.181	1.198
0.6	0.74	0.748	0.815	1.351	1.337	1.227
0.7	0.645	0.698	0.743	1.55	1.433	1.346
0.8	0.632	0.638	0.716	1.582	1.567	1.397
0.9	0.505	0.548	0.655	1.98	1.825	1.527
1	0.441	0.511	0.576	2.268	1.957	1.736

**Figure 5.1** Headway Adjustment Factors under Different MPRs of CAVs

Figure 5.2 Saturation Flow Rate Adjustment Factors under Different MPRs of CAVs

5.3.2. Intersection-level Results

In the simulation, the maximum throughput of the isolated intersection is obtained with the increase in traffic demands. The capacity (simulated maximum throughput) of the isolated intersection is obtained under different MPRs of CAVs conditions. After that, the traffic performances are investigated under maximum throughput scenarios. The fitted curves and adjustment factors for the intersection capacity under different MPRs of CAVs are analyzed.

At first, all simulated vehicles are set as all human driven vehicles. During the simulation, the traffic demand for the whole intersection increases from 500 to 8000 veh/hr. As shown in Figure 5.3, the throughput reaches a maximum value of 4938 veh/hr with the increase in traffic demands. This maximum throughput value for the only-HDVs condition is set as a basic value for scenarios with different MPRs of CAVs.
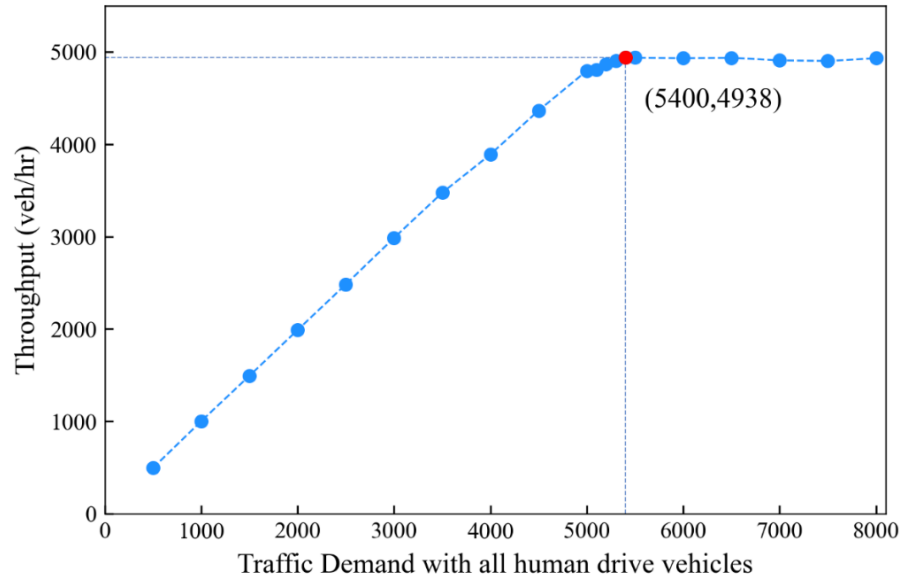
**Figure 5.3** Traffic Throughput with All Human Driven Vehicles

Additionally, scenarios with different MPRs of CAVs are simulated with different traffic demands. When a CAV is following a HDV, the car-following system is changed into the ACC mode. When a CAV is following a CAV, the car-following system is switched into the CACC mode for a closer car-following behavior. As shown in Figure 5.4, the maximum throughputs (points marked with red color) of the whole intersection are obtained with the increase in traffic demands under different MPRs of CAVs (MPR increases from 10% to 100% by 10% per step). The specific traffic performances (including the total waiting time, total CO2 emission, and total fuel consumption) under different traffic demands are also given in Table 5.3. With the increase of MPRs of CAVs, the maximum throughput of the intersection also increases accordingly. With 100% MPRs of CAVs, the maximum throughput reaches 8413 veh/hour.
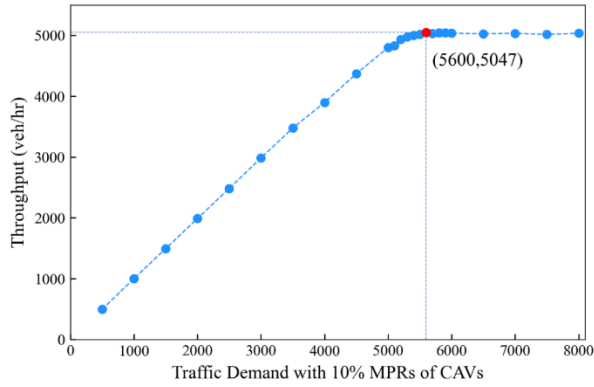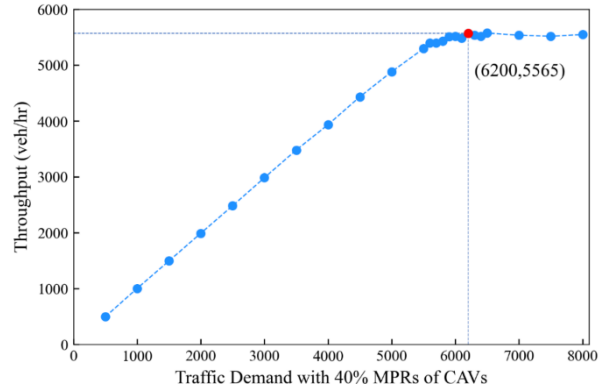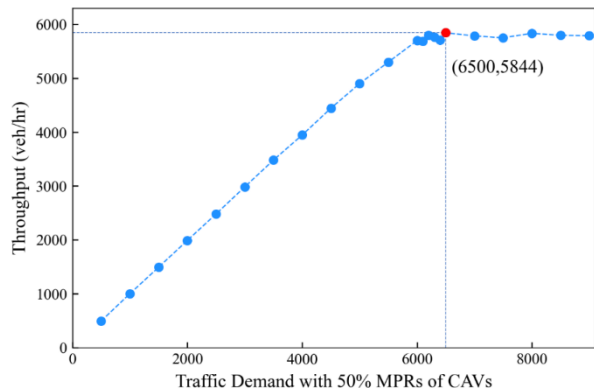
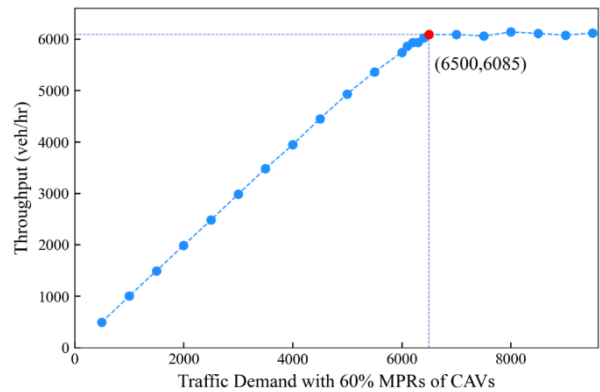(1) 10% MPRs of CAVs
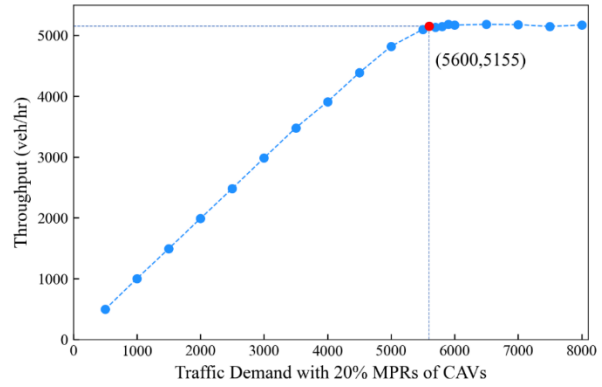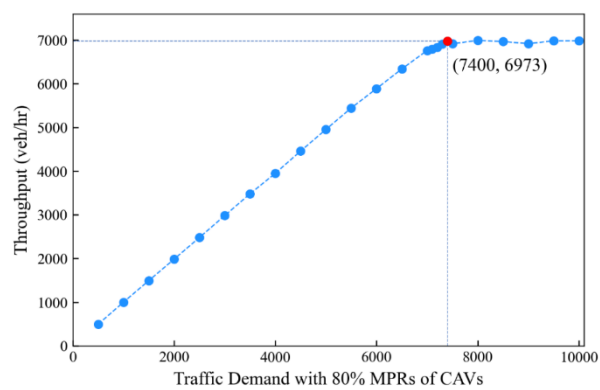
(2) 20% MPRs of CAVs
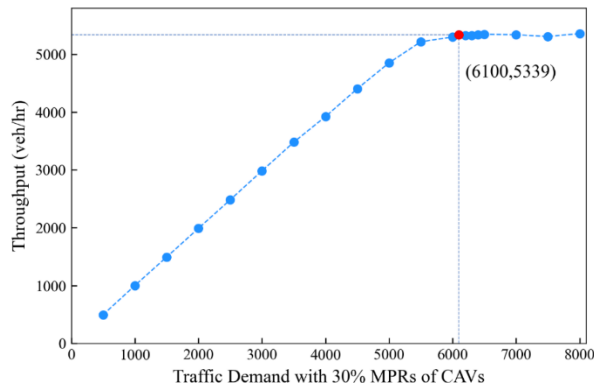
(3) 30% MPRs of CAVs

(4) 40% MPRs of CAVs

(5) 50% MPRs of CAVs

(6) 60% MPRs of CAVs
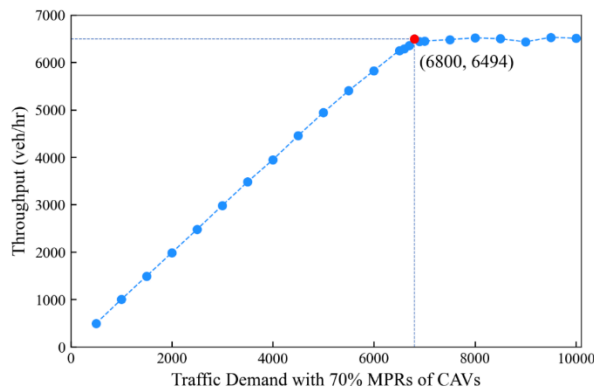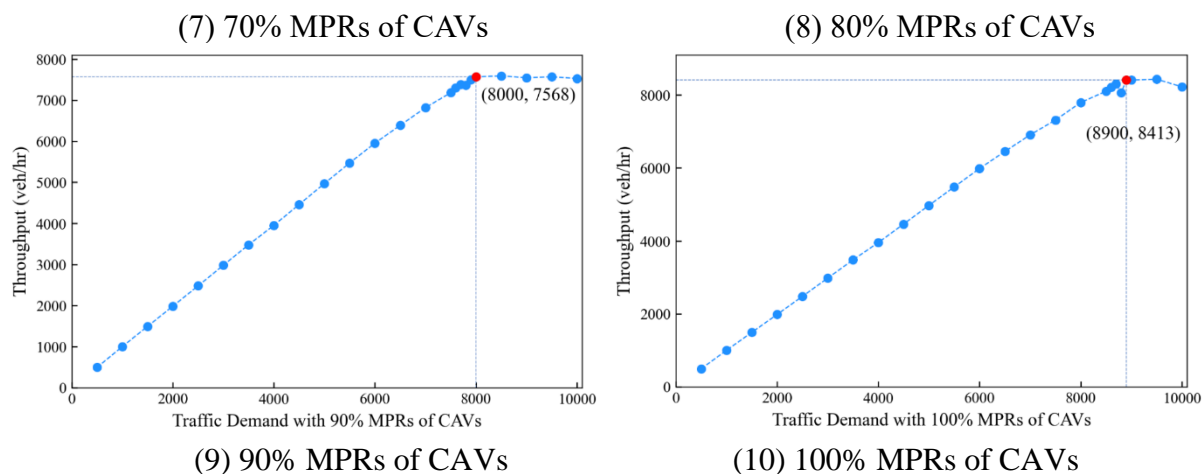
(7) 70% MPRs of CAVs

(8) 80% MPRs of CAVs

(9) 90% MPRs of CAVs

(10) 100% MPRs of CAVs

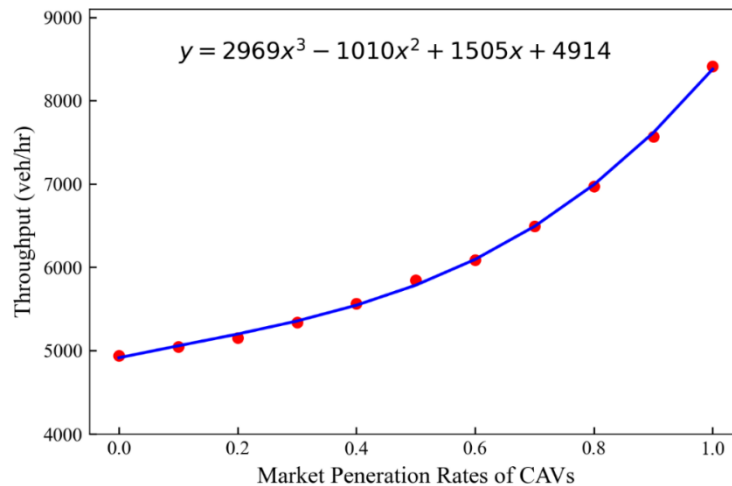**Figure 5.4** Traffic Throughput under Different MPRs of CAVs

All traffic performances under the saturated traffic flow with different MPRs of CAVs are summarized in Table 5.3. The maximum throughput increases with the increase of CAV penetration rates. Also, the change rates of the maximum throughput are summarized in the last column of Table 5.3. It is noted that, with 100% MPRs of CAVs, the maximum throughput of this isolated intersection could increase about 70.4% compared to the scenario with no CAVs.

Table 5.3 Traffic Performance under Saturated Traffic Flow with Different MPRs of CAVs

MPR	Traffic demand	Total waiting time (s)	Average waiting time (s)	Total CO_2 (kg)	Avg. CO_2 (kg)	Total Fuel (L)	Avg. Fuel (L)	Maximum Throughput	Change rate
0	5400	658796.4	122	2180.461	0.404	937.329	0.174	4938	
0.1	5600	697819	124.61	2385.617	0.426	1025.52	0.183	5047	1.022
0.2	5600	695985.4	124.28	2282.991	0.408	981.403	0.175	5155	1.044
0.3	6100	860257.7	141.03	2922.059	0.479	1256.132	0.206	5339	1.081
0.4	6200	848790.4	136.9	2854.666	0.46	1227.158	0.198	5565	1.127
0.5	6500	906076.3	139.4	3001.592	0.462	1290.318	0.199	5844	1.183
0.6	6500	787004.7	121.08	2662.238	0.41	1144.432	0.176	6085	1.232
0.7	6800	734282.3	107.98	2636.286	0.388	1133.273	0.167	6494	1.315
0.8	7400	955250	129.09	3204.906	0.433	1377.712	0.186	6973	1.412
0.9	8000	1008473.3	126.06	3539.99	0.442	1521.757	0.19	7568	1.533
1	8900	1157348.1	130.04	4323.411	0.486	1858.534	0.209	8413	1.704

With the maximum throughput (veh/hour) summarized in Table 5.3, the fitting curve of the maximum throughput (y) is obtained with regard to the MPRs of CAVs (x). The fitting curve is presented in Figure 5.5, and the fitting formula is shown in equation (5.5). The maximum throughput increases steadily under 60% MPRs of CAVs and increases rapidly after 70% MPRs of CAVs.

$$Maximum\ Throughput = 2969MPR^3 - 1010MPR^2 + 1505MPR + 4914 \qquad (5.5)$$

Figure 5.5 Maximum Throughput under Different MPRs of CAVs

5.4. Intersection Performance Under Different MPRs of CAVs

This research also aims to investigate the impacts of MPRs of CAVs on intersections (Song et al., 2021). Three different traffic demand scenarios for the intersection are calculated by the critical volume-to-capacity (v/c) ratio, i.e., v/c = 0.4 for low-demand (512 *vph*), v/c = 0.8 for medium-demand (1024 *vph*), and v/c = 1 for high-demand (1280 *vph*). The proportions of straight, left-turn, and right-turn rates are set as 65%, 15%, and 20%, respectively. CAVs controlled with the CACC mode, AVs controlled with the ACC mode, and AVs controlled with IDM mode are analyzed separately in the mixed traffic with HDVs. The MPR of the AV/CAV

increases from 0% to 100% by 20% per step. To study the effects of AV/CAV at the hypothetical intersections, each traffic demand scenario encompasses three widely used signal control schemes, i.e., pre-timed signal (or fixed signal) control, gap-based actuated control, and delay-based actuated control schemes. The pre-timed signal scheme with four phases is optimized by the performance index approach in Synchro. Two actuated signal schemes are controlled based on the pre-timed signal scheme while setting 5 *s* for the minimum duration and 20 *s* for the maximum extension of the green phase. For the gap-based actuated control, the green-time phase is prolonged when the maximum time gap between two successive vehicles is less than 3 *s*. For the delay-based actuated control scheme, a prolongation of the green-time phase would be activated when the delay (i.e., cumulative time loss) of a vehicle is larger than 1 *s* within the detector/communication range of 300 *m*.

All scenarios are simulated in the Simulation of Urban MObility (SUMO) platform by the TraCI-Python interface. The simulation time for each scenario is 3600 *s* with a 0.1 *s* time step. The speed limit of the roadway is 50 *km/h*. To avoid identical driving behaviors, the initial speed and depart lane of the vehicle are all generated randomly. Also, to avoid homogeneous speeds, the desired speed for each vehicle is calculated by the product of the speed factor and speed limit. The speed factor in this research obeys a normal distribution of N(1.2, 0.1). Meanwhile, the driver's capability in holding the desired speed (between 0 and 1) is determined by the speed control factor according to (Mintsis, 2018). The default lane-changing model (LC2013) in SUMO is used for all vehicles (Erdmann, 2015). Specific parameters for the car-following models are shown in Table 5.4 according to (Mintsis, 2018; Porfyri et al., 2018; Xiao et al., 2017).

Table 5.4 Basic Factors in Car-following Models

Vehicle Type	Control Mode	Acceleration (m/s^2)	Deceleration (m/s^2)	Desired time gap (s)	Speed control factor	Reaction time (s)
HDV	Krauss	1.25	3	1.64	0.5	0.7
AV	IDM	2	4	1.4	0.1	0.1
AV	ACC	2	4	1.1	0.1	0.1
CAV	CACC	2	4	0.6	0.1	0.1

5.4.1. Effects of the AVs with the IDM System

The average delay of all vehicles, which is calculated by the average travel time minus the desired travel time of the trip, is used to measure the performance of the intersection system under pre-timed, gap-based actuated, and delay-based actuated signal scenarios. The results of the average delay for AVs with the IDM system under three traffic demands with different MPRs are shown in Figure 5.6. Table 5.5 also presents the change rate of the average delay compared to the result of the 100% HDVs scenario. For the scenario with low traffic demand and 100% IDM controlled AVs, the average delay decreases by 28%, 45%, and 36% for pre-timed, gap-based, and delay-based signalized intersection, respectively.
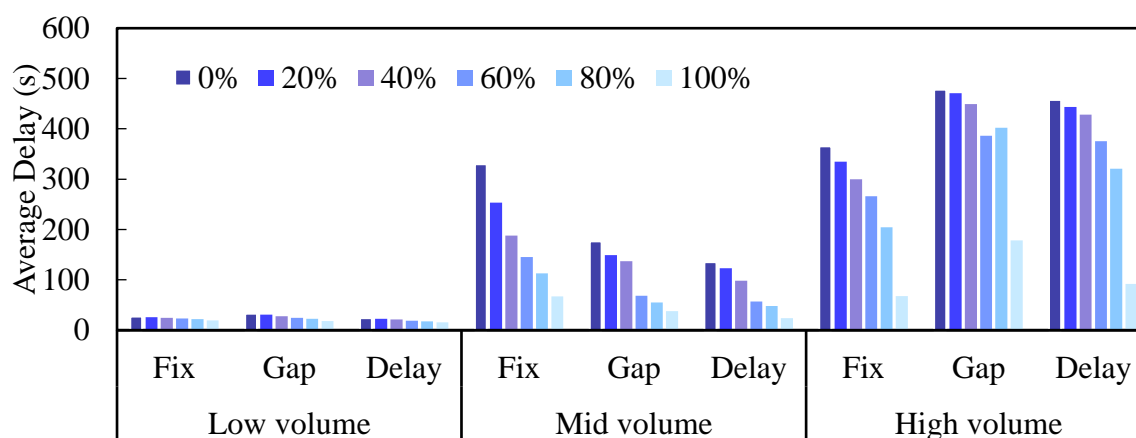
Figure 5.6 Average Delay under Different MPRs of AVs with the IDM System

Table 5.5 Average Delay and the Change Rate of the Average Delay (In Brackets) for AVs with IDM System Compared to 100% HDVs Scenario (unit: s)

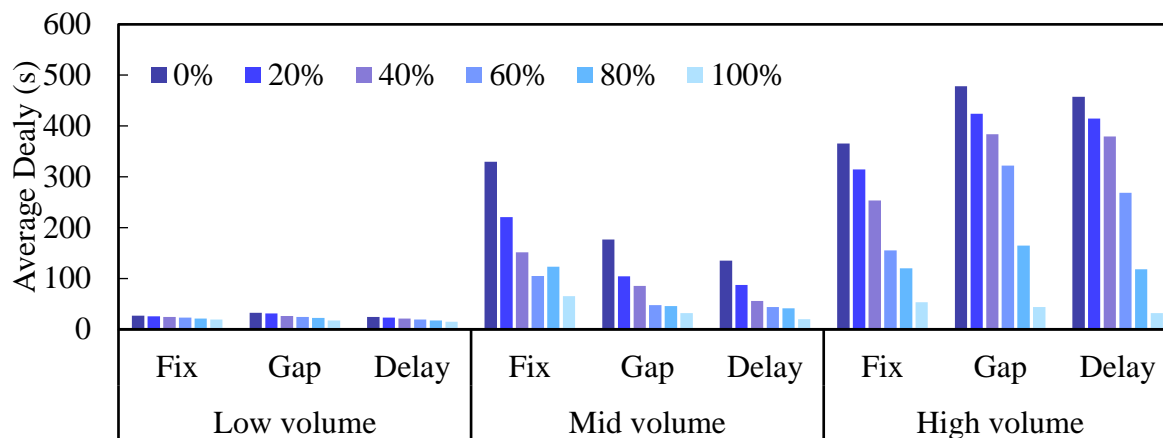| IDM	Low volume			Medium volume			High volume		
MPRs	Fix	Gap	Delay	Fix	Gap	Delay	Fix	Gap	Delay
0	27.1	32.6	24	330	176.7	134.9	365.6	478	457.7
0.2	26.1 (0.04)	30.9 (0.05)	22.9 (0.05)	253.2 (0.23)	149.5 (0.15)	123.1 (0.09)	334.7 (0.08)	470.6 (0.02)	443.6 (0.03)
0.4	24.8 (0.09)	28 (0.14)	21.2 (0.12)	187.8 (0.43)	137.1 (0.22)	98.3 (0.27)	299.6 (0.18)	449.4 (0.06)	428 (0.06)
0.6	23.4 (0.14)	24.5 (0.25)	18.8 (0.22)	145.4 (0.56)	68.5 (0.61)	57 (0.58)	265.8 (0.27)	386.1 (0.19)	375.8 (0.18)
0.8	22.1 (0.18)	22.7 (0.3)	17.8 (0.26)	112.9 (0.66)	54.8 (0.69)	47.8 (0.65)	204.6 (0.44)	402 (0.16)	321.1 (0.3)
1	19.6 (0.28)	18 (0.45)	15.4 (0.36)	67.2 (0.8)	38 (0.79)	24.1 (0.82)	68 (0.81)	178.3 (0.63)	91.7 (0.8)

For the medium traffic demand scenarios, the average delay decreases significantly in all three signalized intersections as the MPR of IDM controlled AVs increases. When the MPRs of the IDM controlled AVs exceed 60%, both actuated signalized intersections reduce about 50% of the average delay compared to the pre-timed signal scenario. With a 100% MPR of IDM controlled AVs, about 79% and 82% decrease of the average delay could be observed at gap-based and delay-based actuated signalized intersections, respectively.

When the traffic is high enough and reaches the saturated flow, significant drops of the average delay could be observed after an 80% MPR of the IDM controlled AVs. With 100% MPRs of IDM controlled AVs, the pre-timed signal scheme outperforms two actuated signal schemes and decreases about 81% of the average delay. Hence, the actuated signal scheme may not be suitable for peak hours or other high traffic demand circumstances when using IDM controlled AVs. Also, in the scenario of high traffic demand, there is an increase in the average delay when the MPR of the IDM controlled AVs increases from 60% to 80% at gap-based

signalized intersection. This indicates the unstable delay at the intersection in the mixed flow of HDVs and IDM controlled AVs.

5.4.2. Effects of the AVs with the ACC System

The results of the average delay and the corresponding change rate of the average vehicle delay for ACC controlled AVs under different scenarios are shown in Figure 5.7 and Table 5.6. The results of ACC controlled AVs are similar to the results of the IDM controlled AVs in low and medium traffic demand scenarios. With a 100% MPR of ACC controlled AVs, the average delay decreases by 85% at the delay-based signalized intersection under medium traffic demand. Also, a slight increase in the average delay is observed when the MPR of the ACC controlled AVs increases from 60% to 80% at the pre-timed signalized intersection under medium traffic demand. This further proves the instability interaction between HDVs and ACC controlled AVs. For the high traffic demand scenarios, the average delay decreases more quickly when the MPRs of the ACC controlled AVs exceed 60% compared to IDM controlled AVs. Different from the IDM scenario, the average delay for two actuated signal-controlled intersections under high traffic demand with a 100% MPR of ACC controlled AVs is less than that for the pre-timed signal scenario. The average delay is decreased by 93% at the delay-based signalized intersection with a 100% MPR of ACC controlled AVs, while the pre-timed signal scenario only decreases 85% of the average delay. These results indicate that ACC controlled AVs outperform the IDM controlled AVs. Also, the implementation of ACC controlled AVs could better cooperate with gap-based and delay-based actuated signal schemes under high traffic demand scenario.

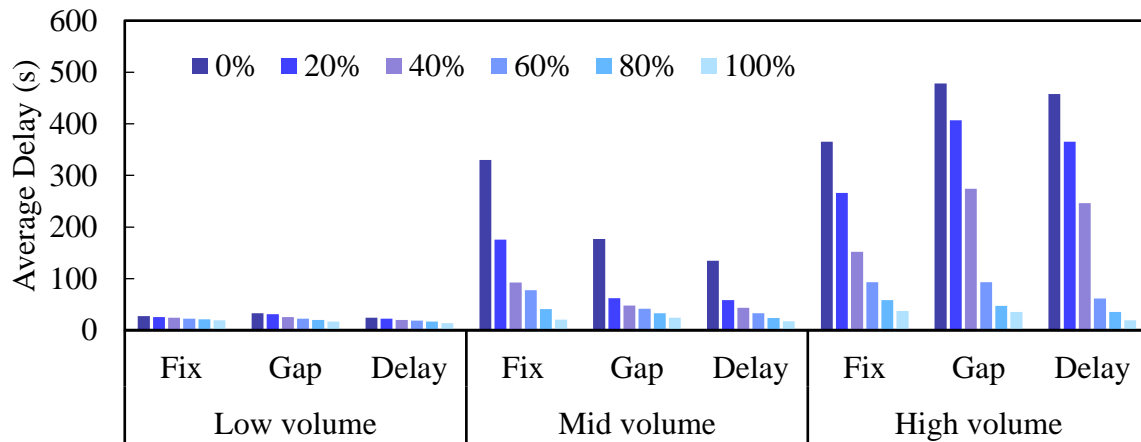**Figure 5.7** Average Delay under Different MPRs of AVs with the ACC System

Table 5.6 Average Delay and the Change Rate of the Average Delay (In Brackets) for AVs with

ACC system Compared to 100% HDVs Scenario (unit: s)

ACC	Low volume			Mid volume			High volume		
MPR	Fix	Gap	Delay	Fix	Gap	Delay	Fix	Gap	Delay
0	27.1	32.6	24	330	176.7	134.9	365.6	478	457.7
0.2	25.7	31.3	22.9	220.6	104.4	87.6	314.5	424.1	414.7
	(0.05)	(0.04)	(0.05)	(0.33)	(0.41)	(0.35)	(0.14)	(0.11)	(0.09)
0.4	24.5	26.5	21.4	151.6	85.1	56	253.3	384.1	379.1
	(0.1)	(0.19)	(0.11)	(0.54)	(0.52)	(0.59)	(0.31)	(0.2)	(0.17)
0.6	22.9	24.2	19.1	105	47.8	43.6	155.1	322.1	268.8
	(0.16)	(0.26)	(0.21)	(0.68)	(0.73)	(0.68)	(0.58)	(0.33)	(0.41)
0.8	21.1	22.7	17.5	122.9	45.6	41.1	120.1	164.5	117.8
	(0.22)	(0.31)	(0.27)	(0.63)	(0.74)	(0.7)	(0.67)	(0.66)	(0.74)
1	19.4	17.5	15.1	64.9	32.1	19.6	53.4	43.8	32.1
	(0.28)	(0.46)	(0.37)	(0.8)	(0.82)	(0.85)	(0.85)	(0.91)	(0.93)

5.4.3. Effects of the CAVs with the CACC System

Figure 5.8 and Table 5.7 present the average delay and the corresponding change rate of

the average delay for CACC controlled CAVs under different scenarios. The average delay

decreases with the increase of MPRs of CACC controlled CAVs. Also, the results of CACC

controlled CAVs outperform IDM and ACC controlled AVs in all scenarios. For medium traffic

demand scenarios, the average delay drops significantly after 20% MPRs of CACC controlled

CAVs for all signal schemes. The average delay drops by 94% at the pre-timed signal scheme with 100% MPRs of CACC controlled CAVs. The results of two actuated signalized intersections indicate that actuated signal schemes are more suitable under medium traffic demand compared to the pre-timed signal scheme. For high demand scenarios, the average delay drops significantly with the increase of MPRs of CACC controlled CAVs. About 87% and 96% drops in the average delay at the delay-based intersection are observed when the MPRs of CACC controlled CAVs reach 60% and 100%, respectively. All these indicate the superiority of the CACC system since the communication function of the CAVs could further decrease the headway and help vehicles to react cooperatively.

Figure 5.8 Average Delay under Different MPRs of CAVs with the CACC System

Table 5.7 Average Delay and the Change Rate of the Average Delay (In Brackets) for CAVs with CACC system Compared to 100% HDVs Scenario (unit: s)

CACC	Low volume			Mid volume			High volume		
MPR	Fix	Gap	Delay	Fix	Gap	Delay	Fix	Gap	Delay
0	27.1	32.6	24	330	176.7	134.9	365.6	478	457.7
0.2	25.7 (0.05)	31.1 (0.05)	22.3 (0.07)	175.5 (0.47)	62 (0.65)	58.2 (0.57)	265.8 (0.27)	407 (0.15)	365.5 (0.2)
0.4	24.2 (0.11)	25.2 (0.23)	20(0.17)	92.2 (0.72)	47.9 (0.73)	43.5 (0.68)	151.9 (0.58)	273.9 (0.43)	246.1 (0.46)

0.6	22.5 (0.17)	22.1 (0.32)	18.6 (0.23)	77.3 (0.77)	41.4 (0.77)	32.7 (0.76)	92.9 (0.75)	92.7 (0.81)	61.2 (0.87)
0.8	20.8 (0.23)	20 (0.39)	16.8 (0.3)	41.1 (0.88)	32.7 (0.82)	23.6 (0.82)	58.5 (0.84)	47.3 (0.9)	35.4 (0.92)
1	19 (0.3)	16.5 (0.49)	13.9 (0.42)	20.2 (0.94)	24 (0.86)	17.2 (0.87)	37.1 (0.9)	35.2 (0.93)	19.4 (0.96)

5.5.   Summary

In this section, the lane level and intersection level capacity are both calibrated and analyzed. In the lane level capacity investigation, adjustment factors for saturation headway and saturation traffic flow rate for each lane under different MPRs of CAVs are calculated. In the intersection level capacity investigation, the maximum throughputs of the intersection under different MPRs of CAVs are calculated. The traffic performances of the total waiting time, CO_2 emission, and fuel consumption under maximum throughputs are also documented. Meanwhile, the fitting curve and fitting function of the maximum throughput under different MPRs of CAVs are calibrated. With 100% CAVs, the saturation headways for the exclusive through traffic lane, exclusive left-turn traffic lane, and shared-right-and-through traffic lane decrease by 55.8%, 48.9%, and 42.4%, respectively. Traffic engineers and planners are expected to directly use the adjustment factors to calculate the intersection capacity under different MPRs of CAVs.

Moreover, this chapter investigates the impacts of different control modes of AVs and CAVs (i.e., IDM-controlled AVs, ACC-controlled AVs, and CACC-controlled CAVs) on the intersections with different signal control methods (i.e., pre-timed signal, gap-based actuated signal, and delay-based actuated signalized intersections) and traffic demands. Results indicate that CACC-controlled CAVs outperform IDM/ACC-controlled AVs. A 96% drop in the average delay is observed at the delay-based signalized intersection under high traffic demand with a 100% MPR of CACC-controlled CAVs. Furthermore, CACC-controlled CAVs could

significantly decrease the average delay under medium and high demand scenarios after the MPRs exceed 20% and 40%, respectively.

CHAPTER 6: IMPACTS OF CAVS ON DEEP REINFORCEMENT LEARNING

CONTROLLED INTERSECTIONS

6.1.   Introduction

Chapter 6 presents the basic settings for the proposed transfer-based DRL traffic signal control (TSC) system. The transfer-based DRL-controlled signal intersection framework is proposed in Section 6.2. The transfer-based DQN models are utilized in scenarios with different traffic demands and MPRs of CAVs as introduced in Section 6.3. In Section 6.4, different model settings, including reward parameters, exploration rates, and action step lengths, are tested. In Section 6.5, the training efficiency and model performances of the transferred model are compared to direct training models. Moreover, the validity of the transfer-based DQN method is tested in scenarios with different MPRs of CAVs. This could determine the basic requirement of the information level of vehicles. Finally, this chapter concludes with a summary.

6.2.   Methodologies

In this section, a transfer-based DRL TSC method is proposed (Song & Fan, 2021). The traffic signal controller of the intersection is controlled by a single DRL agent that communicates with the traffic environment. With the V2I communication, the DRL agent could choose an action a_t based on the inputs of state s_t and reward r_t in timestep t. A benchmark DRL framework, i.e., Deep Q Network (DQN), is utilized in this study to train the traffic signal controller. The action set A_t includes eight green-time phases for traffic movements. When the current action a_t is different from the last time step action a_{t-1}, a 3 s yellow and 1 s all-red time phase is added. Also, if the DRL agent selects the same action and this green phase exceeds the maximum cumulative green time (60 s in this paper), then the agent will switch into the next

green phase accordingly. The state s_t is a matrix combined with the traffic volume in each inlet segment of the intersection. The detailed definitions for the action and state are given in the empirical settings part. The framework of the transfer-based DRL traffic signal control system is presented in Figure 6.1.
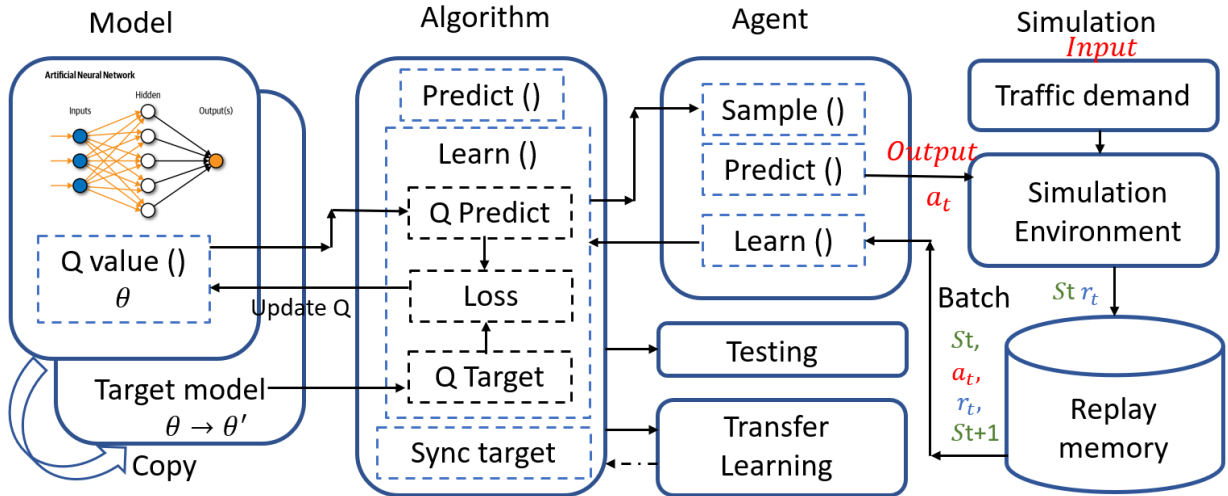
Figure. 6.1 Framework of the Transfer-Based Deep Q Learning Method

The reward r_t denotes the feedback after the DRL agent chosen an action a_t. Several traffic performance criteria could be used to calculate the reward in TSC systems, such as the throughput, queue length, and total waiting time (Haydari & Yilmaz, 2020; Vidali, 2018). The total waiting time is the sum of the time for vehicles when the vehicle speed is less than 0.1 m/s. Different from the throughput and queue length, the total waiting time could consider both traffic volume and stopping time. Hence, the research employs the total waiting time to calculate the reward. Also, according to Vidali (2018), a hyperparameter is added to the reward function to improve the training efficiency. The revised reward function is defined as:

$$r_t = \delta \times twt_{t-1} - twt_t \qquad (6.1)$$

where twt_t denotes the total waiting time at the time step t. The hyperparameter $\delta \leq 1$. δ could increase the magnitude of the reward value and is supposed to improve the training efficiency. When $\delta = 1$, the reward function changes to a normal reward function. The positive reward value r_t denotes a better performance as the current action decreases the twt_t.

Q learning is a benchmark model-free and value-based RL technology (Haydari & Yilmaz, 2020). The Q value denotes all rewards that the agent could obtain when taking an action a_t in state s_t, and it could be approximated by selecting the action a_{t+1} that obtains the maximum Q value Q':

$$Q(s_t, a_t) = r_{t+1} + \gamma \cdot r_{t+2} + \cdots + \gamma^{y-1} \cdot r_{t+y} \approx r_{t+1} + \gamma \cdot \max_A Q'(s_{t+1}, a_{t+1}) \quad (6.2)$$

where $Q'(s_{t+1}, a_{t+1})$ is the Q value for taking an action a_{t+1} in the state s_{t+1}. γ is the discount rate that adds a penalization of the future reward compared to the immediate reward r_{t+1}. γ is set as 0.25 according to the test results in Vidali (2018).

With the development of deep learning technology, neural networks are implemented to estimate the Q value. Experience replay is also utilized to store and extract a batch of samples from the reply memory database. The random selection of the samples could mitigate correlations in samples and improve the utilization rate of the samples. As presented in Figure 6.1, the DQN framework contains two neural networks to improve the stability of the training result. A training neural network predicts the future Q' value base on the input samples. Meanwhile, the target neural network copies/updates its neuron weights from the training neural network after a certain simulation step. The training neural network is trained based on the simple square error between the predicted Q values from the training network and the target network.

$$L(w) = E\left[\left(r + \gamma \max_{a'} Q_t(s', a', w) - Q_t(s, a, w)\right)^2\right] \quad (6.3)$$

To minimize the loss function $L(w)$, the stochastic gradient descent method (i.e., Adam in this research) is used. The neuron weights w are updated with the learning rate α as follows,

$$\frac{\partial L(w)}{\partial w} = E\left[\left(r + \gamma \max_{a'} Q(s', a') - Q(s, a)\right)\frac{\partial Q(s,a,w)}{\partial w}\right] \tag{6.4}$$

$$w_{t+1} = w_t - \alpha \frac{\partial L_t}{\partial w_t} \tag{6.5}$$

Moreover, the epsilon-greedy method is implemented to explore possible actions in the early training steps. The agent would choose an action randomly with a probability of ϵ_h. Otherwise, the agent chooses the action a_{t+1} that obtains the maximum Q' value predicted from the training network,

$$\epsilon_h = 1 - \frac{h}{H} \tag{6.6}$$

where h is the current episode number. H is the total number of simulation episodes.

Transfer learning enables the reuse of a previously trained model between similar scenarios. For TSC scenarios with similar traffic conditions, the trained policy, which determines actions, in one model is also supposed to be useful and could be treated as an initial policy to train another model (Kiran et al., 2021; Xu et al., 2019). As the training procedure of the DRL is time-consuming and cumbersome, the implementation of transfer learning is also expected to improve the training efficiency and performance (when transferring models with higher MPRs of CAVs which could provide more information of the vehicles to the signal controller). In this research, the network weights w in a trained model are transferred into a target model in scenarios with similar traffic demands or traffic information levels (determined by the MPRs of CAVs). The detailed algorithms of the DQN with the transfer learning procedure are shown in Table 6.1.

Table 6.1 Algorithms of Deep Q Network with the Experience Replay and Transferred Procedure

---

Initialize experience replay memory D

Initialize the agent to interact with the environment

Get the current episode number h and the total number of simulation episodes H

If transferred from previous model

    Synchronize base and target neural network weights w and w' from previous model

Else

    Randomly initialize base and target neural network weights w and w'

End if

While cumulative reward value not converged **do**

    /*Sample phase

    Choose an action from states using policy ϵ_h-greedy(Q)

    If probability $\epsilon_h \leq 1 - \dfrac{h}{H}$

        Select a random action a_t

    Else

        Select a $a_t = \underset{a'}{argmax}\, Q_t(s_t, \text{a}, w)$

    End If

    Agent takes action a_t, observe reward r_t, and next state s_{t+1}

    Store sample (s_t, a_t, r_t, s_{t+1}) in the experience replay memory D

    If enough experiences in D **then**

        /*Learn phase

        Sample a random batch of N samples from D

        For every sample (s_t, a_t, r_t, s_{t+1}) in N **do**

            Set $\hat{Q}_t = \begin{cases} r_t & \text{If episode terminated at time step t} \\ r_{t+1} + \gamma \cdot \underset{A}{max}\, Q'(s_{t+1}, a_{t+1}) & \text{Otherwise} \end{cases}$

            Calculate the loss function value $L(w)$

            Update weight w using the SGD algorithm by minimizing $L(w)$

            Every C steps, copy weights from base network to target network

        End For

End If

End While

Backup the trained NN weights w and w'

Test the performance of the TSC system

The research uses the total waiting time, CO2 emission, and fuel consumption to investigate the traffic performance of the intersection. These three criteria are all directly obtained from the SUMO. The waiting time of a vehicle/lane is calculated by accumulating the time when the vehicle speed decreases to a value below 0.1m/s. Also, after the vehicle moves, the total waiting time would be reset to 0. In SUMO, the emission and fuel consumption models of the gasoline-driven passenger car (Euro norm 4) are calculated according to the HBEFA3 (version 3.1). The details of the calculation procedure and emission/fuel consumption factors can be found in HBEFA3 (Hausberger S., Rexeis M., Zallinger M., 2009).
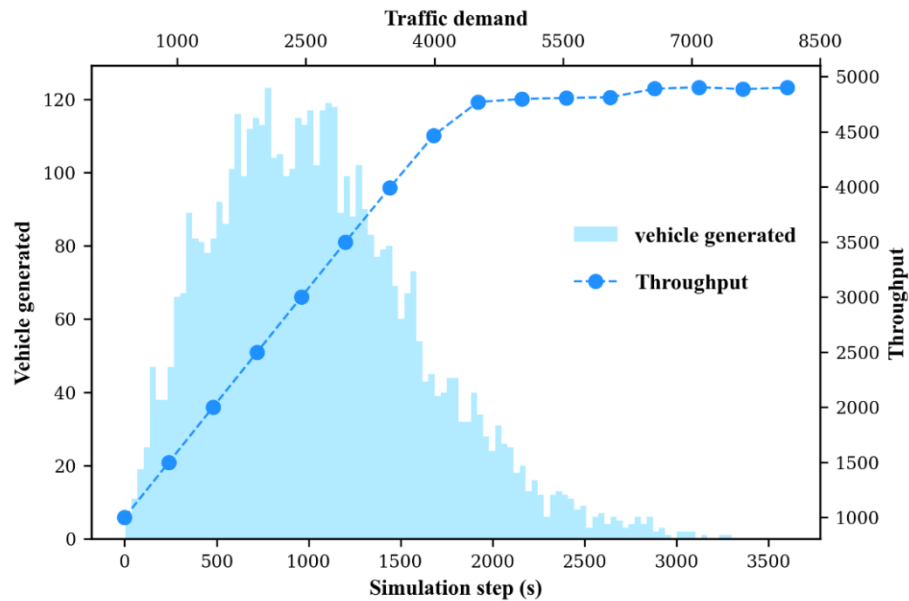
6.3. Simulation Scenarios

As shown in Figure 6.2, a four-way intersection with four lanes per approach is selected for the case study. The vehicle-based state of the traffic environment (an array composed of the number of vehicles in each segment/grid) is determined by the discrete traffic state encoding (DSTE) method and is the input for the DRL model. Eight green phases are set as possible actions for the TSC agent. If the signal changes its phase, a 4 s yellow and all red-time is added. For urban roadways, the speed limit is set at 15.6 m/s (i.e., 35 mph). The peak-hour traffic is generated according to a Weibull distribution with a shape equal to 2. Meanwhile, the random seed, which equals the episode value, is implemented to generate heterogeneous traffic for different training episodes. The traffic demands of the intersection are determined by the simulated maximum throughput of a basic pre-timed signal scheme with a 100-s cycle length. As

shown in Figure 6.3, with the increase of the traffic demand in the simulation, the maximum throughput of the intersection increases to 4800 vehicles/hour, and this saturated traffic is set as the high traffic demand scenario. The low, medium, and medium-high traffic demands are set at 20%, 40%, and 60% of the high traffic demand, respectively. The detailed traffic demand for each traffic movement is presented in Table 6.2.
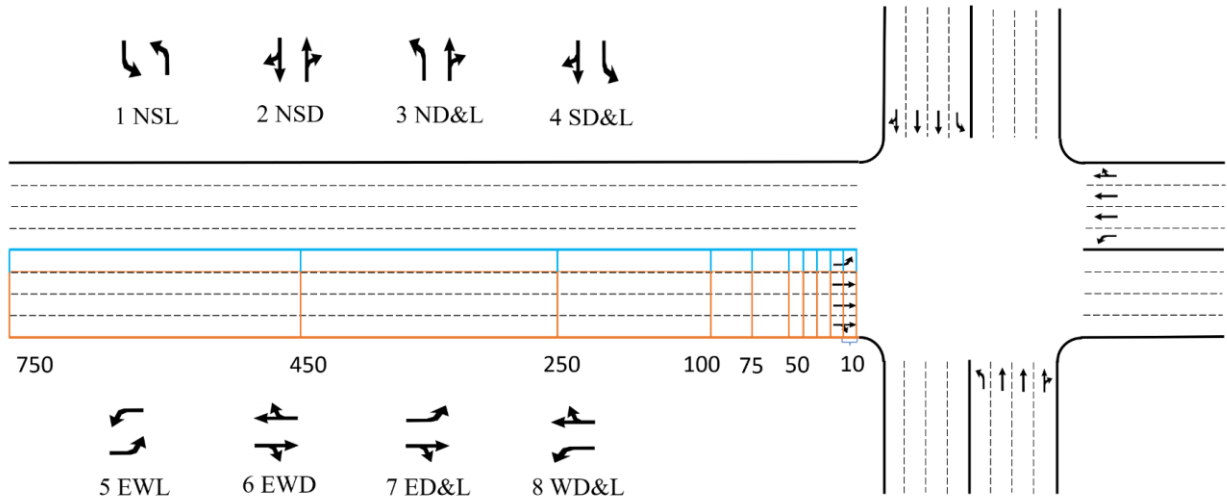
Figure 6.2 Discrete Traffic State Encoding of the Vehicle-Based State Array and Available Traffic Signal Actions of the Intersection

Figure 6.3 Traffic Generated Per Simulation Step and Throughputs under Different Traffic Demands

Table 6.2 Different Traffic Demand Scenarios

Traffic demand (veh/hr)	Low	Medium	Medium-High	High
Left traffic per approach	72	108	144	180
Through traffic per approach	336	504	672	840
Right traffic per approach	72	108	144	180
Total traffic per approach	480	720	960	1200
Total Throughput	1920	2880	3840	4800

All scenarios are simulated in the SUMO by TraCI-Python interface. Each simulation episode is 3600 s with a 0.1 s per time step. The IDM is used for HDVs according to (Martin Treiber et al., 2000). The CACC system is implemented for CAV simulation according to (Liu et al., 2018; Xiao et al., 2017). The default lane change model "LC2013" in SUMO is utilized for all vehicles. Both HDVs and CAVs have the same ability for acceleration (2 m/s2) and deceleration (-4 m/s2). The desired time gaps for HDVs and CAVs are 1.6 s and 0.7 s, respectively. Considering heterogeneous driving behaviors of the human drivers, the maximum speed for the HDV follows a normal distribution N(1.2, 0.1) with respect to the speed limits. Other parameters for CACC controlled CAVs are set according to previous research (Mintsis, 2018; Porfyri et al., 2018; Xiao et al., 2017).

In this research, all vehicles are set as CAVs at first. A direct training procedure with 800 simulation episodes is employed under the low traffic demand scenario. Then, the trained model is transferred to the next scenario with a higher traffic demand (from low to medium, medium to medium-high, and medium-high to high). After that, this study tests the validity of the transfer-based DQN TSC system by considering different MPRs of CAVs (i.e., information levels of the vehicles). For scenarios with the same traffic demand, the MPR of CAVs decreases from 100% to 20% by 20% per step. The trained model with higher MPRs of CAVs will be transferred into the scenario with lower MPRs of CAVs.

6.4. Model Settings

A medium-size neural network with 4 fully connected layers (400 neurons per layer) is utilized as the same as the one determined by (Vidali, 2018). The discount factor of the reward equation is 0.25. At the end of each episode, the training iterations of the neuron weights will execute 800 times with a 0.01 learning rate, and each iteration will retrieve 100 samples according to the memory replay (Vidali, 2018). The following parts test the reward function parameter, the exploration rate, and the action step length.

6.4.1. Reward Function Parameter Test

The revision of the parameter (γ =0.9) in the reward function could increase the magnitude of the reward value and improve the training efficiency (Vidali, 2018). As presented in Figure 6.4, this study compares the results between the general reward parameter (γ =1) and the revised reward parameter (γ =0.9) for the transfer-based DQN procedure under a medium traffic scenario with 100% MPR of CAVs. The reward curves indicate that the proposed reward parameter (γ =0.9) could not always improve the training efficiency and could result in more variations in action selections. Hence, γ =1 is utilized is used in this research.
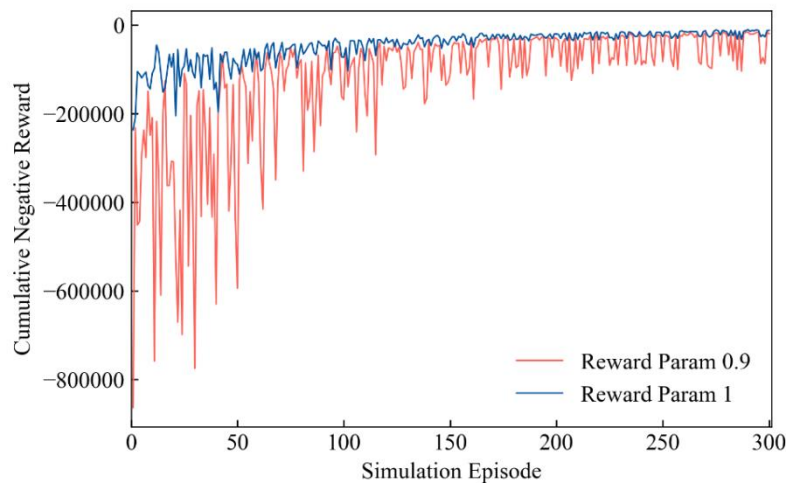
Figure. 6.4 Reward Curves for Different Reward Function Parameters

6.4.2. Tradeoff Between Exploration and Exploitation

In general, the DQN training procedure is expected to explore more possible actions at the beginning of the training. Then, it is expected to exploit more when the action policy is well trained. The ε-greedy exploration is utilized to strike a balance between the exploration and exploitation of the actions. As the transfer-based learning procedure could obtain prior action policy from a previous trained model, the training procedure might obtain a converged value without exploring all possible actions. To confirm this assumption, different ε-greedy exploration rates are tested, and the results are exhibited in Figure 6.5. It is found that the transfer-based models could also obtain a similar stable reward without full exploration (ε changes from 1 to 0), which indicates the validity of transferring models from similar scenarios.
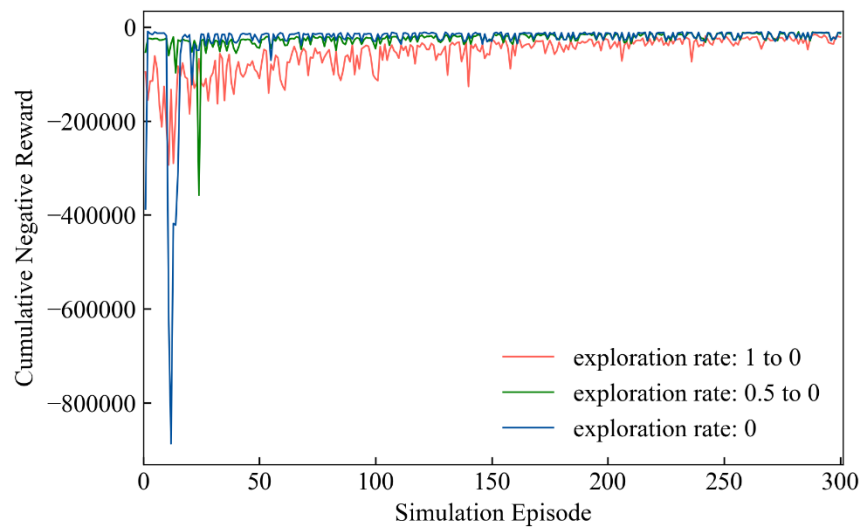
Figure 6.5 Reward Curves under Different ε-greedy Exploration Rate Boundary

6.4.3. Action Step Length Test

As shown in Table 6.3, under a low traffic demand scenario, the model performances with different action step lengths (green time durations) are documented. A significant increase in the total waiting time, CO_2 emission, and fuel consumption are observed after 10 s of the

green time. Also, the frequent change of the green phase could result in more green time loss. Hence, this study selects 10 s green time for each action and 60 s for the maximum green time duration.

Table 6.3 Green Time Duration Per Action for the DQN Signal Controller

Green time (s)	Total waiting time (s)	Total CO_2 (kg)	Total fuel (L)
5	23191.3	318.8	137
10	24942.2	323.7	139.2
15	32772.6	344.9	148.3
20	39815.3	363.2	156

6.5. Results for Single Intersection

6.5.1. Comparison Between Direct and Transfer-Based Learning

To test the efficiency of the transfer-based DQN model, this research compares the direct training and transfer-based training with full exploration (ε-greedy decreases from 1 to 0) under a medium traffic scenario with 100% MPR of CAVs. The cumulative negative reward curves in Figure 6.6 illustrate that the transfer-based method could get stable values with fewer training episodes compared to the direct training procedure. As the direct training procedure for an intersection with different traffic demands is very time-consuming, this result further proves that reusing the prior trained action policy (neural network weights) in target models with fewer adjustments under similar traffic scenarios could improve the training. For example, in Figure 6.6, the direct training and the transfer-based training take about 54.2 hours and 20.1 hours, respectively, in a computer with GTX-1050 GPU and i5-7300 2.5GHz CPU. The significant decrease in the training time provides possible engineering applications of the transfer-based DQN TSC at intersections with similar traffic demands.
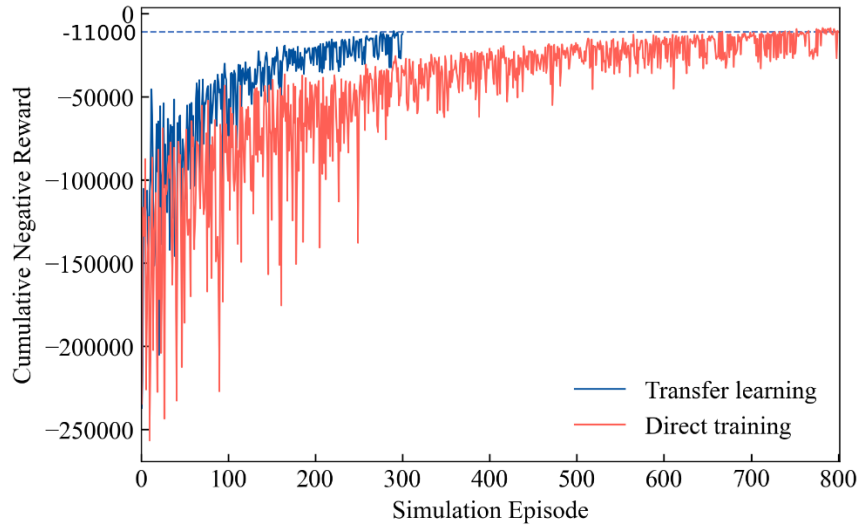
Figure 6.6 Comparison Between the Reward Curves of Direct and Transfer-Based Leaning Approaches

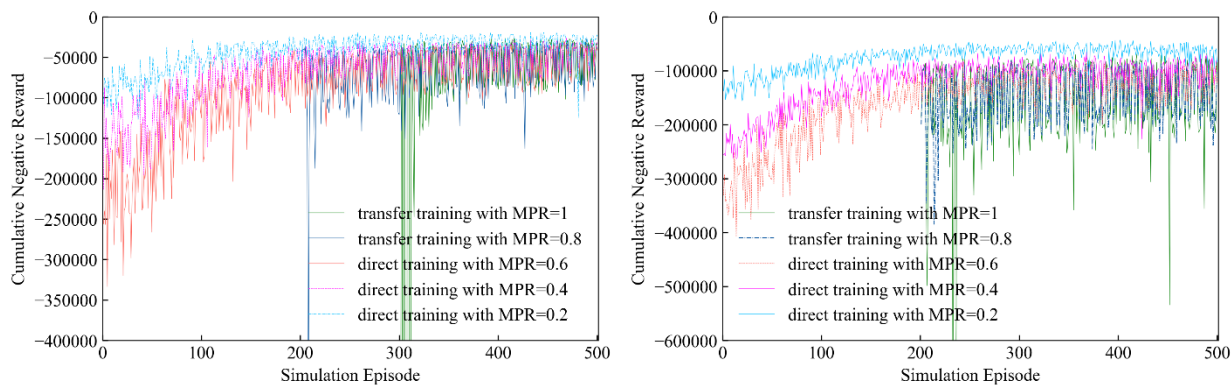### 6.5.2. Impacts Under Different Traffic Demands and MPRs of CAVs

With the V2I communication technology, the TSC agent could obtain traffic state (i.e., speed, traffic volume, waiting time, etc.) from the CAVs approaching the intersection. However, it is expected to have a long transition time during which HDVs and AVs/CAVs will coexist (Sharon & Stone, 2017). This study also investigates the impacts of information levels of the mixed traffic flow on transfer-based DQN TSC systems.

Figure 6.7 presents cumulative reward curves for scenarios with different traffic demands and MPRs of CAVs. The prior action policy of the trained DQN model is first transferred to scenarios with higher traffic demands (from low to medium, medium to medium-high, and medium-high to high) under 100% MPRs of CAVs. After that, this research investigates the impacts of information levels of the vehicles on the DQN TSC system by transferring models with high MPRs of CAVs into models with low MPRs of CAVs (decrease from 100% to 20% by 20% per step). For instance, the trained model with a 100% MPR of CAVs is transferred to a model with an 80% MPR of CAVs. It is also noted that direct training procedures are utilized in

some low MPRs scenarios to obtain more stable reward values at the end of the training. An interesting finding is that the reward values of the transfer-based model overlap with the reward values in models with higher MPRs of CAVs (i.e., higher information level). This overlapping is not observed in direct training models as these models are trained based on partial traffic information. The TSC agent could not select a better choice if the agent only gets limited information on the states and rewards. Moreover, the transfer-based models could obtain higher reward values than direct training models with higher information levels. With the pre-trained action policy provided by a prior model with a higher information level, the transfer-based DQN method could obtain better actions compared to the direct-training-only model.
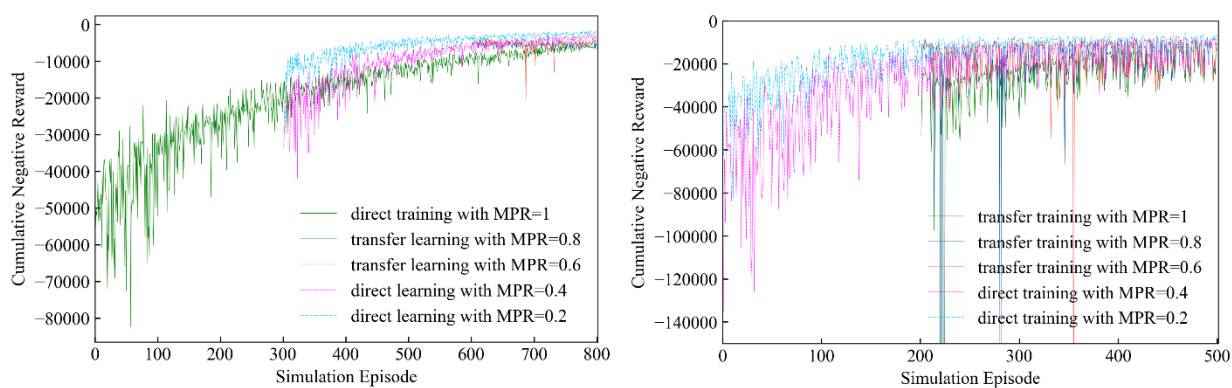
(a) Rewards under low traffic demand   (b) Rewards under medium traffic demand

(c) Rewards under medium-high traffic demand   (d) Rewards under high traffic demand

Figure 6.7 Training Rewards for Scenarios with Different Traffic Demands and MPRs of CAVs

Table 6.4 to Table 6.6 document the test performance (total waiting time, CO_2 emission, and fuel consumption) of the proposed DQN TSC under different traffic demands and MPRs of the CAVs. To better investigate the impacts of different MPRs of CAVs on transfer-based DQN TSC systems, Figure 6.8 shows the total waiting time and CO_2 emission under different traffic demands. Compared to pre-timed signal schemes, the proposed DQN TSC decreases the total waiting time, CO_2 emission, and fuel consumption in scenarios with more than a 40% MPR of CAVs. Meanwhile, a decrease in indicator values (i.e., better system performance) could also be observed with the increase in MPRs of CAVs. Also, the DQN TSC system gets worse traffic performances with a 20% MPR of CAVs under low-, medium-, and high-traffic scenarios. When the MPRs of the CAVs increase from 20% to 40%, the performance indicator values all decrease significantly. These results demonstrate that the proposed transfer-based DQN TSC controller requires a certain information level for the vehicles, and the critical value of the information level is between 20% to 40% under different traffic demands. Moreover, in medium traffic scenarios with 100% MPRs of CAVs, the DQN TSC system decreases total waiting time by 58%, which is the best performance in the total waiting time. For high traffic scenarios, pre-timed signal schemes result in significant congestion as all performance values almost doubled compared to medium-high traffic scenarios. However, with a 100% MPR of CAVs, DQN TSC decreases the total waiting time, CO_2 emission, and fuel consumption by about 38%, 34%, and 34%, respectively.

Table 6.4 Total Waiting Time for Scenarios with Different MPRs of CAVs and Traffic Demands

Total waiting time (s)	Traffic demand			
	Low	Medium	Medium-high	High
Pre-timed signal	48009.7	129770.2	424350.3	816397.9

20% MPR	57641 (-0.201)	165163.1 (-0.273)	388409.3 (0.085)	882875 (-0.081)
40% MPR	35624 (0.258)	93565 (0.279)	341656.4 (0.195)	729716.3 (0.106)
60% MPR	29635.2 (0.383)	83949.1 (0.353)	317232.5 (0.252)	670957.4 (0.178)
80% MPR	29912.3 (0.377)	67767.1 (0.478)	251353.4 (0.408)	604543.4 (0.259)
100% MPR	24942.2 (0.48)	54472.9 (0.58)	218563.7 (0.485)	508737.1 (0.377)

*note: numbers in parentheses denote the change rate compare to pre-timed signal schemes

**Table 6.5** Total CO_2 Emission for Scenarios with Different MPRs of CAVs and Traffic Demands

Total CO_2 (kg)	Traffic demand			
	Low	Medium	Medium-high	High
Pre-timed signal	363.1	684.2	1647.7	3086.1
20% MPR	369.3 (-0.017)	744.9 (-0.089)	1615.4 (0.02)	3089.3 (-0.001)
40% MPR	324.9 (0.105)	582.6 (0.148)	1419.2 (0.139)	2650.1 (0.141)
60% MPR	318.9 (0.122)	573.7 (0.162)	1311.3 (0.204)	2519.5 (0.184)
80% MPR	328.2 (0.096)	554.1 (0.19)	1152.2 (0.301)	2206.9 (0.285)
100% MPR	323.7 (0.109)	537.2 (0.215)	1105.2 (0.329)	2023.8 (0.344)

*note: numbers in parentheses denote the change rate compare to pre-timed signal schemes

Table 6.6 Total Fuel Consumption for Scenarios with Different MPRs of CAVs and Traffic Demands

Total fuel (L)	Traffic demand			
	Low	Medium	Medium-high	High
Pre-timed signal	156.1	294.1	708.3	1326.6
20% MPR	158.8 (-0.017)	320.2 (-0.089)	694.4 (0.02)	1328 (-0.001)
40% MPR	139.6 (0.106)	250.4 (0.149)	610.1 (0.139)	1139.2 (0.141)
60% MPR	137.1 (0.122)	246.6 (0.162)	563.7 (0.204)	1083.1 (0.184)
80% MPR	141.1 (0.096)	238.2 (0.19)	495.3 (0.301)	948.7 (0.285)
100% MPR	139.2 (0.108)	230.9 (0.215)	475.1 (0.329)	870 (0.344)

*note: numbers in parentheses denote the change rate compare to pre-timed signal schemes

(a) Total waiting time (s)   (b) Total CO$_2$ emission (kg)
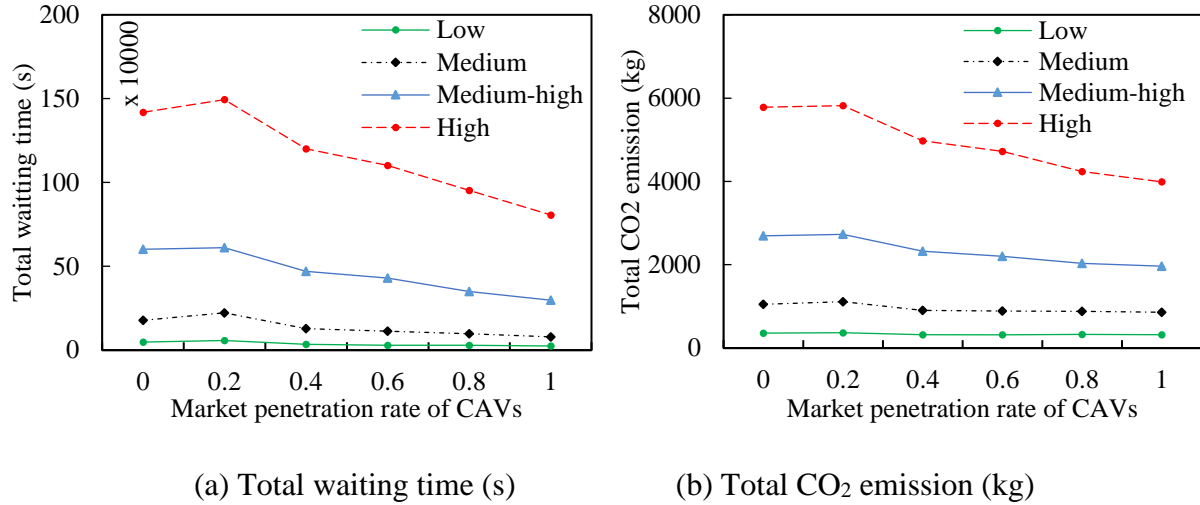
Figure. 6.8 Impacts of Different MPRs of CAVs under Different Traffic Demand Scenarios

6.6.   Summary

Chapter 6 proposes a transfer-based DRL-controlled signal intersection framework and analyzes the performance of the DRL-controlled TSC under different traffic demands and MPRs of CAVs. Different parameter settings are also tested. The results indicate that transfer-based models could improve training efficiency and performance. With a 100% MPR of CAVs, the transfer-based DQN approach could significantly improve the system performance compared to pre-timed signal schemes. In high traffic demand scenarios, the total waiting time, CO$_2$ emission, and fuel consumption decrease by about 38%, 34%, and 34%, respectively. Moreover, the transfer-based TSC system performs better than pre-timed signal schemes after 20% to 40% MPRs of CAVs under different traffic demands. In conclusion, the good performances in efficiency, validity, and transferability of the transfer-based DQN-TSC models indicate a possible engineering application in intersections with similar traffic scenarios. Meanwhile, the basic requirement of the MPRs of CAVs (between 20% and 40%) for the transfer-based DQN TSC system is expected to be met in the near future. These findings should be valuable to

transportation researchers, decision-makers, and traffic engineers to improve intersection efficiency by implementing transfer-based DQN-controlled traffic signals.

CHAPTER 7: MULTI-AGENT DEEP REINFORCEMENT LEARNING CONTROLLED

TRAFFIC SIGNAL SYSTEMS

7.1. Introduction

Chapter 7 presents the basic settings for the proposed multi-agent DRL TSC system. The multi-agent DQN models are implemented in a corridor with seven intersections. All intersections are decentrally controlled by the DQN controller. With the V2I communication technology, the intersections can obtain the traffic states from vehicles in each approach. Meanwhile, with the infrastructure to infrastructure (I2I) communication technology, the intersections can share the state value with one another. Hence, the multi-agent reinforcement learning (MARL) with the state of total waiting time and the MARL with shared total waiting time are both analyzed. The traffic performances including the total waiting time, average queue length, and total CO_2 emission of each intersection are investigated. Finally, this chapter concludes with a summary.

7.2. Methodologies

In this chapter, all intersections in the corridor are decentrally controlled by independent DRL agents. The Deep Q Network (DQN) framework as introduced in Chapter 6 is used in this section for the DRL control. Also, as shown in Figure 7.1, several revisions are made to the research work conducted by (Ault & Sharon, 2021). With the V2I technology, the intersection could obtain the state of traffic in each lane of the approach. In this case, the state of the intersection is a matrix composed of the green-time-phase indicator P_{ij} ($P_{ij} = 1$ if green-time phase and 0 otherwise) and the total waiting time TWT_{ij} for each inlet lane j of the intersection i. Meanwhile, with the I2I communication technology, the intersections can also share the state

value with one another. In this case, the shared state is a matrix composed of the states of the target intersection i, upstream intersection $i-1$, and downstream intersection $i+1$. The reward of the intersection is the negative total waiting time of vehicles. The communication range is set as 200 m. Considering the large size of the state matrix, the input layer of the DQN is firstly set as a convolution layer with a 2×2 convolution kernel. After the flatten layer, 3 full connection layers with 64 neurons are implemented. Rectified Linear Unit (ReLU) is set as the activation function for the neural network. Adam method is set as the optimizer for the neural network. The final layer outputs are the discrete values for the action space.
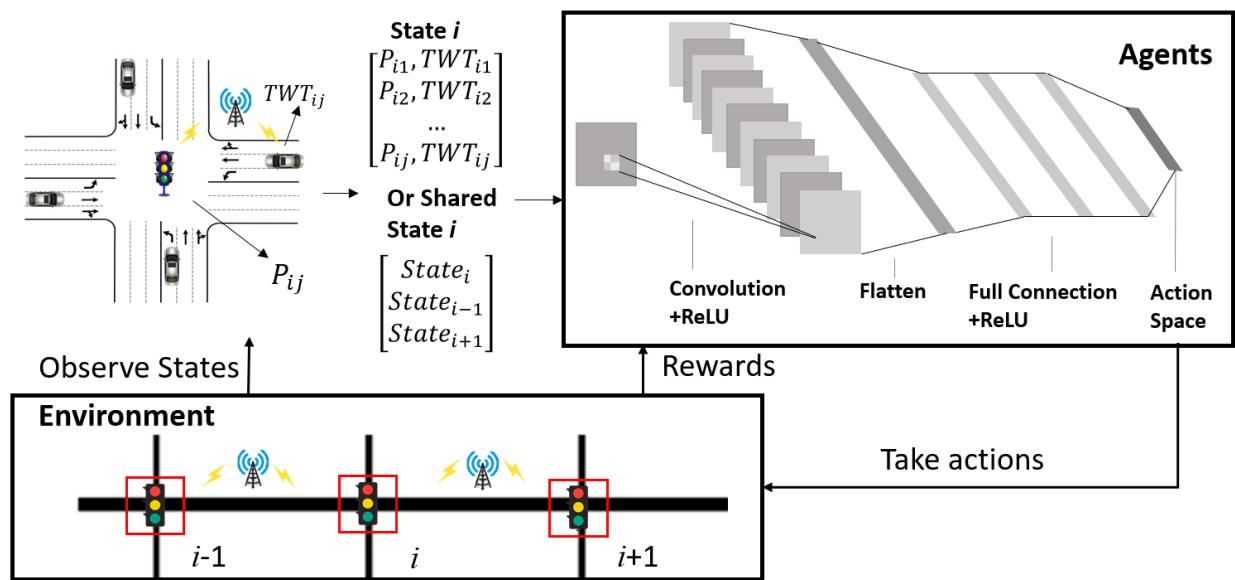
Figure. 7.1 Framework of the Multi-agent Deep Q Learning Method

The framework of the independent DQN is shown in Figure 7.2. Each DQN agent also includes the experience replay and epsilon-greedy functions. The batch size is 32 and the experience replay buffer is 10000. The update interval of the target network weight is 500. The DQN TSC agent could choose an action a_t based on the state s_t and reward r_t from the

simulation environment in the timestep t. The action set A_t includes green phases for traffic movements at the intersection. When the current action a_t is different from the previous action a_{t-1}, a phase that includes 3-s yellow is added.
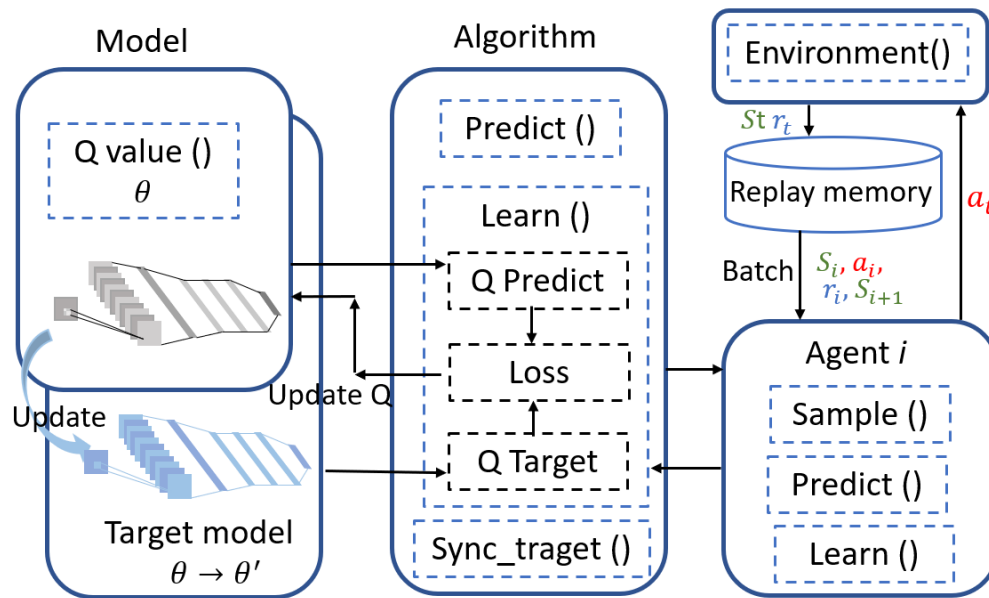


Figure. 7.2 Framework of the Deep Q Learning Method

7.3. Simulation Settings

A corridor with 7 intersections in Ingolstadt, Germany, is selected as a case study in this research. The Ingolstadt Traffic Scenario (InTAS) for SUMO is obtained by the previous research (Lobo et al., 2020). Ingolstadt traffic has been modeled and validated using real traffic information from 24 measurement points. As shown in Figure 7.3, a corridor with seven intersections is selected as a case study for the simulation. The detailed layout of each intersection is shown in Figure 7.4. Green-time phases (10 s) are set as possible actions for each intersection. A 3-s yellow time is added if the traffic light changes its phase. The speed limit is set at 35 mph (i.e., 15.6 m/s). The detailed traffic demands for each movement at the intersection

are also presented in Table 7.1. All simulations are implemented in the Simulation of Urban MObility (SUMO) by the TraCI-Python interface. Each training episode of the simulation is 3600 s with the first 600 s being the warm-up time. The default car-following model and lane change model documented in InTAS are utilized for all vehicles.

Figure 7.3 InTAS Roadway Topology and Selected Corridor Scenario settings
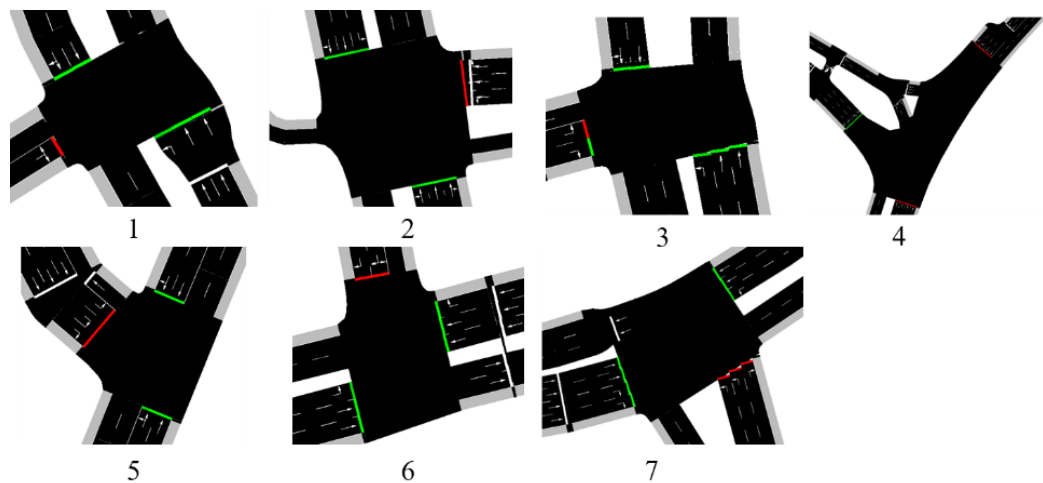
Figure 7.4 Layouts of Seven Intersections in the Corridor

Table 7.1 Traffic Demand of Each Inlet of The Intersection During 14:00 to 15:00

Int.	SB _W	SB _S	SB _E	WB _N	WB _W	WB _S	NB _E	NB _N	NB _W	EB _S	EB _E	EB _N	All
1	218	473	0	0	0	0	0	50	0	78	0	78	897
2	222	707	286	281	92	32	141	552	257	0	0	0	2570
3	333	457	0	338	0	0	0	457	0	334	0	174	2093
4	0	145	74	0	0	0	0	220	238	217	0	147	1041
5	278	317	0	0	0	0	0	304	211	50	0	112	1272
6	199	239	0	0	0	0	0	232	80	306	0	258	1314
7	0	215	19	12	0	267	250	217	0	0	0	0	980

During the training of the MARL, three traffic control cases are analyzed: 1) pre-timed signal control, 2) MARL, and 3) MARL with shared states. It is noted that in the MARL model, the state matrix is composed of the green-time-phase indicator P_{ij} ($P_{ij} = 1$ if green-time phase and 0 otherwise) and the total waiting time TWT_{ij} for each inlet lane j of the intersection i. Also, in the MARL with shared states, the target intersection could obtain the states of its nearest neighbors (upstream and downstream intersections). Hence, the shared state is a matrix composed of the states of the target intersection i, upstream intersection i-1, and downstream intersection i+1. During the training of the MARL models, each training includes 5 trials and each trial includes 200 simulation episodes. Meanwhile, each simulation episode runs 3600s with the first 600s being the warm-up time. Three main traffic performances are calculated including the total waiting time, average queue length, and the total CO2 emission. The performance result is the average value of test results from 5 episodes in 5 trials.

7.4.   Results for Multi-agent Corridor Intersections

After 200 simulation episodes, the average values of the total waiting time in 5 trials for each intersection (presented in dash line) are presented in Figure 7.5. The red dash line shows the result of the pre-timed signal controller. The blue color indicates the results for the MARL

controller and the purple line shows the results for the MARL with the shared states. Also, the color boundary indicates the maximum and minimum values in 5 trials. The negative total waiting time is set as the training reward for each independent DQN agent. Hence, these curves also exhibit negative rewards. All curves in Figure 7.5 indicate that the training procedures reach a converged value after 200 training episodes. It is also noted that the trained models are all better than traditional pre-timed signal controllers with regard to the performance of the total waiting time. It is noted that both MARL and MARL with shared states could decrease the total waiting time from 72% (in intersection 3) to 93% (in intersection 1) compared to pre-timed signal controllers.
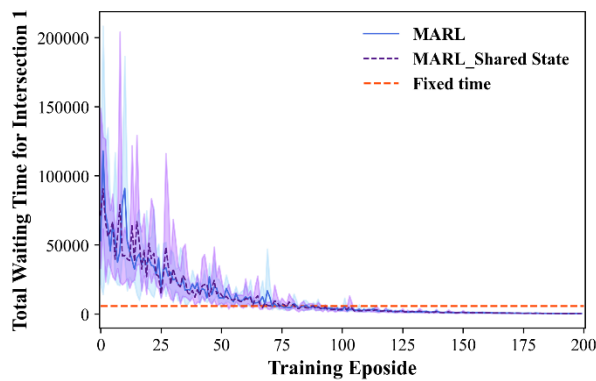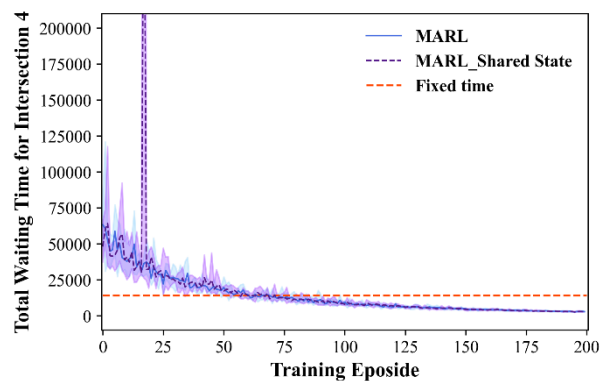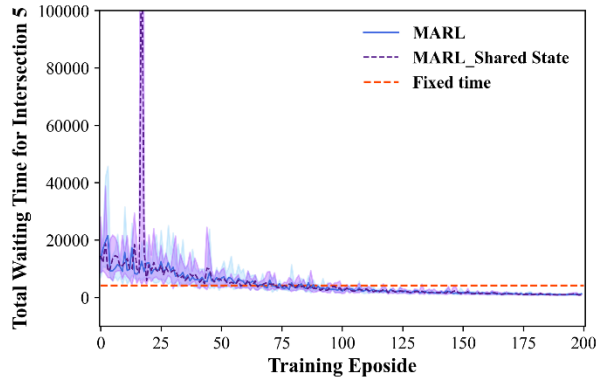

(a) Total waiting time for Int. 1
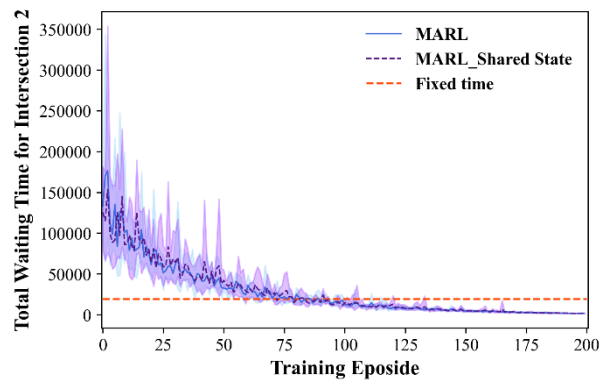
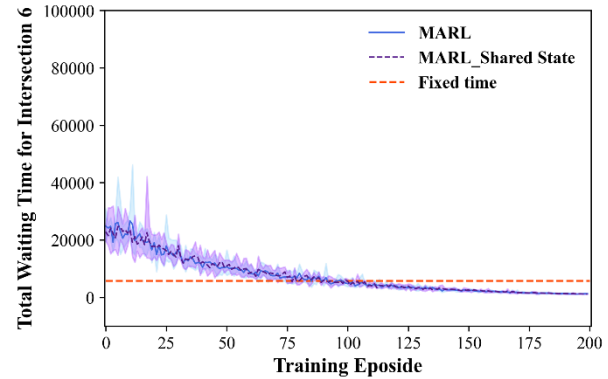(b) Total waiting time for Int. 2
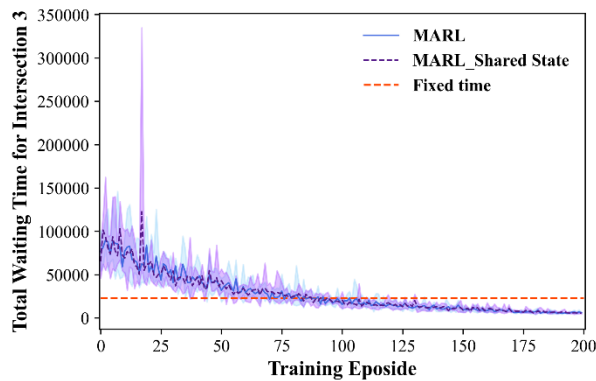
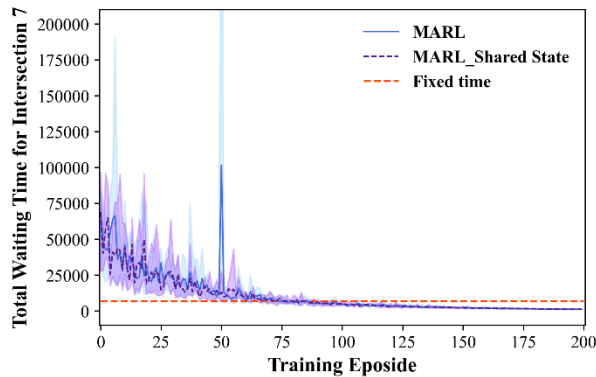(c) Total waiting time for Int. 3

(d) Total waiting time for Int. 4

(e) Total waiting time for Int. 5

(f) Total waiting time for Int. 6

(g) Total waiting time for Int. 7

Figure 7.5 Total Waiting Time for Each Intersection

From Figure 7.6 to Figure 7.8, the total waiting time, average queue length, and total CO_2 emission for all intersections are presented. It is noted that MARL and MARL with shared states could all have a better performance compared to the pre-timed signal controller. Tables 7.2 to 7.4 also exhibit the detailed results for three performance indicators. The values in parentheses are change rates with regard to pre-timed signal results. The values in brackets are change rates with regard to MARL results. Compared to the pre-timed controller, the MARL controller could decrease the total waiting time, average queue length, and total CO_2 emission of all intersections by 81%, 75%, and 75%, respectively. Meanwhile, the MARL with shared states shows a further improvement in three performance indicators compared to the MARL controller. Compared to the MARL controller, the MARL with shared states could further decrease the total waiting time,

average queue length, and total CO2 emission of all intersections by 6%, 3%, and 3%, respectively.
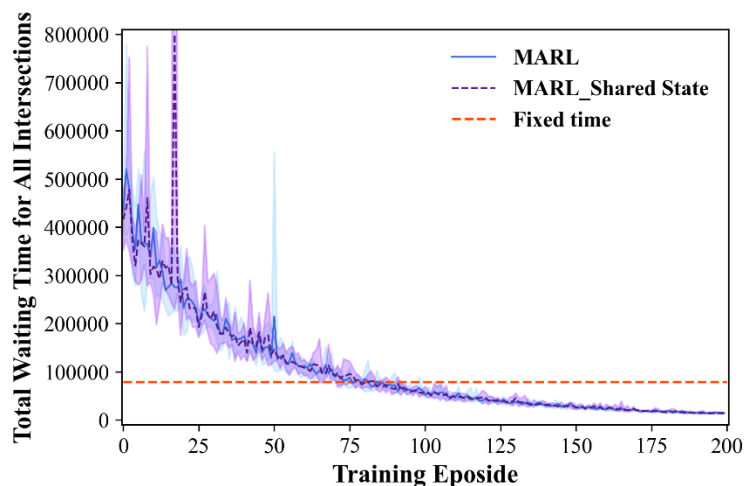
Figure 7.6 Total Waiting Time for All Intersections

Table 7.2 Total Waiting Time at Each Intersection

Waiting time (s)	Int. 1	Int. 2	Int. 3	Int. 4	Int. 5	Int. 6	Int. 7	All
Pre-timed signal	5765	19336	23091	13986	4261	5779	6910	79128
MARL	412.96 (0.93)	1733.32 (0.91)	6413.92 (0.72)	2787.08 (0.8)	1072.72 (0.75)	1232.36 (0.79)	1110.8 (0.84)	14763.16 (0.81)
MARL-Shared State	371 [0.1]	1715.72 [0.01]	5764.44 [0.1]	2706.76 [0.03]	1057.6 [0.01]	1197.16 [0.03]	1111 [0]	13923.68 [0.06]

*note: the values in parentheses are change rates with regard to pre-timed signal results. The values in brackets are change rates with regard to MARL results.
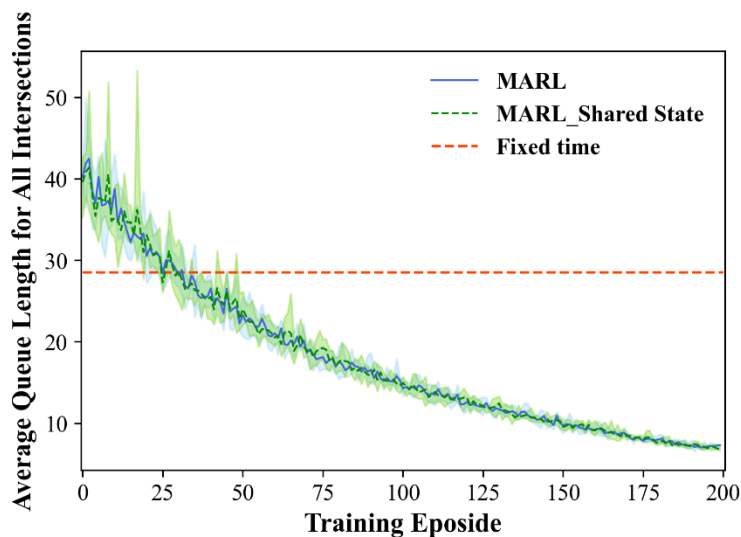
Figure 7.7 Average Queue Length for All Intersections

Table 7.3 Average Queue Length at Each Intersection

Queue Length	Int. 1	Int. 2	Int. 3	Int. 4	Int. 5	Int. 6	Int. 7	All
Pre-timed signal	2.08	6.99	8.02	4.92	1.61	2.25	2.67	28.55
MARL	0.31 (0.85)	1.28 (0.82)	1.86 (0.77)	1.51 (0.69)	0.57 (0.65)	0.91 (0.6)	0.78 (0.71)	7.21 (0.75)
MARL-Shared State	0.27 [0.11]	1.24 [0.03]	1.71 [0.08]	1.5 [0]	0.56 [0.02]	0.91 [0.01]	0.78 [0]	6.96 [0.03]

*note: the values in parentheses are change rates with regard to pre-timed signal results. The values in brackets are change rates with regard to MARL results.
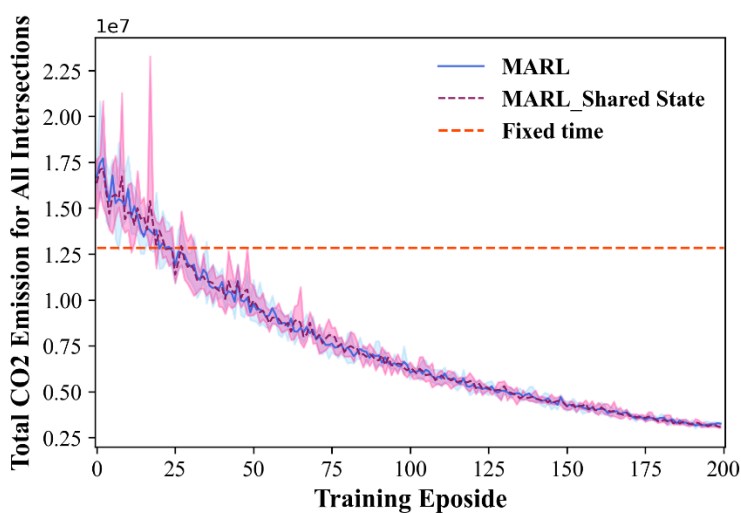
Figure 7.8 Total CO_2 Emission for All Intersections

Table 7.4 Total CO_2 Emission at Each Intersection

CO_2 (g)	Int. 1	Int. 2	Int. 3	Int. 4	Int. 5	Int. 6	Int. 7	All
Pre-timed signal	1012.89	3422.05	3777.67	2073.87	702.09	842.57	1010.8	12841.94
MARL	228.95 (0.77)	883.14 (0.74)	1018.36 (0.73)	457.15 (0.78)	200.53 (0.71)	249.21 (0.7)	195.63 (0.81)	3232.96 (0.75)
MARL-Shared State	224.31 [0.02]	864.22 [0.02]	953.15 [0.06]	450.97 [0.01]	196.87 [0.02]	245.46 [0.02]	197.08 [-0.01]	3132.06 [0.03]

*note: the values in parentheses are change rates with regard to pre-timed signal results. The values in brackets are change rates with regard to MARL results.

7.5. Summary

In this chapter, the framework and basic settings for the multi-agent DRL TSC system are introduced. A corridor with seven intersections in Ingolstadt, Germany, is selected as a case study in this research. All intersections are decentrally controlled by independent DQN agents. Considering the I2I communication technology, the MARL controlled intersections are further improved by sharing the state value with upstream and downstream intersections. The training results indicate that both MARL and MARL with shared states could both have significant improvements in traffic performance at all intersections. Compared to the pre-timed controller, the MARL controller could decrease the total waiting time, average queue length, and total CO_2 emission at all intersections by 81%, 75%, and 75%, respectively. Compared to the MARL controller, the MARL with shared states could further decrease the total waiting time, average queue length, and total CO_2 emission of all intersections by 6%, 3%, and 3%, respectively.

CHAPTER 8: SUMMARY AND CONCLUSIONS

8.1. Introduction

CAV technologies could make intelligent driving decisions based on multi-source data and significantly affect the performance of the intersection systems. The requirement of the time gap for CAVs could also be drastically decreased with the help of V2V communication technology, and this could significantly change the car-following behaviors and impact the capacity of the intersection. However, it is expected to have a long transition time to achieve high MPRs of CAVs (Sharon & Stone, 2017). Hence, there is an urgent need to investigate the impacts of CAVs on the intersection systems under different MPRs of CAVs. Meanwhile, the intersection capacity calculation is essential to intersection design and traffic performance evaluation. The calibration of the intersection capacity adjustment factors under different CAV penetration rates could provide a useful guideline for transportation engineers and planners to calculate intersection capacity and retrofit/design future intersection systems.

Also, the rapid developments of DRL technologies provide an innovative solution to improve the efficiency, safety, and sustainability of the intersection systems. However, the high performance of the DRL-controlled TSC system requires high-quality inputs of the traffic information from the environment. Since there is still a long way to achieve high MPRs of CAVs, training a DRL TSC model under 100% MPRs of CAVs (which assumes that the signal controller could obtain information about all vehicles on the roadways) is not currently feasible for engineering applications. Moreover, the training procedure of the DRL methods requires a lot of samples and takes a long time to converge (Xu et al., 2019). It is not applicable to train a specific DRL model for each intersection on the roadways for real-world applications. Thus, transfer learning, which enables the reuse of previously trained action policy developed from a

similar task to initialize the learning of a target task, provides a possible solution to improve the training efficiency of the DRL model. A modification of the currently used DRL framework and reusing pre-trained model under similar traffic scenarios based on the transfer learning could provide a feasible solution to improve the training procedure of the DRL.

Furthermore, it is common to have several intersections on corridors or networks. However, a single DRL agent is unable to control several intersections because this could result in exponential explosion in the action space. As the coordination between intersections could further improve the system performance, a multi-agent DRL control framework considering the cooperation between intersections (by sharing the state information) is investigated in this dissertation to provide possible new insights for future intelligent intersection systems control and design.

The major goal of this research is to provide an intensive evaluation of the impacts of CAVs on signal intersection systems, as well as an in-depth analysis of intersection capacity adjustment factors considering varying MPRs of CAVs. Also, a transfer-based DRL TSC framework is developed and tested under different MPRs of CAVs and traffic demand levels. A multi-agent DRL TSC with shared traffic states between downstream and upstream intersections is investigated in a corridor. The framework developed in this research could provide a theoretical reference for transportation researchers and traffic engineers in calculating intersection capacity, designing intelligent intersections, improving intersection efficiency, and implementing DRL-controlled traffic signals under mixed traffic environments with CAVs. The main research results and discussions will be summarized in Section 8.2. Suggestions for future research will be also provided in Section 8.3.

8.2. Summary and Conclusions

This study develops specific case studies to evaluate the impacts of CAVs on intersections under different MPRs of CAVs. Micro-simulation methods and specific control models for CAVs (ACC model and CACC model) are introduced. Both the lane-level and intersection-level capacity analyses are conducted in this research. On the lane-level capacity investigation, adjustment factors for saturation headway and saturation traffic flow rate for each lane of the intersection under different MPRs of CAVs are calculated. With 100% CAVs, the saturation headways for the exclusive through traffic lane, exclusive left-turn traffic lane, and shared-right-and-through traffic lane decrease by 55.8%, 48.9%, and 42.4%, respectively. On the intersection-level capacity investigation, the fitting curve of the maximum throughput of the intersection under different MPRs of CAVs is calibrated. Meanwhile, the traffic performances of the total waiting time, CO_2 emission, and fuel consumption under maximum throughputs are also documented. The results are expected to help traffic engineers and planners to develop a useful systematic framework summarizing the rationale and techniques used during the process of simulation modeling, scenario identification, and intersection capacity analysis under different MPRs of CAVs.

Additionally, this research investigates the effects of different control models of AVs and CAVs (i.e., IDM-controlled AVs, ACC-controlled AVs, and CACC-controlled CAVs) on the intersections with different signal control methods (i.e., pre-timed signal, gap-based actuated signal, and delay-based actuated signal) under different MPRs of CAVs and traffic demands. Results indicate that CACC-controlled CAVs outperform IDM/ACC-controlled AVs. The delay-based signalized intersection shows a 96% decrease in the average delay under high traffic demand with a 100% MPR of CACC-controlled CAVs. Also, CACC-controlled CAVs could

significantly decrease the average delay under medium and high demand scenarios after the MPRs exceed 20% and 40%, respectively. The results could provide a foundation for researchers to investigate the impact of CAVs on different signal-controlled intersections and give a reference for better signal control and intelligent vehicle operations.

This study also proposes a transfer-based DRL-controlled signal intersection framework to improve the training efficiency of the DRL procedure. The validity and performance of the DRL-controlled TSC are investigated under different traffic demands and MPRs of CAVs. The result comparison between the transfer-based model and direct-trained model indicates that the training efficiency is improved when the prior action policy of the DQN TSC model is utilized in a model under similar scenarios. The traffic performance is also improved with the increase of MPRs of CAVs. In high traffic scenarios, the total waiting time, CO_2 emission, and fuel consumption decrease by about 38%, 34%, and 34%, respectively. Compared with pre-time signal schemes, the transfer-based DQN TSC systems perform better when the MPRs of CAVs are more than 20% under the medium-high traffic scenario and more than 40% under low, medium, and high traffic scenarios. In summary, the good performance in efficiency, validity, and transferability of the transfer-based DQN TSC indicates a possible engineering application in intersections under similar traffic conditions. Meanwhile, the basic MPR requirement of the CAVs (between 20% and 40%) for this transfer-based DQN TSC system is expected to be met in the near future.

Furthermore, this research introduces a multi-agent DRL TSC system framework and provides basic settings for a corridor with seven intersections in Ingolstadt, Germany. All intersections are decentrally controlled by independent DQN agents. The multi-agent reinforcement learning (MARL) enables cooperation between intersections by sharing the state

value with upstream and downstream intersections. The results indicate that both MARL and MARL with shared states could significantly improve the traffic performance of all intersections. Compared to the pre-timed signal controller, the MARL controller could decrease the total waiting time, average queue length, and total CO_2 emission of all intersections by 81%, 75%, and 75%, respectively. In addition, compared to the MARL controller, the MARL with shared states could further decrease the total waiting time, average queue length, and total CO_2 emission of all intersections by 6%, 3%, and 3%, respectively. These findings should be valuable to transportation researchers, decision-makers, and engineers in improving the intersection efficiency, designing future intersections, and implementing DRL-controlled traffic signals.

8.3.   Future Research Directions

This research documents the adjustment factors for saturation headway and saturation traffic flow rate for each lane of the intersection under different MPRs of CAVs. The results provide useful guidance for traffic engineers and planners to modify and calculate the intersection capacity. To model the CAV behavior, when a CAV is following a HDV, the car-following system is changed into the ACC mode. When a CAV is following a CAV, the car-following system is switched into the CACC mode to achieve a closer car-following gap. However, with the development of CAV technologies, the CAV control strategy and headway acceptance for different vehicles are still largely not determined. A more fundamental investigation of the CAV technologies, especially for car-following models and platooning system, is important to improve the results. Meanwhile, considering the unstable results found in the mixed flow of HDVs with CAVs, a further study on the interactions between CAVs and

HDVs is needed. A specific control mode between HDVs and CAVs is required to ensure safety in the mixed traffic flow.

Additionally, the DRL framework proposed in this study focuses mainly on traffic mobility improvement. Future studies should pay more attention to the safety issues of vehicles. Moreover, the reasonability of the actions determined by the DRL agent still needs more explanations, and the model-based DRL framework may be beneficial to the model interpretation. Furthermore, the reliability of the DRL models could also be improved by multi-source data fusion and reconstruction. Improving the prediction accuracy of the traffic states at limited MPRs of CAVs could greatly promote the use of DRL models in real-world applications.

REFERENCES

Abdelhameed, M. M., Abdelaziz, M., Hammad, S., & Shehata, O. M. (2015). A Hybrid Fuzzy-Genetic Controller for a multi-agent intersection control system. *ICET 2014 - 2nd International Conference on Engineering and Technology*.

Abhishek, Boon, M. A. A., & Mandjes, M. (2019). Generalized gap acceptance models for unsignalized intersections. *Mathematical Methods of Operations Research*, *89*(3), 385–409.

Algomaiah, M., & Li, Z. (2019). Utilizing Lane-Based Strategy to Incorporate Mixed Traffic in Interchange Control for Connected and Autonomous Vehicles. *TransportationResearch Record: Journal of the Transportation ResearchBoard*, *2673*(5), 454–465.

Amoozadeh, M., Raghuramu, A., Chuah, C. N., Ghosal, D., Michael Zhang, H., Rowe, J., & Levitt, K. (2015). Security vulnerabilities of connected vehicle streams and their impact on cooperative driving. *IEEE Communications Magazine*, *53*(6), 126–132.

Arel, I., Liu, C., Urbanik, T., & Kohls, A. G. (2010). Reinforcement learning-based multi-agent system for network traffic signal control. *IET Intelligent Transport Systems*, *4*(2), 128–135.

Arem, B Van, & Vos, A. P. De. (1997). *The microscopic traffic simulation model Commissioned by the Transport Research Centre*. REPORT INRO-VVG 1997.

Arnaout, G. M., & Arnaout, J. P. (2014). Exploring the effects of cooperative adaptive cruise control on highway traffic flow using microscopic traffic simulation. *Transportation Planning and Technology*, *37*(2), 186–199.

Ault, J., & Sharon, G. (2021). *Reinforcement Learning Benchmarks for Traffic Signal Control | OpenReview*. https://openreview.net/forum?id=LqRSh6V0vR

Bloomberg. (2017). *Is your city getting ready for AVs?* http://avsincities.bloomberg.org/global-atlas

Brilon, W., & Wu, N. (2001). Capacity at Unsignalized Intersections Derived by Conflict Technique. *Transportation Research Record: Journal of the Transportation Research Board*, *1776*(1), 82–90.

Chen, G., & Kang, K. D. (2016). Win-fit: Efficient intersection management via dynamic vehicle batching and scheduling. *2015 International Conference on Connected Vehicles and Expo, ICCVE 2015 - Proceedings*, 263–270.

Christie, D., Koymans, A., Chanard, T., Lasgouttes, J. M., & Kaufmann, V. (2016). Pioneering Driverless Electric Vehicles in Europe: The City Automated Transport System (CATS). *Transportation Research Procedia*, *13*, 30–39.

Chu, T., Wang, J., Codeca, L., & Li, Z. (2020). Multi-agent deep reinforcement learning for large-scale traffic signal control. *IEEE Transactions on Intelligent Transportation Systems*, *21*(3), 1086–1095.

Dahl, J., & Lee, C. (2012). Empirical Estimation of Capacity for Roundabouts Using Adjusted Gap-Acceptance Parameters for Trucks. *Transportation Research Record: Journal of the Transportation Research Board*, *2312*(1), 34–45.

Delis, A. I., Nikolos, I. K., & Papageorgiou, M. (2015). Macroscopic traffic flow modeling with adaptive cruise control: Development and numerical solution. *Computers and Mathematics with Applications*, *70*(8), 1921–1947.

Deng, Q. (2016). A General Simulation Framework for Modeling and Analysis of Heavy-Duty Vehicle Platooning. *IEEE Transactions on Intelligent Transportation Systems*, *17*(11), 3252–3262.

Derbel, O., Péter, T., Zebiri, H., Mourllion, B., Basset, M., & Zebiri Benjamin Mourllion, H.

(2012). Modified Intelligent Driver Model. *Transportation Engineering*, *40*(2), 53–60.

Do, W., Rouhani, O. M., & Miranda-Moreno, L. (2019). Simulation-Based Connected and Automated Vehicle Models on Highway Sections: A Literature Review. *Journal of Advanced Transportation*, *2019*.

Dresner, K., & Stone, P. (2008). A multiagent approach to autonomous intersection management. *Journal of Artificial Intelligence Research*, *31*, 591–656.

Du, Z., Homchaudhuri, B., & Pisu, P. (2017). Coordination strategy for vehicles passing multiple signalized intersections: A connected vehicle penetration rate study. *Proceedings of the American Control Conference*, 4952–4957.

Duncan, M., Charness, N., Chapin, T., Horner, M., Stevens, L., Richard, A., Souders, D., Crute, J., Riemondy, A., & Morgan, D. (2015). Enhanced mobility for aging populations using automated vehicles. BDV30 977-11. *The National Academies of Sciences, Engineering, and Medicine*.

Erdmann, J. (2015). SUMO's Lane-changing model. *Lecture Notes in Control and Information Sciences*, *13*, 105–123.

Fagnant, D. J., & Kockelman, K. (2015). Preparing a nation for autonomous vehicles: Opportunities, barriers and policy recommendations. *Transportation Research Part A: Policy and Practice*, *77*, 167–181.

Faisal, A., Yigitcanlar, T., Kamruzzaman, M., & Currie, G. (2019). Understanding autonomous vehicles: A systematic literature review on capability, impact, planning and policy. *Journal of Transport and Land Use*, *12*(1), 45–72.

Genders, W., & Razavi, S. (2016). Using a Deep Reinforcement Learning Agent for Traffic Signal Control. *ArXiv Preprint*. http://arxiv.org/abs/1611.01142

Genders, W., & Razavi, S. (2019). Asynchronous n-step Q-learning adaptive traffic signal control. *Journal of Intelligent Transportation Systems: Technology, Planning, and Operations*, *23*(4), 319–331.

Guo, Q., Li, L., & Ban, X. (2019). Urban traffic signal control with connected and automated vehicles: A survey. *Transportation Research Part C: Emerging Technologies*, *101*(April), 313–334.

Hausberger S., Rexeis M., Zallinger M., L. R. (2009). *Emission Factors from the Model PHEM for the HBEFA Version 3*.

Haydari, A., & Yilmaz, Y. (2020). Deep Reinforcement Learning for Intelligent Transportation Systems: A Survey. *IEEE Transactions on Intelligent Transportation Systems*, 1–22.

HCM. (2016). *Highway Capacity Manual* (6th ed.). Transportation Research Board.

He, Z., Zheng, L., Lu, L., & Guan, W. (2018). Erasing Lane Changes from Roads: A Design of Future Road Intersections. *IEEE Transactions on Intelligent Vehicles*, *3*(2), 173–184.

Hendrickson, C., Biehler, A., & Mashayekh, Y. (2014). *Conected and autonomous vehicles 2040 vision*.

Ilgin Guler, S., Menendez, M., & Meier, L. (2014). Using connected vehicle technology to improve the efficiency of intersections. *Transportation Research Part C: Emerging Technologies*, *46*, 121–131.

Ioannou, P. A., & Stefanovic, M. (2005). Evaluation of ACC vehicles in mixed traffic: Lane change effects and sensitivity analysis. *IEEE Transactions on Intelligent Transportation Systems*, *6*(1), 79–89.

Jiang, H., Hu, J., An, S., Wang, M., & Brian, B. (2017). Eco approaching at an isolated signalized intersection under partially connected and automated vehicles environment.

Transportation Research Part C, *79*, 290–307.

Kesting, A., Treiber, M., & Helbing, D. (2010). Enhanced intelligent driver model to access the impact of driving strategies on traffic capacity. *Philosophical Transactions of the Royal Society A: Mathematical, Physical and Engineering Sciences*, *368*(1928), 4585–4605.

Kesting, A., Treiber, M., Schönhof, M., & Helbing, D. (2007). Extending Adaptive Cruise Control to Adaptive Driving Strategies. *Transportation Research Record: Journal of the Transportation Research Board*, *2000*(1), 16–24.

Kesting, A., Treiber, M., Schönhof, M., & Helbing, D. (2008). Adaptive cruise control design for active congestion avoidance. *Transportation Research Part C: Emerging Technologies*, *16*(6), 668–683.

Kiran, B. R., Sobh, I., Talpaert, V., Mannion, P., Sallab, A., Yogamani, S., & Perez, P. (2021). Deep Reinforcement Learning for Autonomous Driving: A Survey. *IEEE Transactions on Intelligent Transportation Systems*.

Kockelman, K., & Boyles, S. (2018). *Smart Transport for Cities and Nations: The Rise of Self-D riving and Connected Vehicles*. http://www.caee.utexas.edu/prof/kockelman/public_html/C AV_Book2018.pdf

Lee, J., & Park, B. (2012). Development and evaluation of a cooperative vehicle intersection control algorithm under the connected vehicles environment. In *IEEE Transactions on Intelligent Transportation Systems*. *13*(1), 81–90.

Lee, J., Park, B., & Yun, I. (2013). Cumulative travel-time responsive real-time intersection control algorithm in the connected vehicle environment. *Journal of Transportation Engineering*, *139*(10), 1020–1029.

Li, T., & Kockelman, K. M. (2016). Valuing the safety benefits of connected and automated vehicle technologies. *Transportation Research Board 95th Annual Meeting*, No. 16-1468.

Li, Z., Elefteriadou, L., & Ranka, S. (2014). Signal control optimization for automated vehicles at isolated signalized intersections. *Transportation Research Part C: Emerging Technologies*, *49*, 1–18.

Liang, X., Guler, S. I., & Gayah, V. V. (2019). Joint Optimization of Signal Phasing and Timing and Vehicle Speed Guidance in a Connected and Autonomous Vehicle Environment. *TransportationResearch Record: Journal of the Transportation ResearchBoard*, *2673*(4), 70–83.

Liang, X., Du, X., Wang, G., & Han, Z. (2019). A Deep Reinforcement Learning Network for Traffic Light Cycle Control. *IEEE Transactions on Vehicular Technology*, *68*(2), 1243–1253.

Litman, T. (2020). *Autonomous Vehicle Implementation Predictions: Implications for Transport Planning*. https://www.vtpi.org/avip.pdf

Liu, B., Shi, Q., Song, Z., & Kamel, E. (2018). Trajectory Planning for Autonomous Intersection Management of Connected Vehicles. *Simulation Modelling Practice and Theory*, *90*, 16–30.

Liu, H., Xiao, L., Kan, X. D., Shladover, S. E., Lu, X. Y., Wang, M., Schakel, W., & van Arem, B. (2018). *Using Cooperative Adaptive Cruise Control (CACC) to Form High-Performance Vehicle Streams*. University of California, Berkeley, PATH Program. https://escholarship.org/uc/item/8pw857gb

Lobo, S. C., Neumeier, S., Fernandez, E. M. G., & Facchi, C. (2020). *InTAS -- The Ingolstadt Traffic Scenario for SUMO*. https://doi.org/10.48550/arxiv.2011.11995

Milanés, V., & Shladover, S. E. (2014). Modeling cooperative and autonomous adaptive cruise control dynamic responses using experimental data. *Transportation Research Part C:*

Emerging Technologies, *48*, 285–300.

Milanés, V., & Shladover, S. E. (2016). Handling Cut-In Vehicles in Strings of Cooperative Adaptive Cruise Control Vehicles. *Journal of Intelligent Transportation Systems: Technology, Planning, and Operations*, *20*(2), 178–191.

Milanes, V., Shladover, S. E., Spring, J., Nowakowski, C., Kawazoe, H., & Nakamura, M. (2014). Cooperative adaptive cruise control in real traffic situations. *IEEE Transactions on Intelligent Transportation Systems*, *15*(1), 296–305.

Mintsis, E. (2018). Modelling, simulation and assessment of vehicle automations and automated vehicles' driver behaviour in mixed traffic. *TransAID Deliverable D3.1*, *2018*(723390), 113. https://www.transaid.eu/wp-content/uploads/2017/Deliverables/WP3/TransAID_D3.1_Mo delling-simulation-and-assessment-of-vehicle-automations.pdf

Navigant Research. (2016). *Autonomous Vehicles: Advanced Driver Assistance Systems and the Evolution of Self-Driving Functionality: Global Market Analysis and Forecasts*. http://www.navigantresearch.com/research/autonomous-vehicles

NHTSA. (2016). *Federal automated vehicles policy: Accelerating the next revolution in roadway safety*. https://www.transportation.gov/AV/federal-automated-vehicles-policy-september-2016

Nilsson, J., Brannstrom, M., Coelingh, E., & Fredriksson, J. (2015). Longitudinal and lateral control for automated lane change maneuvers. *Proceedings of the American Control Conference*, *2015-July*, 1399–1404.

Pendleton, S., Andersen, H., Du, X., Shen, X., Meghjani, M., Eng, Y., Rus, D., & Ang, M. (2017). Perception, Planning, Control, and Coordination for Autonomous Vehicles. *Machines*, *5*(1), 6.

Ploeg, J., Serrarens, A. F. A., & Heijenk, G. J. (2011). Connect & Drive: design and evaluation of cooperative adaptive cruise control for congestion reduction. *Journal of Modern Transportation*, *19*(3), 207–213.

Porfyri, K. N., Mintsis, E., & Mitsakis, E. (2018). Assessment of ACC and CACC systems using SUMO. *EPiC Series in Engineering*, *2*, 82–69.

Pourmehrab, M., Elefteriadou, L., & Ranka, S. (2018). Smart intersection control algorithms for automated vehicles. *2017 10th International Conference on Contemporary Computing, IC3 2017*, 1–6.

PTOLEMUS. (2017). *The Autonomous Vehicle Global Study | PTOLEMUS Consulting Group*. https://www.ptolemus.com/research/theautonomousvehicleglobalstudy2017

SAE. (2016). *Taxonomy and definitions for terms related to driving automation systems for on-road motor vehicles*. http://standards.sae.org/j3016_201609

Sharon, G., & Stone, P. (2017). A Protocol for Mixed Autonomous and Human-Operated Vehicles at Intersections. *International Conference on Autonomous Agents and Multiagent Systems*, 151–167.

Shi, S., & Chen, F. (2018). Deep Recurrent Q-learning Method for Area Traffic Coordination Control. *Journal of Advances in Mathematics and Computer Science*, *27*(3), 1–11.

Shi, T., Wang, P., Cheng, X., Chan, C. Y., & Huang, D. (2019). Driving Decision and Control for Automated Lane Change Behavior based on Deep Reinforcement Learning. *2019 IEEE Intelligent Transportation Systems Conference, ITSC 2019*, 2895–2900.

Shladover, S. E. (2018). Connected and automated vehicle systems: Introduction and overview. *Journal of Intelligent Transportation Systems: Technology, Planning, and Operations*, *22*(3), 190–200.

Shladover, S. E., Su, D., & Lu, X. Y. (2012). Impacts of cooperative adaptive cruise control on freeway traffic flow. *TransportationResearch Record: Journal of the Transportation ResearchBoard*, *2324*, 63–70.

Song, L., & Fan, W. (2021). Traffic Signal Control under Mixed Traffic with Connected and Automated Vehicles: A Transfer-Based Deep Reinforcement Learning Approach. *IEEE Access*, *9*, 145228–145237.

Song, L., Fan, W., & Liu, P. (2021). Exploring the effects of connected and automated vehicles at fixed and actuated signalized intersections with different market penetration rates. *Transportation Planning and Technology*, *44*(6), 577–593.

Sun, W., Zheng, J., & Liu, H. X. (2018). A capacity maximization scheme for intersection management with automated vehicles. *Transportation Research Part C: Emerging Technologies*, *94*, 19–31.

Talebpour, A., & Mahmassani, H. S. (2016). Influence of connected and autonomous vehicles on traffic flow stability and throughput. *Transportation Research Part C: Emerging Technologies*, *71*, 143–163.

TransAID. (2019). *Transition Areas for Infrastructure-Assisted Driving D2.2*. https://www.transaid.eu/deliverables/

Treiber, M., & Kesting, A. (2013). *Traffic Flow Dynamics. Traffic Flow Dynamics: Data, Models and Simulation*. Springer.

Treiber, Martin, Hennecke, A., & Helbing, D. (2000). Congested traffic states in empirical observations and microscopic simulations. *Physical Review E - Statistical Physics, Plasmas, Fluids, and Related Interdisciplinary Topics*, *62*(2), 1805–1824.

USDOT. (2020). *Intelligent Transportation Systems - Connected Vehicle Basics*. https://www.its.dot.gov/cv_basics/index.htm

Van Arem, Bart, Van Driel, C. J. G., & Visser, R. (2006). The impact of cooperative adaptive cruise control on traffic-flow characteristics. *IEEE Transactions on Intelligent Transportation Systems*, *7*(4), 429–436.

Vidali, A. (2018). *Simulation of a traffic light scenario controlled by a Deep Reinforcement Learning agent*. University of Milano-Bicocca.

Virdi, N., Grzybowska, H., Waller, S. T., & Dixit, V. (2019). A safety assessment of mixed fleets with Connected and Autonomous Vehicles using the Surrogate Safety Assessment Module. *Accident Analysis and Prevention*, *131*(June), 95–111.

Wan, C. H., & Hwang, M. C. (2018). Value-based deep reinforcement learning for adaptive isolated intersection signal control. *IET Intelligent Transport Systems*, *12*(9), 1005–1010.

Wang, P., Li, H., & Chan, C. Y. (2019). Continuous control for automated lane change behavior based on deep deterministic policy gradient algorithm. *IEEE Intelligent Vehicles Symposium, Proceedings*, *2019-June*, 1454–1460.

Wei, Haoran, Mashayekhy, L., & Papineau, J. (2018). Intersection Management for Connected Autonomous Vehicles: A Game Theoretic Framework. *IEEE Conference on Intelligent Transportation Systems, Proceedings, ITSC*, *2018-November*, 583–588.

Wei, Hua, Yao, H., Zheng, G., & Li, Z. (2018). IntelliLight: A reinforcement learning approach for intelligent traffic light control. *Proceedings of the ACM SIGKDD International Conference on Knowledge Discovery and Data Mining*, 2496–2505.

Xiao, L., Wang, M., & Van Arem, B. (2017). Realistic car-following models for microscopic simulation of adaptive and cooperative adaptive cruise control vehicles. *TransportationResearch Record: Journal of the Transportation ResearchBoard*, *2623*, 1–9.

Xu, N., Zheng, G., Xu, K., Zhu, Y., & Li, Z. (2019). Targeted knowledge transfer for learning traffic signal plans. *Pacific-Asia Conference on Knowledge Discovery and Data Mining*, *11440*, 175–187.

Yang, H., Rakha, H., & Ala, M. V. (2017). Eco-Cooperative Adaptive Cruise Control at Signalized Intersections Considering Queue Effects. *IEEE Transactions on Intelligent Transportation Systems*, *18*(6), 1575–1585.

Yang, K., Guler, S. I., & Menendez, M. (2016). Isolated intersection control for various levels of vehicle technology: Conventional, connected, and automated vehicles. *Transportation Research Part C: Emerging Technologies*, *72*, 109–129.

Zhang, R., Ishikawa, A., Wang, W., Striner, B., & Tonguz, O. K. (2021). Using Reinforcement Learning with Partial Vehicle Detection for Intelligent Traffic Signal Control. *IEEE Transactions on Intelligent Transportation Systems*, *22*(1), 404–415.

Zhao, W., Ngoduy, D., Shepherd, S., Liu, R., & Papageorgiou, M. (2018). A platoon based cooperative eco-driving model for mixed automated and human-driven vehicles at a signalised intersection. *Transportation Research Part C*, *95*(April), 802–821.

Zhou, M., Qu, X., & Jin, S. (2017). On the Impact of Cooperative Autonomous Vehicles in Improving Freeway Merging: A Modified Intelligent Driver Model-Based Approach. *IEEE Transactions on Intelligent Transportation Systems*, *18*(6), 1422–1428.